1-1-2007

Thermal analysis of active catalytic diesel particulate filter regeneration.

Siddhartha Banerjee
University of Windsor

THERMAL ANALYSIS OF ACTIVE CATALYTIC DIESEL PARTICULATE FILTER REGENERATION

By

Siddhartha Banerjee

A Thesis
Submitted to the Faculty of Graduate Studies
through Mechanical Engineering
in Partial Fulfillment of the Requirements for
the Degree of Master of Applied Science at the
University of Windsor

Windsor, Ontario, Canada

2007

Your file Votre référence
ISBN: 978-0-494-62756-3
Our file Notre référence
ISBN: 978-0-494-62756-3

ABSTRACT

A one-dimensional computational fluid dynamics (CFD) model has been developed to simulate the exhaust flow and chemical reactions in the Diesel Oxidation Catalyst (DOC) and Diesel Particulate Filter (DPF) under different active flow schemes. Experiments have been carried out with the DPF and DOC units with a single cylinder diesel engine. Supplemental fuel has been delivered through the variations in exhaust gas temperatures by the supplemental exhaust gas heating. The thermal response analysis has been carried out on the basis of the simulation results of various active flow control schemes and the supplemental energy efficiencies for different active flow configurations has been compared. The theoretical and experimental analyses indicates that the active flow control schemes have fundamental advantages in optimizing the converter thermal management that includes reduced supplemental heating, increased thermal retention and recuperation, and improved overheating protection. Further investigations have been carried out to identify the energy efficient pathway to enable aftertreatment operation and to sustain conditions favourable to the aftertreatment operations without overheating.

DEDICATION

This work is dedicated to my parents Tapandeb Banerjee and Mallika Banerjee for their unconditional support throughout all my endeavours, to my late grandmother Gauri Banerjee for her love and encouragement. I would also like to dedicate this work to my wife Beeta Saha for her love and encouragement.

ACKNOWLEDGEMENTS

I would like to thank my supervisors, Dr. Ming Zheng and Dr. Graham T. Reader for their continued support and guidance throughout the course of this research work. Their wisdom and constant encouragement has given me the right passion to dedicate to the research and accomplish the best work that I can.

I would like to acknowledge Dr. Meiping Wang for her constant assistance and constructive criticism. I would also like to thank my colleagues Raj Kumar, Mwila Clarence Mulenga, Usman Asad, Yuyu Tan, Xiaoye Han, Richard (Suek-Jin) Ko, and William Bombardier at the Clean Diesel Engine Laboratory, for their help and assistance throughout my endeavours. I would also like to acknowledge Dr. Nihar Biswas for his encouragement to graduate research.

This research is partially sponsored by the Canada Research Chair Program, Ford Motor Company of Canada, Canada Foundation of Innovation, Ontario Innovation Trust, Natural Science and Engineering Research Council of Canada, AUTO 21 Network of Centers of Excellence and the University of Windsor.

LIST OF PUBLICATIONS

The following publication resulted from the research conducted during the course of this work:

1. Usman Asad, **Siddhartha Banerjee**, Graham T. Reader, Meiping Wang, Zing Zheng, "*Energy Efficiency Analysis Between In-Cylinder and External Supplemental Fuel Strategies*", Society of Automotive Engineers (SAE) Paper Number 2007-01-1125, SP – 2140, April 2007.
2. Graham T. Reader, **Siddhartha Banerjee**, Meiping Wang, Ming Zheng, "*Energy Efficiency Analysis of Active-flow Operations in Diesel Engine Aftertreatment*", Society of Automotive Engineers (SAE) Paper Number 2006-01-3286, 2006.
3. Xiaoye Han, Usman Asad, Raj Kumar, Mwila Clarence Mulenga, **Siddhartha Banerjee**, Meiping Wang, Graham T. Reader, Ming Zheng, "*Emperical Studies of Diesel Low Temperature Combustion on a Modern Diesel Engine*", Combustion Institute/ Canadian Section 2007 Spring Technical Meeting, University of Alberta, Canada.
4. Usman Asad, Ming Zheng, David S-K Ting, Raj Kumar, **Siddhartha Banerjee**, Graham T. Reader, Jimi Tjong, "*Real-time Heat Release Analysis towards On-fly Combustion Control for Diesel Engines*", Combustion Institute/ Canadian Section 2006 Spring Technical Meeting, University of Waterloo, Canada.

TABLE OF CONTENTS

LIST OF TABLES

LIST OF FIGURES

LIST OF APPENDICES

oxidation efficiency of NO reaches its maximum in the temperature range of 300 °C ~ 380 °C. However the NO conversion efficiency decreases at the temperatures above 380 °C.

The chemical reactions take place at a certain rate depending on the temperature, the reactant concentration (availability) and the presence of catalyst. In order to initiate chemical reaction in forward direction (from reactants to product formation), an energy is required to overcome the activation energy barrier. The activation energy for a particular reaction is the energy required to supply to the reaction site in order to successfully initiate the reaction in a certain direction. If a chemical reaction releases heat on formation of its product(s), it is called exothermic reaction. Therefore it is obvious that an exothermic reaction can in turn utilise part of the released heat energy to overcome its activation energy barrier and sustain reaction in a particular direction. All chemical reactions takes place in both the directions, that is the forward direction (from reactants to products formation) as well as the backward direction (from products to reactant formation). A chemical reaction is said to be exothermic reaction if the forward reaction is exothermic and the backward reaction is endothermic in nature. A chemical equilibrium is said to be reached if the of forward reaction rate becomes equal to the backward reaction rate. From the start of chemical reaction the forward reaction rate is higher than the backward reaction rate till the equilibrium is reached. In the DOC the combination of both chemical equilibrium and the mass transfer (diffusion) equilibrium acts together in order to achieve the steady state conditions. Diffusion of the exhaust species from gas to solid phase occurs at a rate depending on the temperature, and the

difference in the concentration of the exhaust species between two phases. The chemical reactions take place in the catalyst surface. The reactants are adsorbed and the products are desorbed back to the exhaust stream in the gaseous phase from the catalyst surfaces. The rate of adsorption for a particular reactant depends on the concentration of the reactant, the temperature of the catalyst and the availability of the catalyst surface. A reaction rate is commonly defined as the rate of decrease of reactants in a chemical reaction. Catalyst is defined as the substance that influences the reaction by lowering the activation energy barrier thereby increasing the reaction rate but otherwise remains unaffected from any chemical change. Without the catalyst in DOC, the chemical reactions cannot occur due to the low diesel exhaust temperature that is unable to overcome the activation energy barrier for the chemical reactions. The effectiveness of the catalyst lies in its ability to reduce the harmful pollutant gases due to reduction of the activation energy barrier and enhanced reaction rate at comparatively lower temperatures.

The catalysts are embedded in the washcoat of the DOC channel. The number of catalyst sites available in a DOC channel influences the easiness of occurance of the chemical reactions. The catalysts are dispersed into high surface area in order to maximize the number of active sites for the chemical reactions and to increase the surface area for diffusion. This is accomplished by carriers known as washcoat bonded in a stable substrate structure. The active catalyst sites dispersed into the surface of flow through honeycomb monolith channel is responsible for adsorption of the reactants and enhances the chemical reactions. Two most important properties of the catalysts are activity and selectivity. Activity refers to the catalyst's ability to enhance the reaction rate, and the

selectivity refers to the catalyst's ability to promote certain reactions over others. An example is selectivity of NO oxidation over sulphur dioxide (SO_2) oxidation [11].

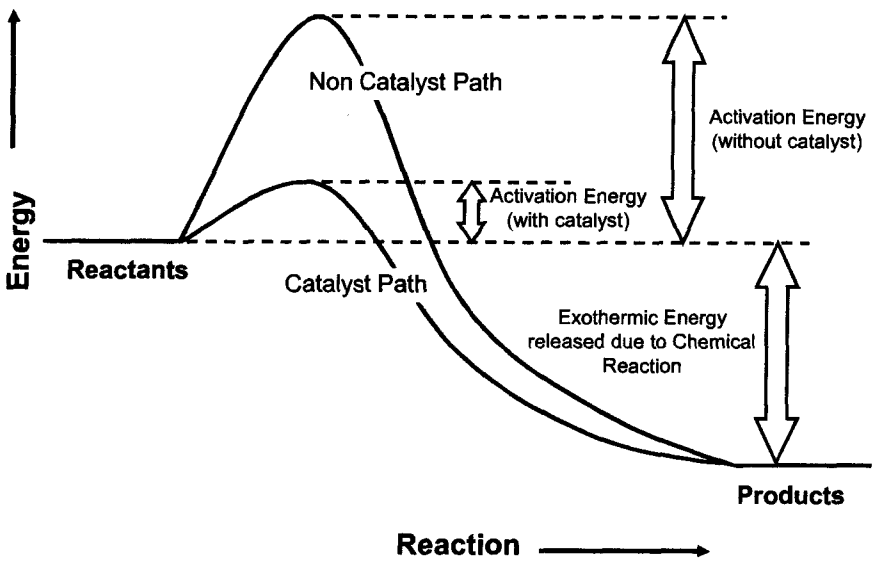

Figure 2-2: Effect of Catalyst in Chemical Reaction

The oxidation catalysts that are most commonly used for the diesel aftertreatment applications are an extruded ceramic honeycomb monolith made of cordierite. The operation principle of monolithic DOC involves both the physical (mass transfer of reactant species) and chemical (reaction kinetics of oxidation reaction at the site of catalyst) processes. The catalysts commonly used for the DOC applications are platinum (Pt), palladium (Pd) and Rhodium (Rh). The catalysts are loaded in a thin washcoat paper and embedded on the walls of honeycomb channels. Typically the DOC in automotive applications consists of approximately more than 10000 cells at 400 cells per square inch of frontal area. Generally catalyst loading ranges from 1 ~ 5 g/L of the substrate volume. The reactant gaseous species (CO and HC) diffuses from the gas phase to the solid

washcoat phase of the DOC channel. The reaction rate is commonly represented by arrhenious equations as a function of catalyst surface temperature.

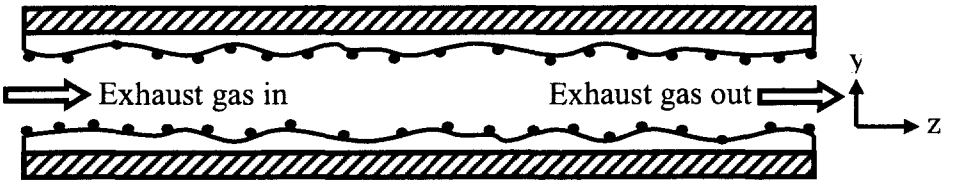

Figure 2-3: Single Channel of DOC

The conversion of the reactants in a DOC is a complicated phenomenon involving both physical mass transfer and chemical reaction kinetics. The conversion rate of a particular species is the minimum of the chemical reaction rate, pore diffusion rate and physical bulk mass transfer from the gas to solid phase. The chemical kinetics is the rate limiting factor at low temperatures (temperature below catalytic "light off"). As the temperature of the substrate increases, due to exponential relationship between chemical reaction rate and the temperature, the kinetics of chemical reaction becomes faster than physical mass transfer process. In the high temperatures (temperature above catalytic "light off") the pore diffusion and mass transfer become the rate limiting factor for the conversion efficiency of the DOC.

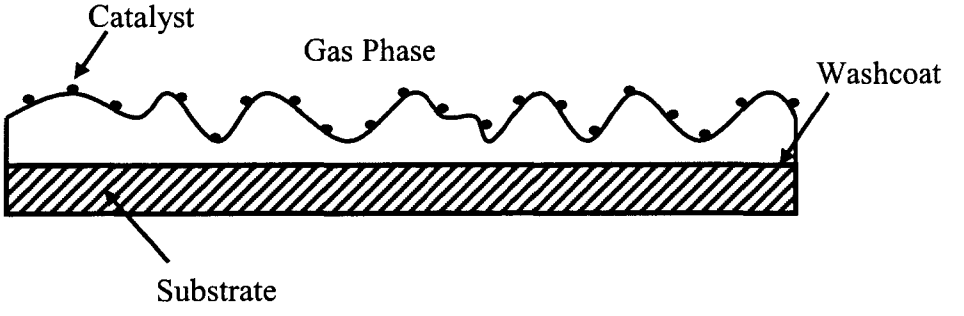

Figure 2-4: Representation of Catalyst Dispersed in Washcoat of DOC Channel

2.2. DIESEL PARTICULATE FILTER (DPF)

The Diesel Particulate Filter (DPF) is generally placed at the downstream of DOC that enables the physical removal of the suspended particulates matters (SPM) from the exhaust stream by filtration mechanism. In this research work the DPF design that is most commonly used for the diesel engine applications is considered. The DPF design in various diesel applications is a ceramic porous wall flow honeycomb structure made of cordierite. The SPMs are filtered due to the deep bed filtration of the raw exhaust gas during its passage through the porous ceramic substrate wall. The unfiltered exhaust gas enters the inlet channel of the DPF whose outer end is plugged. The exhaust gas flows through the wall of the porous substrate resulting in the physical separation of the solid particulates of diameter exceeding 10 nm. The filtered exhaust gas is then allowed to pass through the outlet as shown in the Figure 2-5.

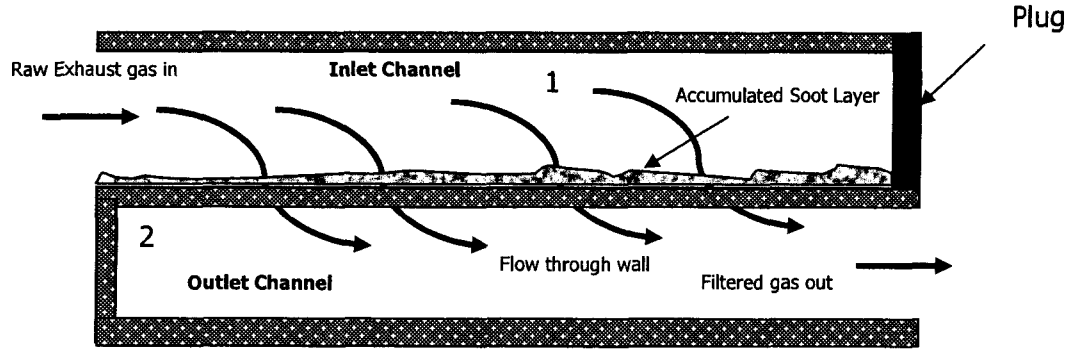

Figure 2-5: Single Channel of DPF

The PM over the period of time accumulates in the pores of the filter wall as well as the inner wall of the inlet channel as shown in the Figure 2-5. Over the period of filtration operation, the thickness of accumulated soot layer increases and eventually clogs the exhaust flow path. Moreover the accumulated soot layer in the inlet channel of the DPF

results in increased resistance of the exhaust flow through the soot layer and the clogged filter wall. This also leads to the increase of pressure drop across the DPF. Higher pressure drop across the DPF results in higher back pressure in the in-cylinder engine combustion process, therefore reducing significantly the engine power output and overall energy efficiency. Therefore it is required that the PMs accumulated inside the inlet channels be periodically removed by the regeneration process to keep the exhaust manifold pressure within the acceptable limits for lower energy penalty. The most convenient and common method for regeneration is to oxidize the accumulate soot in the presence of oxygen with sufficient high temperature to facilitate burning of the soot. The thermal regeneration process can be initiated either by the high substrate temperature or the high exhaust temperature.

In the wall flow DPFs the PMs are filtered from the exhaust gas by the combined effects of the deep bed filtration and cake filtration. In the deep bed filtration, the mean sizes of PMs are smaller than the mean pore size of the filter wall and in the cake filtration the mean particulate size is bigger than the mean pore diameter. There are different mechanisms for the filtration of PMs in the DPF. These are inertial impaction and interception, Brownian diffusion, gravitational settling, electrostatic attraction, thermophoresis and diffusiophoresis. For typical diesel exhausts, the particulate filtration is dominated by inertial deposition, flow-line interception and diffusion deposition [12]. Inertial deposition is the primary filtration mechanism for the particulates bigger than 1 μm. The particulates with larger mean diameters, have higher inertial mass and tend to deviate from the gas flow stream of the inlet channel. In this work for the mathematical

simplicity it is assumed that particulates will be deposited in the filter wall by inertial divergence of the particulate matter from the flow stream.

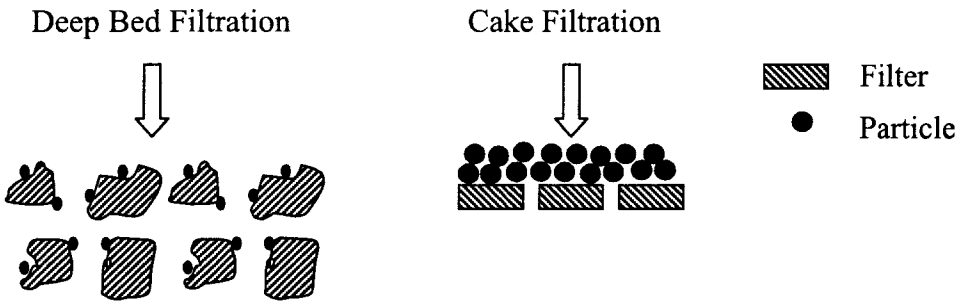

Figure 2-6: Filtration Mechanisms in DPF

The DPF regeneration is to effectively remove the soot from the inlet channel. In practical diesel engine operations, it is efficiently done by oxidising the PMs at a high temperature by oxidising agents present in the exhaust stream. The diesel engine exhaust temperature ranges between 150 ~ 350 °C for the light duty application and 300 ~ 400 °C for the heavy duty applications. These diesel exhaust temperatures are not able to impart required energy to initiate thermal regeneration. For the catalytic DPF, the regeneration takes place at the temperatures lower than the thermal regeneration conditions. This is because the regeneration activation energy is reduced by the participation of the catalysts in the reaction process. Due to difference in the energy required to initiate regeneration and the energy available in the diesel exhaust, there is a requirement for an additional external energy to the exhaust stream in order to enable DPF regeneration. One of the many ways to impart external energy is in the form of microwave heating of the inner walls of the DPF channels. Other commonly used method is to deliver fuel in the exhaust stream by the supplemental fuel addition or by in-cylinder post injection.

2.3. ACTIVE AND PASSIVE AFTERTREATMENT CONTROL

In an active flow-control aftertreatment system, an independent controller adaptively modifies the raw exhaust to the favourable conditions for efficient operation of aftertreatment devices. In a passive flow-control aftertreatment system, the engine tailors the raw exhaust to enable the aftertreatment operations. An exhaust aftertreatment system may use the active or passive flow control strategies. The essence of the active flow-control aftertreatment is to control the complex thermal and chemical processes of the exhaust species using a variety of gas flow configurations. In the active control system the initiation of the DPF regeneration is carried out by high temperature of the exhaust gas at the DPF inlet channel located at the downstream of the DOC. The active-flow control of the exhaust gases is capable of effectively improving the energy efficiency of the diesel aftertreatment systems [13, 14, 15, 16]. The theoretical analysis indicates that the active flow control schemes have fundamental advantages in optimizing the converter thermal management that includes reduced supplemental heating, increased thermal retention and recuperation, and improved overheating protection. The exhaust active-flow control schemes includes the parallel alternating flow, partial restricting flow, periodic flow reversal, and the extended flow stagnation. The external fuel injection is often proved to be more effective in rising the substrate temperature because of the direct fuel dispersion on the catalytic flow bed [2].

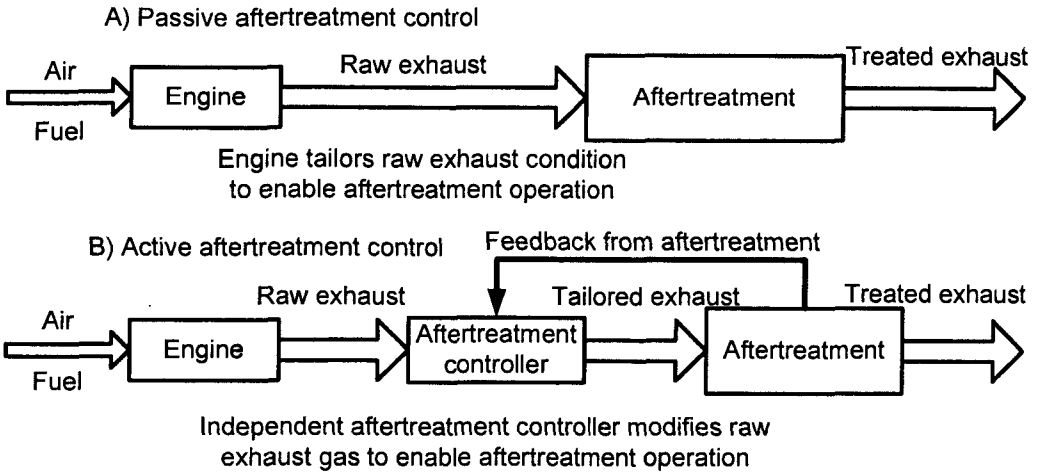

Figure 2-7: Passive versus Active Aftertreatment Control Strategies

There are different types of active flow control methods. In the automotive industry, the common practice is to use a passive aftertreatment system with an active engine fuel management control. However by periodically alternating the direction of the exhaust flow through the aftertreatment device, the heat retention capacity of the substrate is increased, which in turn helps in improving the thermal efficiency of the system. Due to the oscillation of thermal wave of the substrate temperature, the temperature in the central portion of the substrate can be retained higher than the boundary temperatures during the cooling of the substrate by the exhaust gas. In a non flow reversal (NFR) system the thermal wave sweeps through the substrate and cools down the substrate progressively with time due to convection heat transfer between the hot substrate and cold exhaust gas as shown in the Figure 2-9 and Figure 2-10. Therefore in non flow reversal setup the substrate is not capable of retaining the substrate temperature above the catalytic light-off for DOC or regeneration condition for DPF for longer period of time. In the flow reversal (FR) system, the central portion temperature of the substrate is not cooled down as quickly as the NFR system. The temperature of the central portion is retained higher than

the catalytic "light off" limit for DOC or regeneration condition for DPF as shown in the Figure 2-11 and Figure 2-12. Therefore the FR operation helps to retain the thermal energy thereby enabling the aftertreatment operations. The FR operation in practical application can be carried out by installing a 4 way valve which alters the flow direction periodically as shown [3].

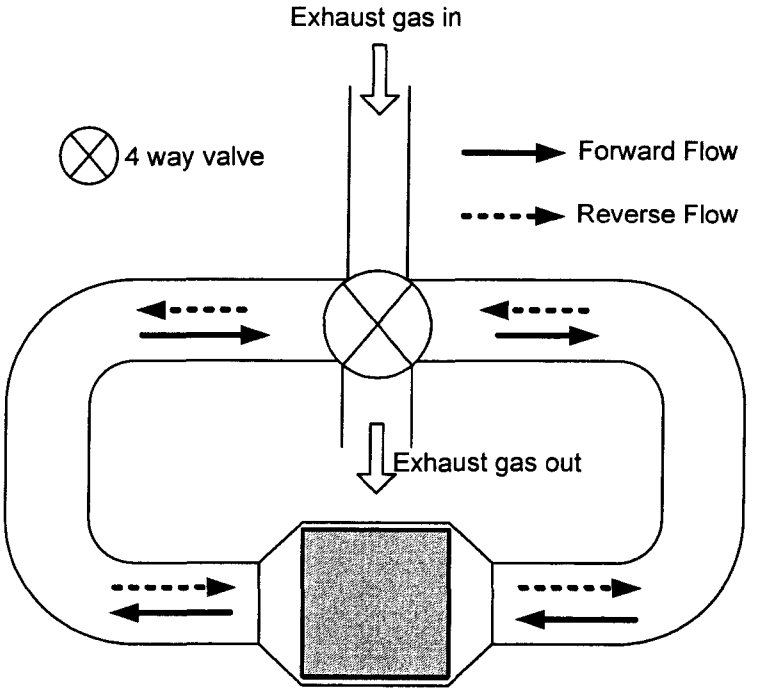

Figure 2-8: Flow Reversal Operation

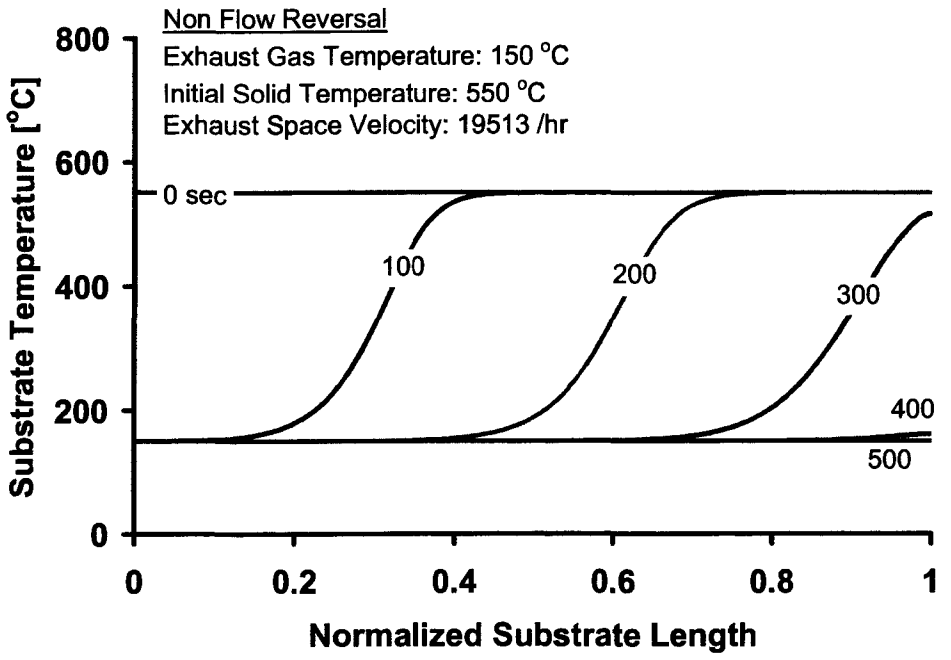

Figure 2-9: NFR Solid Temperature Profile (Cooling Process)

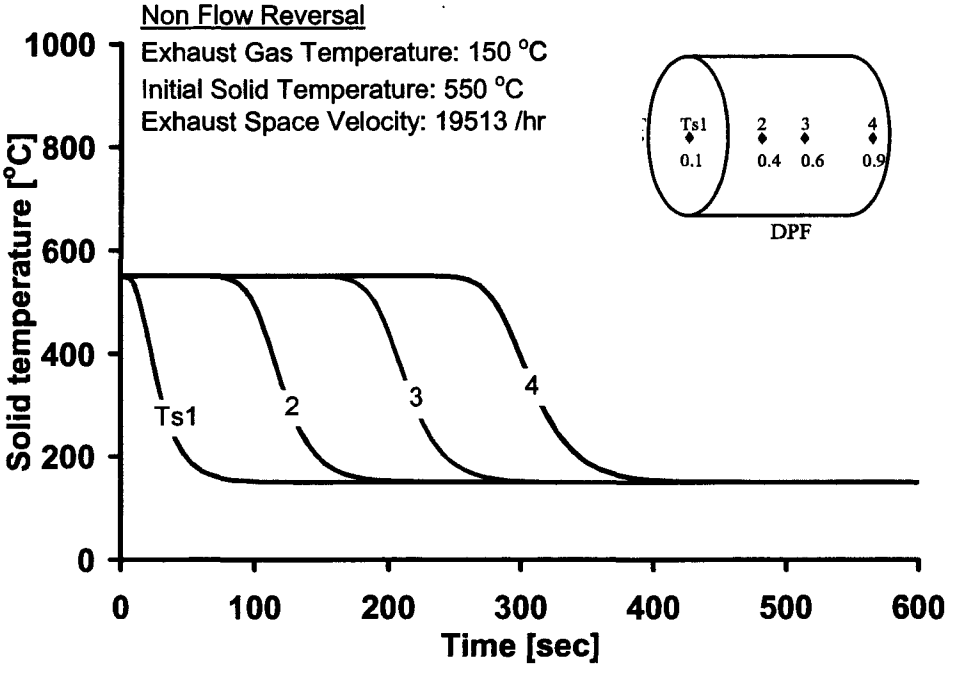

Figure 2-10: NFR Temperature Response (Cooling Process)

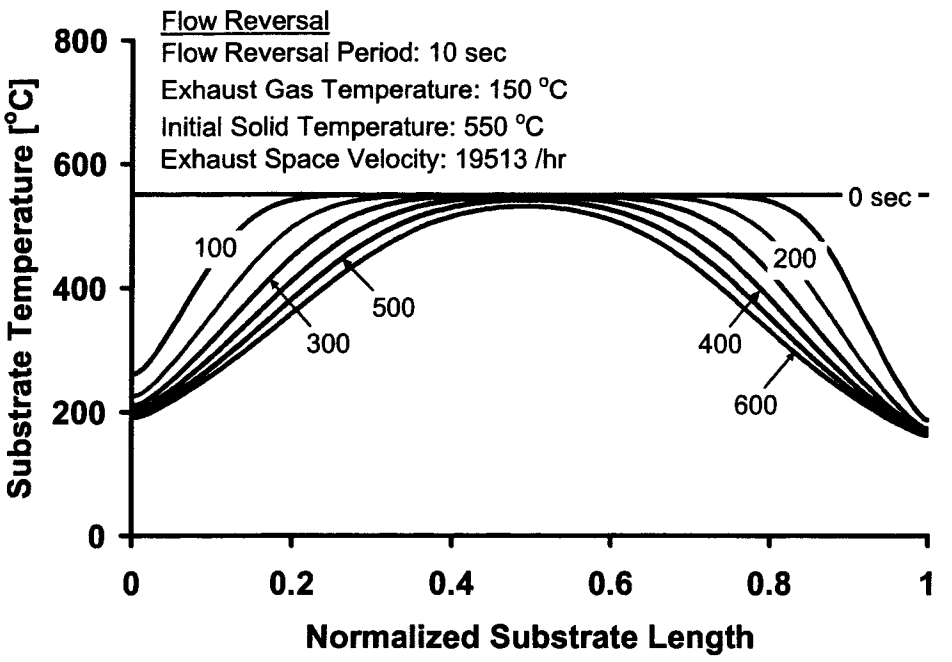

Figure 2-11: FR Solid Temperature Profile (Cooling Process)

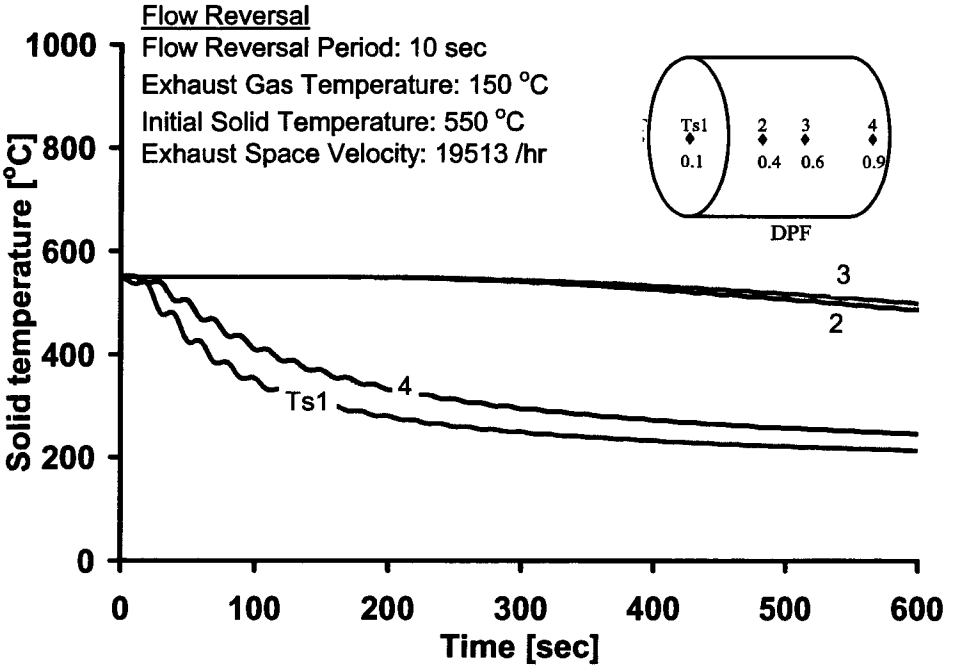

Figure 2-12: FR Temperature Response (Cooling Process)

The FR operation therefore helps in saving supplemental energy to keep aftertreatment in operable condition when the diesel exhaust temperature is well below the temperature required for the proper functioning of the aftertreatment. The cold thermal boundary is defined as the portion of substrate where the substrate temperature is below the temperature for the effective operations of aftertreatment and the hot core is defined as the portion of the substrate where the temperature is higher than the temperature for the effective operations of aftertreatment. In FR process the rate of growth of cold thermal boundary is much slower than the NFR reversal process as shown in the APPENDIX C. Space velocity is defined as the ratio of exhaust velocity to the substrate length.

An active flow control technique that arranges the exhaust flow through two or more parallel aftertreatment devices with differential flow rates is commonly referred as the parallel flow (PR) system. A PR system with DOC-DPF units operates in alternating cycles of filtration and regeneration. An active regeneration using external supplemental energy is more energy efficient with low space velocities, when the exhaust temperature is below the threashold limit for the aftertreatment operations. By sharing the operating cycle with other parallel devices the PR operation can effectively reduce the supplemental energy consumption to successfully carry out active regeneration [13]. For energy efficient operations the PR switches between different modes as shown in the Table 2-1. Different modes of flow control are made based on the requirements of the regeneration. Generally mode 1 operation is stayed over longer period of time as the rate of filtration is slower than the rate of regeneration. The flow control valve is placed in

order to control the flow distribution during various modes of PR operation as shown in the Figure 2-13. The PR operates in sequence from mode 1 to 5.

Table 2-1: Sequence of PR Operation

Mode	Injector		Flow Distribution		Operation	
	Loop 1	Loop 2	Loop 1 (%)	Loop 2 (%)	Loop 1	Loop 2
1	OFF	OFF	50	50	Filtration	Filtration
2	ON	OFF	10	90	Regeneration	Filtration
3	OFF	OFF	0	100	Stagnation	Filtration
4	OFF	ON	90	10	Filtration	Regeneration
5	OFF	OFF	100	0	Filtration	Stagnation

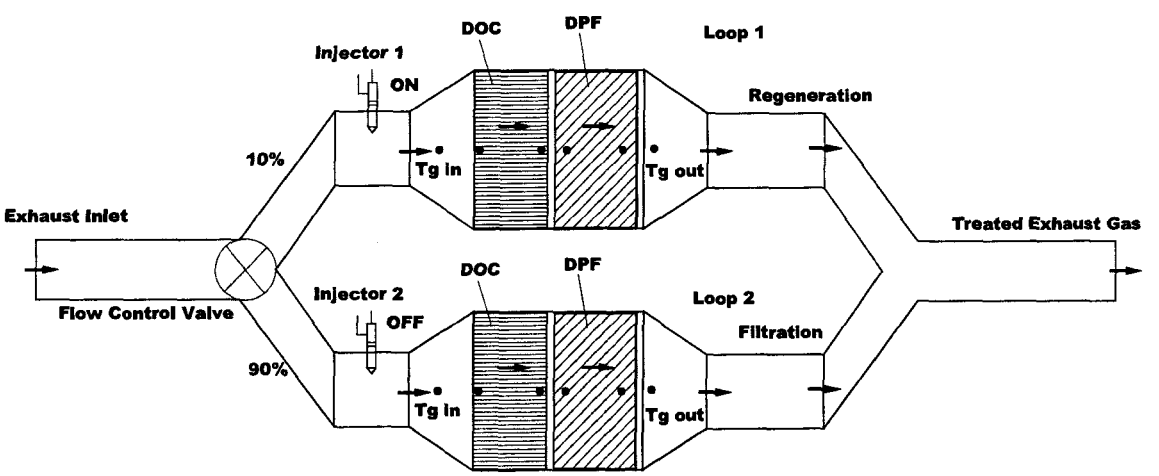

Figure 2-13: Parallel Flow Operation (Mode 2)

CHAPTER III

3. DESIGN AND METHODOLOGY

A one dimensional numerical simulation model has been developed considering single channel of the monolith structure. The DOC and DPF are represented each by a single channel assuming no radial variations of the flow velocity and temperature at the inlet. The primary objective of the model is to carry out transient thermal response simulation of the exhaust gas and the substrate wall. The model accounts for the convective heat transfer between the solid and the gas phase, conductive heat transfer from high temperature to low temperature region through substrate. The effect of thermal radiation from the substrate wall to the surroundings is not considered. The transfer of heat and mass across the channels are not considered in the model due to its intrinsic nature of simulation in the one dimension along the direction of flow.

A FORTRAN program is written to simulate the DOC-DPF system. The program is written with user friendly interface. A brief summary of the simulation program is given in the Figure 3-1. The simulation is carried out in the three broad steps namely pre-processing, simulation run and post-processing. Pre-processing consists of defining the simulation conditions such as initial and boundary conditions, calibration parameters such as the reaction kinetics parameters and property definition of the exhaust gas and substrate material. The program pre checks the validity of the input data before the start of the simulation. The post-processing includes writing the output data in a desired format such that the results can be imported to an MS-EXCEL® template to generate meaningful plots for further analysis.

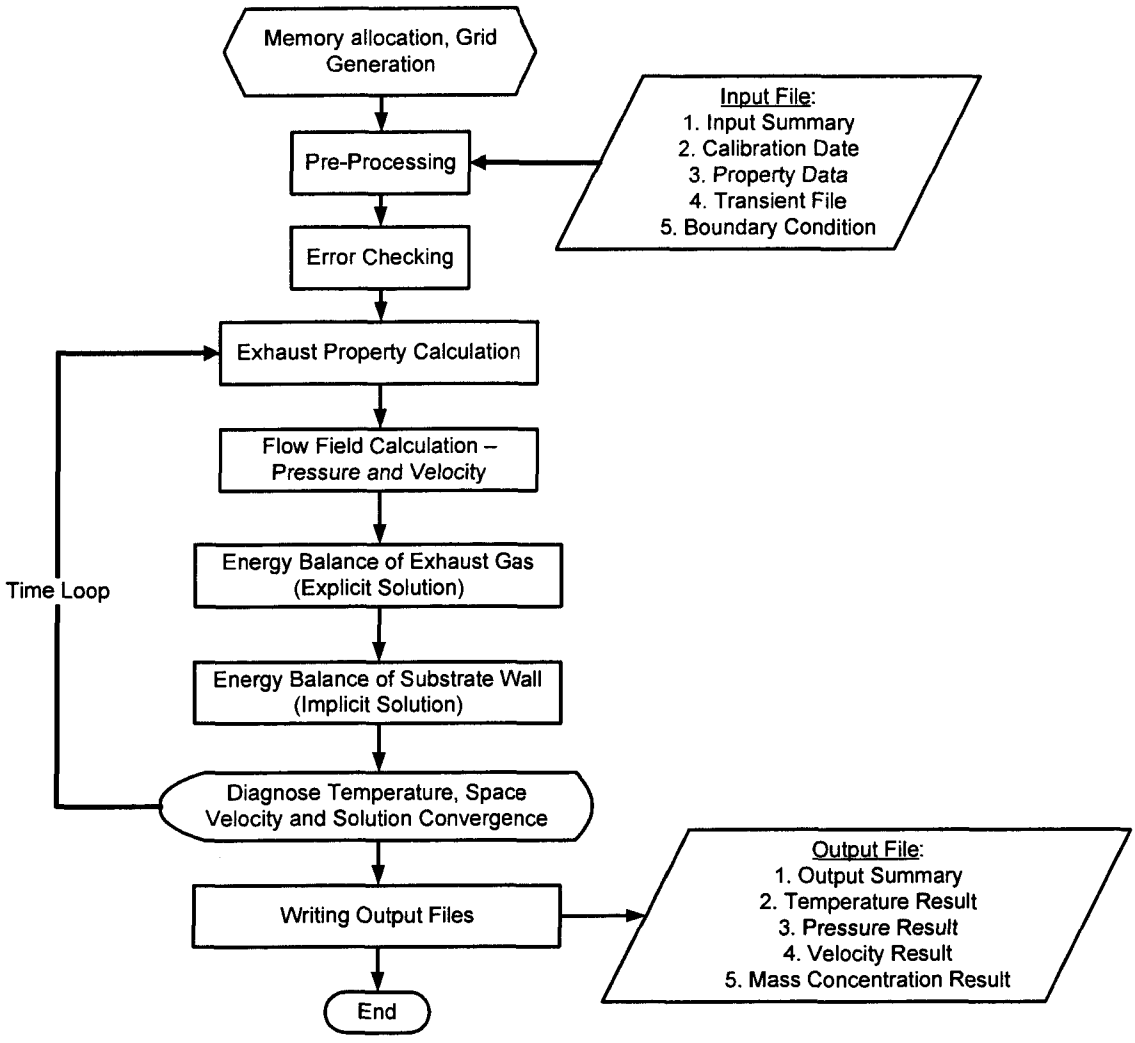

Figure 3-1: Simulation Data Flow

3.1. DOC MODEL

The primary assumptions of the DOC model are:

- The diffusion of exhaust gas species along the direction of exhaust flow is neglected due to gas phase bulk mass transfer.
- The gas phase heat conduction is neglected due to bulk mass transfer.
- The free convection heat transfer between gaseous phase and the substrate wall is neglected due to the dominance of forced convection.

- The gas phase chemical reactions are not considered due to the dominance of catalyst's participation in the reaction.
- The temporal heat and mass transfer in the gaseous phase are neglected assuming quasi-steady condition.
- The exhaust gas properties are considered as a function of bulk gas temperature only.
- The radiation heat transfer between the substrate wall and the surroundings are neglected.
- The exhaust gas is assumed to follow ideal gas behavior.
- The effects of turbulence inside the channels are neglected due to low reynold's number of exhaust gas inside the substrate channels.
- The compressibility of exhaust gas is not considered due to low operating pressures in the substrate channels.
- The entrance and exit losses in pressure are not considered for the simplicity of mathematical model.
- The exhaust gas flow is assumed to be laminar in nature due to low reynold's number.
- The channel hydraulic friction is not considered due to negligible effect of momentum transfer in the DOC channel.
- Propylene (C_3H_6) is chosen to represent the THC in the exhaust gas.

The chemical reactions taking into account for the model are:

$$CO + \frac{1}{2}O_2 \rightarrow CO_2 \tag{3.1}$$

$$C_3H_6 + \frac{9}{2}O_2 \rightarrow 3CO_2 + 3H_2O \tag{3.2}$$

$$NO + \frac{1}{2}O_2 \rightarrow NO_2 \tag{3.3}$$

The reaction rate constants k_s for different reactions are taken as an Arrhenious function of the temperature and the activation energy as given in equation (3.4). The activity factor represented by G_i is given in equation (3.5) is a mathematical representation of the catalyst performance at various temperature of the embedded solid substrate. The reaction rate given by equation (3.6) considers the chemical kinetics, the availability of reactant species, the activity factor of the catalyst and the catalyst loading in the DOC washcoat.

$$k_{s,i} = A_{s,i}\, e^{\left(-E_i/RT_s\right)} \qquad i = CO, HC, NO \tag{3.4}$$

$$G_i = \frac{1}{1 + k_{1i}\, e^{(T_s - k_{2i})/k_{3i}}} \qquad i = CO, HC, NO \tag{3.5}$$

$$r_i = k_{s,i}\, \sigma\, G_i\, Y_{s,O_2} / \left(\alpha_i\, Y_{s,i}\right) \quad i = CO, HC, NO \tag{3.6}$$

where, $\alpha_{CO} = 0.5$, $\alpha_{HC} = 4.5$, $\alpha_{NO} = 0.5$ respectively and σ indicates the catalyst loading in the DOC washcoat. The rate of reaction of O_2 in the DOC channel is given by the equation (3.7).

$$r_{O_2} = \alpha_{CO}\, r_{CO} + \alpha_{HC}\, r_{HC} + \alpha_{NO}\, r_{NO} \tag{3.7}$$

The mass balance of the exhaust gas in the DOC channel is written in the partial differential form in the equation (3.8).

$$\frac{d\left(\rho_g u_z\right)}{dz} = 0 \tag{3.8}$$

The mass balance of the gas phase exhaust species is given by the equation (3.9).

$$SVF\,\frac{\partial Y_i}{\partial t} = -SVF\,u_z\,\frac{\partial Y_i}{\partial z} - \sigma\,k_{a,i}\,SSF\,\left(Y_i - Y_{s,i}\right) \quad i = CO, HC, NO, O_2 \tag{3.9}$$

where, ***SVF*** denotes the specific volume fraction of the gaseous phase and ***SSF*** denotes the specific surface area fraction between solid and gaseous phase over the total volume of DOC denoted by V_{DOC} in the equations (3.10), (3.11), (3.12). In other words, ***SVF*** represents the specific volume fraction of void space and ***SSF*** represents the specific surface area of monolith as a fraction of total volume of DOC. From the principle of gas phase exhaust species balance the equation (3.9) is derived. During the quasi-steady state, the accumulation of exhaust species inside the control volume is neglected and therefore the transient term becomes negligible.

$$V_{DOC} = \frac{\pi D^2}{4} L \tag{3.10}$$

$$SVF = \frac{N_c\,d^2 L}{V_{DOC}} = \frac{N_c\,d^2 L}{\frac{\pi D^2}{4} L} = 4N_c\left(\frac{d^2}{\pi D^2}\right) \tag{3.11}$$

$$SSF = \frac{A_{total}}{V_{DOC}} = \frac{N_c\,d^2\,L}{\frac{\pi D^2}{4} L} = 16N_c\left(\frac{d}{\pi D^2}\right) \tag{3.12}$$

where A_{total} represents the total surface area of the interface between the solid phase and the gaseous phase. From the equations (3.11) and (3.12) a relationship is established between ***SSF*** and ***SVF*** as given by the equation (3.13).

$$SSF = \frac{4}{d}\,SVF \tag{3.13}$$

The ratio between ***SSF*** and ***SVF*** remains unchanged between any variations of the thermal boundary layer shapes between the exhaust gas and the wall surface, and only depends on the size of the channel cross section. This proves that the model takes care of

any variations in the channel shapes and design. ***SVF*** can also be derived as a function of hydraulic diameter of the channel and the wall thickness as shown the equation (3.14).

$$SVF = \left(\frac{d}{d + w_s} \right)^2 \tag{3.14}$$

The exhaust species balance in the solid phase is dependent on the rate of mass diffusion, rate of catalyst surface adsorption and the rate of disappearance due to chemical reaction. Therefore the mathematical representation of species concentration embedded in the catalyst surface includes all the above mentioned factors. Assuming quasi steady state of the exhaust balance in the solid phase the rate of disappearance of reactant species is equal to the rate of adsorption of the species from the gaseous phase. The net rate of reaction is therefore controlled by the chemical kinetics when the rate of adsorption is higher than the rate of chemical reaction - the condition occurs mostly in the temperatures below "light off". However in the temperatures above catalytic "light off", the rate of diffusion controls the rate of reaction because, at these temperatures the rate of reaction is higher and therefore the reaction is mostly controlled by the availability of the reactant constituents.

$$\sigma \, k_{a,i} \left(Y_{s,i} - Y_i \right) + r_i = 0 \qquad i = CO, HC, NO, O_2 \tag{3.15}$$

The conservation of mass of exhaust gas for one dimensional DOC channel is given by the following equation.

$$\frac{\partial \rho_g}{\partial t} + \frac{\partial \left(\rho_g u_z \right)}{\partial z} = 0 \tag{3.16}$$

Assuming steady state laminar flow process of the exhaust gas flow inside the DOC channel, the transient term of the equation (3.16) is neglected.

The overall mass transfer model of DOC is briefly summarized in the Figure 3-2.

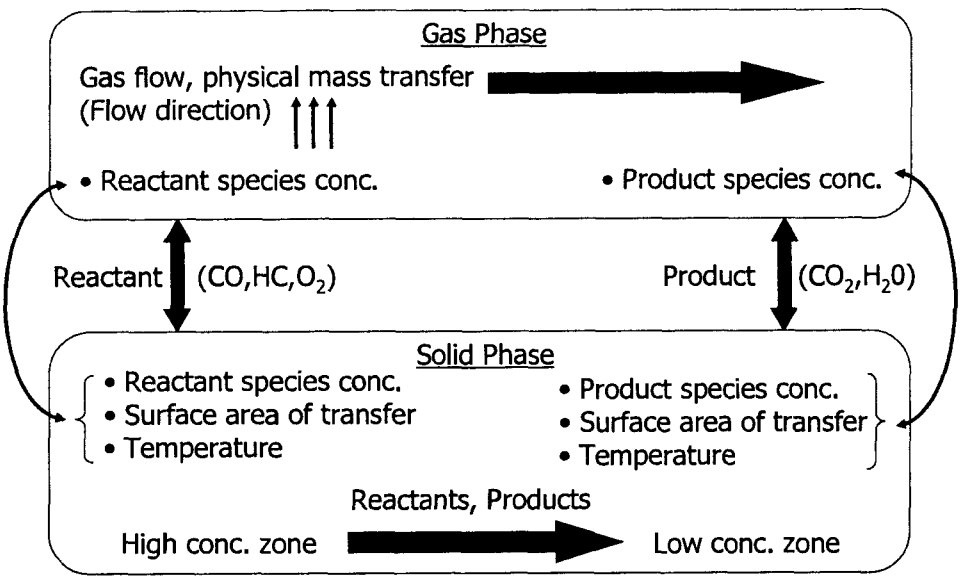

Figure 3-2: Mass Transfer Model of DOC

The gaseous phase energy balance is given by the equation (3.15) and the solid phase energy balance is given by the equation (3.16).

$$SVF\, c_{p,g}\left(\frac{1}{\gamma_g}\frac{\partial(\rho_g T_g)}{\partial t}+\frac{\partial(\rho_g u_z T_g)}{\partial z}\right)+SSF\, h\,(T_g-T_s)=0 \tag{3.17}$$

A typical space velocity of the exhaust gas through the DOC during normal operations is 48000 /h. This signifies that the channels inside DOC will be refreshed with new charge of exhaust gas more than 13 times the volume of DOC channel per second of operation. Therefore the exhaust flow inside the DOC is assumed to be a quasi-steady process due to its short residence time inside the channel. Therefore the temporal term of the equation (3.17) can be neglected.

$$SVF\, c_{p,g}\frac{\partial(\rho_g u_z T_g)}{\partial z}+SSF\, h\,(T_g-T_s)=0 \tag{3.18}$$

The energy balance of the solid substrate due to heat transfer between the solid and the gas phase due to convection and heat transfer inside the solid wall due to conduction and the heat generation due to the exothermic heat release from the oxidation reactions are considered.

$$(1-SVF)\rho_s c_{p,s}\frac{\partial T_s}{\partial t}= \lambda_s(1-SVF)\frac{\partial^2 T_s}{\partial z^2}-h\ SSF\ (T_s-T_g)+SSF\sum_{i=1}^{3}(\Delta H_i)\,r_i \tag{3.19}$$

where, convective heat transfer coefficient is a function of hydraulic diameter of the channel, conductive heat transfer coefficient of the exhaust gas as given by the equation (3.20).

$$h=\frac{Nu\,d}{\lambda_g},\qquad \gamma_g=\frac{c_{p,g}}{c_{v,g}} \tag{3.20}$$

The overall energy balance model of DOC is briefly summarized in the Figure 3-3.

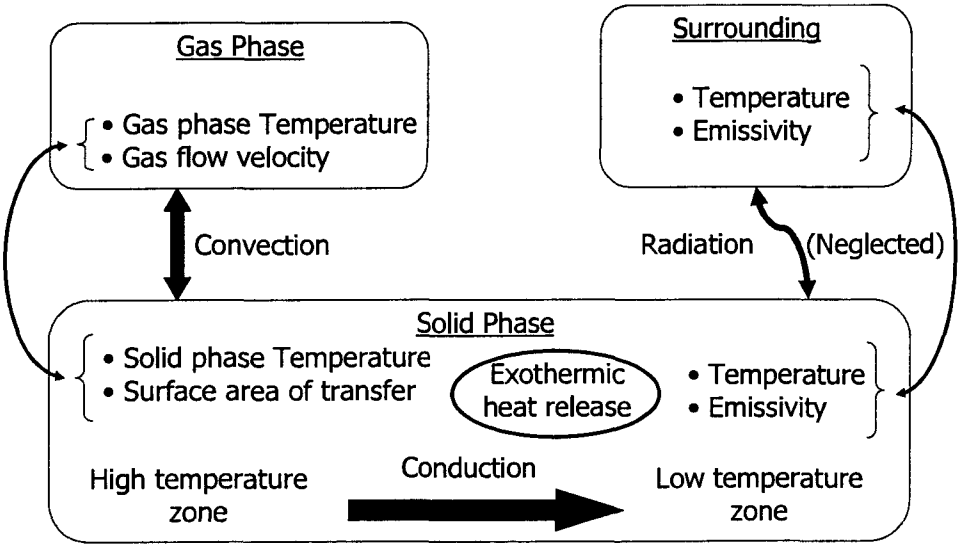

Figure 3-3: Energy Transfer Model of DOC

The inlet boundary conditions of DOC for the exhaust gas temperature and species concentration is given by:

$$Y_i(t,0)=Y_{i,in},\ T_g(t,0)=T_{g,in} \tag{3.21}$$

Neglecing any heat transfers between the substrate and the surroundings, the substrate temperature gradients along the channel length at the inlet and outlet boundaries are neglected.

$$\frac{\partial T_s(t,0)}{\partial z}=\frac{\partial T_s(t,L)}{\partial z}=0 \tag{3.22}$$

where, $z = 0$ represents inlet and $z = L$ represents outlet of the DOC channel.

The substrate temperature profile is initialized with a known value as shown below:

$$T_s(0,z)=T_{s,0}(z) \tag{3.23}$$

3.2. DPF MODEL

The primary assumptions of DPF model remains same as of DOC model except that the viscous friction is considered between the exhaust gas and the channel wall. The chemical reactions in the DPF regeneration model are represented as a one step global reaction given by the equations (3.24) and (3.25).

$$C+\alpha_1 O_2 \rightarrow 2\left(\alpha_1-\frac{1}{2}\right)CO_2+2(1-\alpha_1)CO \tag{3.24}$$

$$C+\alpha_2 NO_2 \rightarrow \alpha_2 NO+(\alpha_2-1)CO_2+(2-\alpha_2)CO \tag{3.25}$$

The terms α_1 and α_2 are the coefficients of chemical selectivity for the reactions of carbon particulate matter with O_2 and NO_2 respectively. The chemical selectivity coefficients are dependent on the reaction rates of respective chemical reactions. In the Catalytic Diesel Particulate Filter (CDPF), the reaction rate of particulate oxidation with oxygen is

enhanced and therefore the chemical selectivity of the carbon oxidation with the available oxygen increases. The selectivity coefficient is given by the equation (3.26).

$$\alpha_1 = 1 - \frac{f_{CO}}{2},\ \alpha_2 = 2 - g_{CO} \tag{3.26}$$

where, f_{CO} and g_{CO} are the selectivity coefficient of CO formation from the soot oxidation by O_2 and NO_2 respectively.

$$f_{CO} = \frac{1}{1 + p_{f1} Y_{O_2}^{\mu_1} \cdot e^{E_{f1}/RT}},$$
$$g_{CO} = \frac{1}{1 + p_{f2} Y_{O_2}^{\mu_2} \cdot e^{E_{f2}/RT}} \tag{3.27}$$

The chemical reaction rate constants are given by:

$$k_{f,1} = A_{f,1}\ e^{\left(-E_1/RT_s\right)},$$
$$k_{f,2} = A_{f,2}\ e^{\left(-E_2/RT_s\right)} \tag{3.28}$$

The rates of reaction are dependent on the available reactant concentrations and therefore represented by:

$$r_{f,1} = k_{f,1}\, Y_{O_2}^{\alpha_1},$$
$$r_{f,2} = k_{f,2}\ Y_{NO_2}^{\alpha_2} \tag{3.29}$$

The control volume is such chosen that only the one dimensional fluid flow and flow through the filter wall from the inlet to the outlet channel is considered. This is also how the overall radial variations in the flow field calculations and the energy balance are neglected. The control volumes of inlet and outlet channels are chosen so that interactions between only adjacent channels are considered for the one dimensional model.

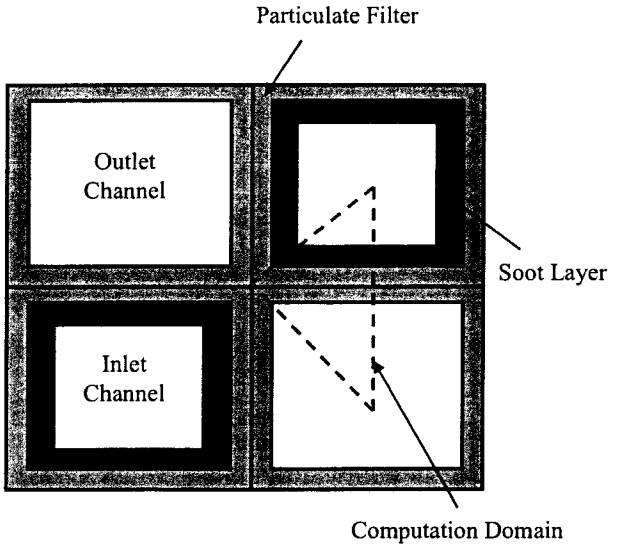

Figure 3-4: Cross Section of Loaded DPF Channels and Computational Domain

The mass, the momentum and the energy balance equations are separately solved between the inlet and the outlet channels. The entire DPF channel is discretised into numerous small control volumes to solve the partial differential equations (PDE) individually for all the control volumes throughout the length of the DPF channel.

The mass transfer of exhaust gas for the inlet and outlet channels is given by the equations (3.30) and (3.31) respectively.

$$\frac{\partial}{\partial z}(\rho_1 u_1) = -\frac{4}{D_1}\rho_w v_w \tag{3.30}$$

$$\frac{\partial}{\partial z}(\rho_2 u_2) = \frac{4}{D_2}\rho_w v_w \tag{3.31}$$

The momentum balance of the exhaust gas in the inlet and outlet channels of the DPF is given by the equations (3.32) and (3.33) respectively. It is assumed that the axial momentum is affected by the change in velocity magnitude and the friction between the exhaust gas and the filter wall.

$$\frac{\partial p_1}{\partial z} + \frac{\partial}{\partial z}\left(\rho_1 u_1^2\right) = -\frac{F}{D_1^2}\mu\, u_1 \tag{3.32}$$

$$\frac{\partial p_2}{\partial z} + \frac{\partial}{\partial z}\left(\rho_2 u_2^2\right) = -\frac{F}{D_2^2}\mu\, u_2 \tag{3.33}$$

The pressure velocity coupling is solved by using Semi-Implicit Pressure Linked Equations between p_1, p_2, u_1 and u_2. The pressure drop across the filter wall between the inlet and the outlet channels is given by Darcy's Law. The law states that the pressure drop across the filter wall is dependent on the wall flow velocity, the thickness of wall consisting of the filter wall and the soot cake and their permeabilities. The dynamic viscosity of the exhaust gas is a temperature dependent variable that contributes to the pressure drop across the wall. It is assumed that the exhaust gas viscosity is a function of the wall temperature. The solid temperature is assumed to be uniform throughout the thickness of the particulate cake and the filter wall.

$$p_1 - p_2 = \frac{\mu}{\kappa_p} v_w w_p + \frac{\mu}{\kappa_s} v_w w_s \tag{3.34}$$

The entire DPF channel is discretised into numbers of small control volumes. The vector terms, such as velocity are defined at the inlet and the outlet faces of the control volumes and the scalar terms, such as pressure, temperature are defined at the nodes of control volumes. This is a staggered grid arrangement to simplify the discritisation of the partial differential equations for pressure – velocity coupling.

The energy balance of the exhaust gas in the inlet and outlet channels of the DPF is given by the following partial differential equations (3.35) and (3.36) respectively.

The energy balance of the exhaust gas in the inlet and outlet channels is due to the net heat flux to the control volume, and the heat transfer to the substrate wall by convection.

$$c_{p_g}\rho_1 u_1 \frac{\partial T_1}{\partial z} = \frac{4}{D} h_1 (T_s - T_1) - \frac{4}{D}\rho_{gw} v_w c_{pgw} T_s \tag{3.35}$$

$$c_{p_g}\rho_2 u_2 \frac{\partial T_2}{\partial z} = \frac{4}{D} h_2 (T_s - T_2) + \frac{4}{D}\rho_{gw} v_w c_{pgw} T_s \tag{3.36}$$

The energy balance of the substrate wall is considered by taking into account the convection heat transfer between the substrate and the exhaust gas at the inlet and the outlet channels, conduction heat transfer in the solid phase and the heat generation due to the exothermic soot oxidation. The solid phase in a loaded DPF channel is composed of the substrate and the soot cake. But the model assumes uniform solid temperature across the exhaust flow throughout the thickness of the soot cake layer and the solid substrate layer within a control volume remains same.

$$\begin{aligned}\frac{\partial}{\partial t}\left(\left(\rho_s c_{p,s} w_s + \rho_p c_{p,p} w_p\right) T_s\right) = \\ h_1 (T_1 - T_s) + h_2 (T_2 - T_s) - \lambda_p \frac{\partial}{\partial z}\left(w_p \frac{\partial T_s}{\partial z}\right) - \lambda_s w_s \frac{\partial^2 T_s}{\partial z^2} + \dot{q}_s\end{aligned} \tag{3.37}$$

With the mass, the axial momentum and the energy balance equations for the inlet and outlet channels of DPF, the flow field can be solved by numerical methods. The pressure drop is greatly influenced by the filtration and the oxidation of the accumulated soot cake in the DPF inlet channel. Therefore it is important to calculate the soot cake thickness in order to determine the pressure drop from the flow field calculation.

The convective effects such as diffusion mass transfer dominate the species transport in the porous wall and the soot cake [17]. The chemical reactions in the gas phase are neglected due to its short residence time inside the DPF channel. The molar concentration of the reactant species like O_2 and NO_2 inside the DPF channel is assumed to be constant throughout the channel length for simplicity of calculation.

The conservation of the species can be expressed in terms of the molar concentrations of the reactant species and the rate of reaction in the embedded reaction sites. The total time derivative of the reactant species concentration is the sum of partial derivatives with respective to time and distance across the flow (i.e. distance along the particulate reaction site).

$$\frac{D(Y_k)}{Dt} = \frac{\partial([Y_k])}{\partial t} + \frac{\partial([Y_k]\, v_w)}{\partial y} \qquad k = O_2, NO_2 \tag{3.38}$$

From the equation (3.38), it is seen that the time rate of change of molar concentration of reactants is governed by the balance between convective transport across the wall (y direction) and the chemical kinetics of the particulate oxidation. It is assumed that the chemical reactions are limited to its kinetics due to the extremely small reaction passage through the porous particulate filter layer. Experimental investigations by various researchers confirms that diffusion mass transfer rates are two orders of magnitude higher than the chemical reaction rates at the range of operating DPF regeneration temperatures (450 °C ~ 1400 °C) [18, 19, 20].

Assuming the order of oxidation reaction as α_k, the conservation equation of the reactant mole fractions are given by the steady state conditions for the overall rate of species accumulation. Equating the total time derivative of the reactant species concentration to zero the reactant species concentration equation can be written as:

$$\frac{\partial(\rho_{gw} Y_k)}{\partial t} = -\frac{\partial(\rho_{gw} Y_k v_w)}{\partial y} = -k_{k,j}\, \rho_{gw}\, \alpha_k\, Y_k \tag{3.39}$$
$$where, k_{k,j} = A_{k,j}\, T_s\, e^{(-E_j/RT_s)}$$

The local reaction rate of particulate oxidation is represented by the modified Arrehenious form that is dependent on the temperature of the reaction site and the

activation energy. The activation energy E_j varies between different sites of reactions such as the thermal, the catalytic and the soot cake is represented by the subscript $_j$. It is assumed that the thermal reaction site is embedded inside the porous particulate filter wall.

Assuming quasi steady state of reaction, the transient term of the equation (3.39) is neglected. Therefore the molar balance of the exhaust gas species across the DPF channel (y direction) is given by:

$$\frac{\partial}{\partial y}\left(\rho_{gw}\, v_w\, Y_k\right) = -k_{k,j}\, \rho_{gw}\, Y_k\, \alpha_k \tag{3.40}$$

The rate of O_2 or NO_2 depletion per unit wall surface area can be obtained by rearranging and integrating the equation (3.40) across the wall thickness.

$$R_k = \int_{y=0}^{w} s_j\, k_{k,j}\, \rho_{gw}\, Y_k\, dy \tag{3.41}$$

where, s_j is the specific surface area of soot particulate [21]. Therefore smaller the size of soot, greater will be the surface area of soot oxidation for a given mass of soot loading in a DPF channel. This will lead to a higher rate of oxidation with higher specific surface area of oxidation.

Solving the integration of the equations (3.40) and (3.41) with the boundary conditions, $y = 0$, $Y_i = Y_{i,in}$:

$$R_k = \frac{s_j \rho_{gw} v_w}{\alpha_k} Y_i \left(1 - e^{\left(-k_{k,j}\alpha_k w / v_w\right)}\right) \tag{3.42}$$

The soot layer depletion rate during the regeneration process is a mathematical product of the rate of oxidation reaction and the order of reaction. The overall rate of change of soot cake thickness is given by:

$$\rho_p \frac{\partial w_p}{\partial t} = -\sum_k \left(\frac{M_C}{M_k} \right) R_k + \dot{w}_{accum} \tag{3.43}$$

The particulate mass balance is solved numerically from the above equations to predict the soot depletion rate and the energy released due to oxidation. In the two layer model developed by Konstandopoulos *et al*, the particulate layer thickness is divided into the thermal layer and catalytic layer [19]. A similar model treatment of the soot oxidation phenomenon is adopted to estimate soot oxidation embedded inside the porous filter walls. The filtration and the accumulation mechanism of the exhaust particulate are modeled and integrated with the regeneration model in order to simulate simultaneous regeneration and accumulation.

The particulates are initially deposited in the porous filter wall by Brownian diffusion and direct and interception called as deep bed filtration. But as soon as the porous filter wall is saturated with the accumulated soot, the particulate matter starts accumulating over the filter wall to form soot cake inside the wall of the inlet channel. In the following simulations the accumulation mechanism is modeled based on the assumption that the soot deposition is dependent on the flow field of the exhaust gas at the inlet channel and the filter wall.

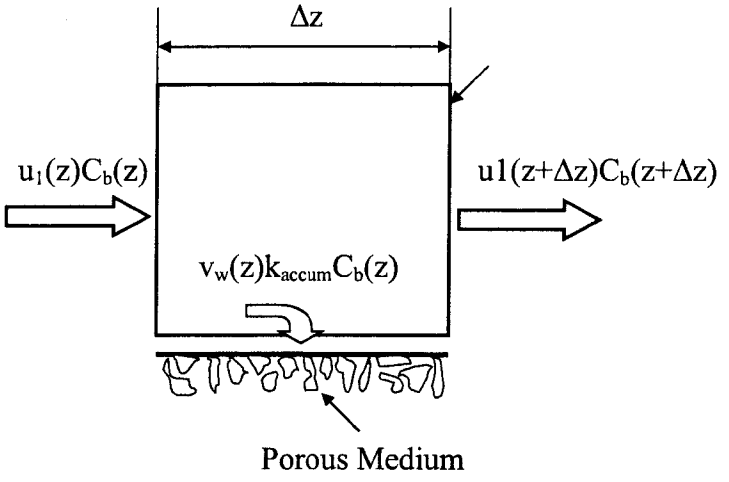

Figure 3-5: Soot Accumulation in Control Volume

The rate of soot accumulation in a control volume is dependent on the influx of soot and the wall flow velocity, and is inversely proportional to the inlet flow velocity. Higher the inlet flow velocity, greater the chance of bulk soot been carried over to the next control volume of the inlet channel.

$$u_1 \frac{\partial([C_g])}{\partial z} = -k_{accum}([C_g])v_w \tag{3.44}$$

The soot accumulation rate is estimated from the above equation.

$$\dot{w}_{accum} = k_{accum}([C_g])\frac{v_w}{u_1}\frac{\dot{m}_{in}}{\left(\frac{1}{2}N_c\right)} \tag{3.45}$$

The inlet exhaust mass is only passed through the inlet channels of DPF which is only half of the total number of channels in the DPF (*Nc*). The mass flow rate of the exhaust gas at the intake of DPF gives an estimate of how much soot is carried over to DPF for the filtration or the accumulation.

In general high soot accumulation coefficient (k_{accum}), represents the less flow ability of SPMs along the inlet channel. The mass flow rate of the exhaust gas at the inlet of DPF channel is given by:

$$\dot{m}_{in} = \rho_g \, u_1(t,0)\left(\frac{N_c}{2}\right) \tag{3.46}$$

The typical diesel exhaust contains particulate matters ranging from 5 ~ 1000 nm in diameter [20]. The particulate matters smaller than 10 nm diameters are commonly not captured by the filter wall. Such small particulates pass through the porous filter media. In other words, mean pore diameter has to be smaller than the particulate size to successfully filter the particulates. Therefore the soot accumulation coefficient is also a representative of the particulate diameter. It is reported by the researchers that the median particulate diameters of diesel exhaust is around 100 nm [20]. In the following simulations, a representative value of soot accumulation coefficient is chosen to calibrate with the experimental literature. The distribution of the particulates by numbers in exhaust gas is different from the distribution of volumetric concentration of PMs in exhaust gas. Smaller number of particulates of bigger diameter can occupy more volume than higher number of particulates of smaller diameter. The distribution of particulate matter by size and volumetric concentration is shown in the Figure 3-6.

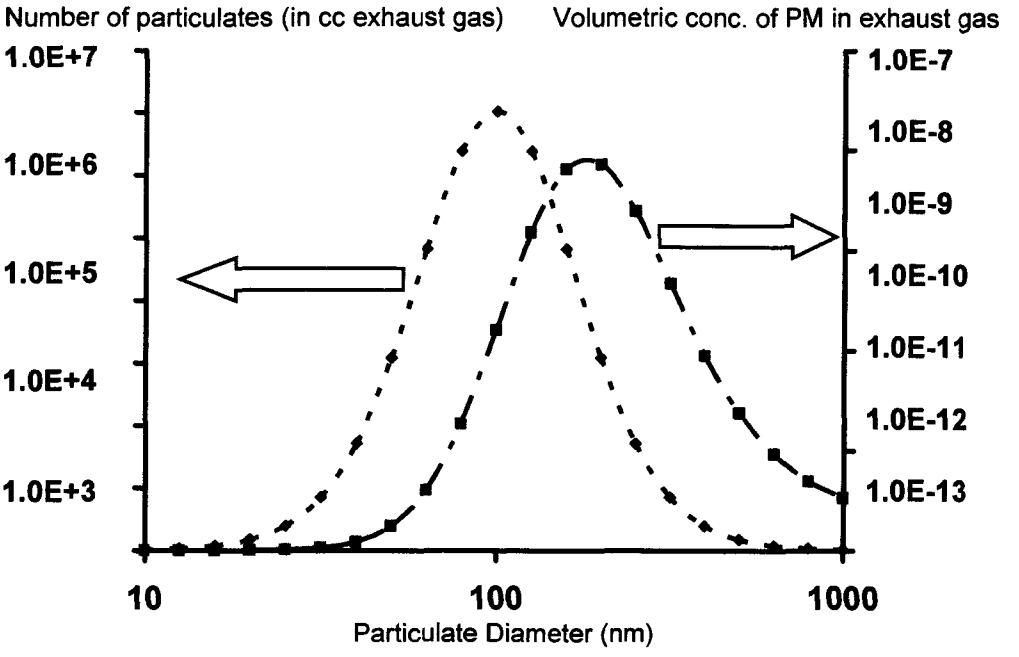

Figure 3-6: Distribution of Particulate Matter in Diesel Exhaust

3.3. NUMERICAL METHOD

The PDEs are solved numerically by applying CFD techniques. The PDE are discretised into simple arithmetic forms and the discretised equations are solved simultaneously within a time loop of the simulation. The scalar variables such as temperatures, pressure species concentrations etc, that are represented by the symbol ϕ in the Figure 3-7 are solved with the vector flow field parameters such as velocity and mass flux by Semi-Implicit Pressure Linked Equation (SIMPLE). However the energy equations for gas phase in DOC and DPF are solved by explicit method. The discretised momentum and energy equations are solved using Tri-Diagonal Matrix Algorithm (TDMA) using forward elimination and backward substitution for fast and efficient solution. The initial boundary conditions for pressure at the inlet of the DPF are solved iteratively till the flow continuity convergence criterion is reached. The solution at every

iteration step is checked for conservativeness, boundedness and transportiveness to avoid solution divergence. In order to apply the pressure velocity equation in DPF the channel is divided into a staggered mesh formation of small control volumes as shown in the Figure 3-8. The scalar variables are solved at each node whereas the vector variables are solved at each faces using central differencing scheme. Considering the different schemes of solving the partial differential equations, the time step and length of discretised control volumes are carefully chosen. The solution is checked for conservativeness, boundedness and transportiveness for each time step for all the control volumes. The discretised time interval for calculation is taken as $\Delta t = 0.1\ sec$ and the discretised length depending on the length of the substrate channel is taken as $\Delta z = 0.001\times \cong 0.15\ mm$ ***(for 6" substrate)***.

The governing equations of the energy the mass and the momentum transfer in the exhaust gas were derived from the Reynolds's Transport equation. From the principles of mass, momentum and energy conservations, the Reynolds's Transport equation gives the generalised equations for the gas phase flow field and energy calculations. The solid phase energy conservation is derived from the Fourier's Law of heat conduction, forced convection and heat generation from chemical oxidation reaction. The FORTRAN code written in order to carry out the numerical computations for the DOC and the DPF model are integrated together in the code structure using different subroutines. The numerical code is written using different subroutines such that it can be integrated with SIMULINK ® using MEX files. FORTRAN programmes can be dynamically linked with MATLAB ® callable MEX files and can be directly implemented in SIMULINK ® S-function to develop feed-forward control algorithms.

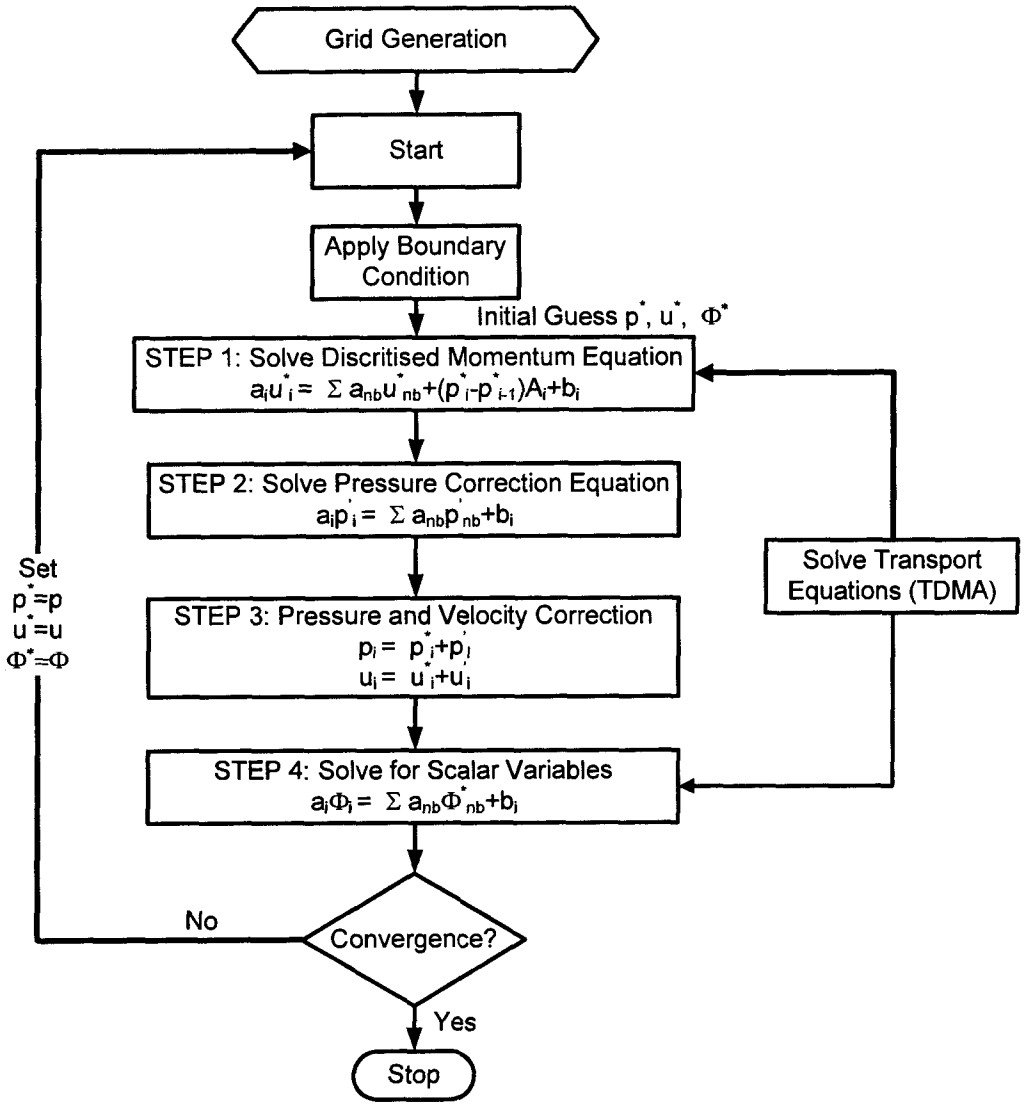

Figure 3-7: SIMPLE Method to Solve Pressure and Velocity

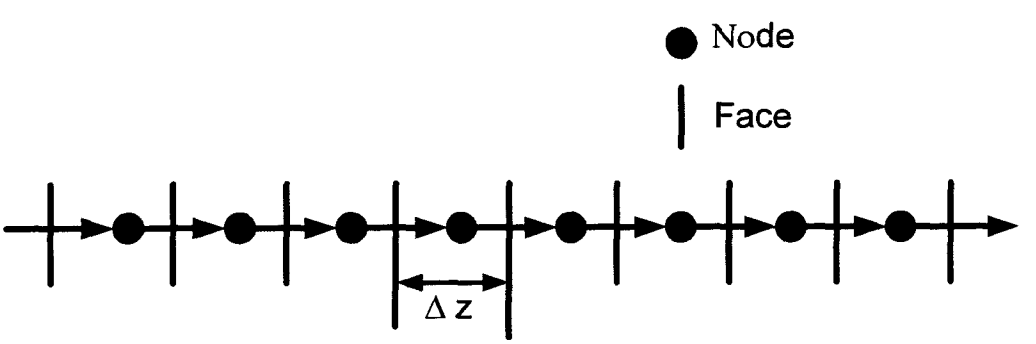

Figure 3-8: Staggered Mesh Formation

CHAPTER IV

4. ANALYSIS OF RESULTS

A preliminary model validation has been carried out using the experimental thermal response of DPF under the controlled regeneration condition. The validation was carried out for both the pressure drop across the DPF channel and the thermal response of the substrate wall at various locations of the DPF substrate. A cordierite DPF of 6" by 5.66" is chosen for the model validation with 200 cells per square inch of channels with 19 mils of wall thickness and 50 % porosity in the filter wall. From the technical literature of the manufacturer's manual, the initial pressure drop and the initial soot loading corresponding to the different exhaust mass flow rates and the inlet temperatures are compared with the simulation results as shown in the Figure 4-1 and Figure 4-2 [22, 23]. The pressure drops due to the entrance and the exit losses from the canister are neglected. For the sake of simplicity for the model validation, it is assumed that the thermocouples that are installed in the DPF channels have no thermal inertia.

In order to validate the regeneration model, a simulation case with initial soot loading of 5 g/L and initial substrate temperature of 250 °C is compared with an experimental result. The initial soot load is assumed on the basis of the initial pressure drop for the DPF. Thermocouples are located at four different locations inside the substrate channel. The model is validated by tuning number of chemical kinetics, thermal and flow field parameters in order to match the pressure drops and the temperatures of the substrate within the acceptable limits of tolerance. It is extremely difficult to predict regeneration

in an experimental setup and therefore the regeneration model is validated by comparing the simulated thermal response and pressure drop of the DPF with the experimental data.

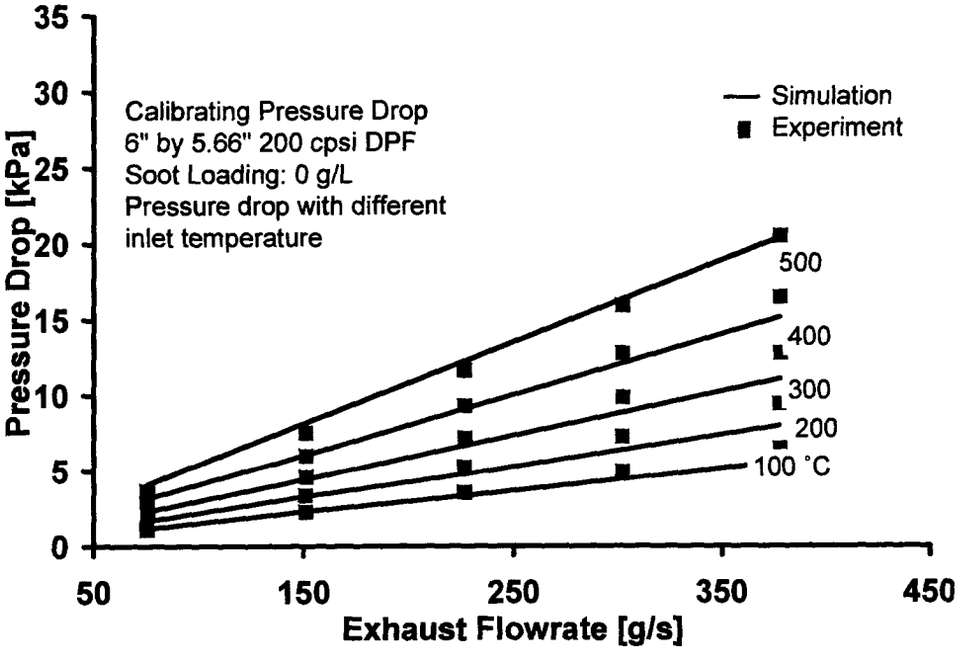

Figure 4-1: Pressure Drop vs. Flow rate (0 g/L Soot Loading)

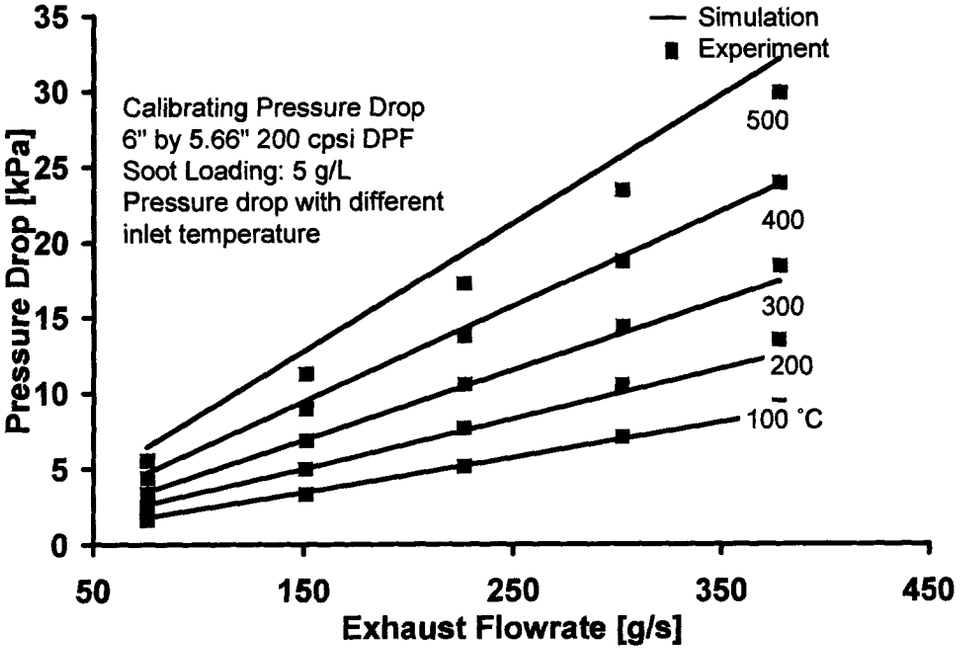

Figure 4-2: Pressure Drop vs. Flow rate (5 g/L Soot Loading)

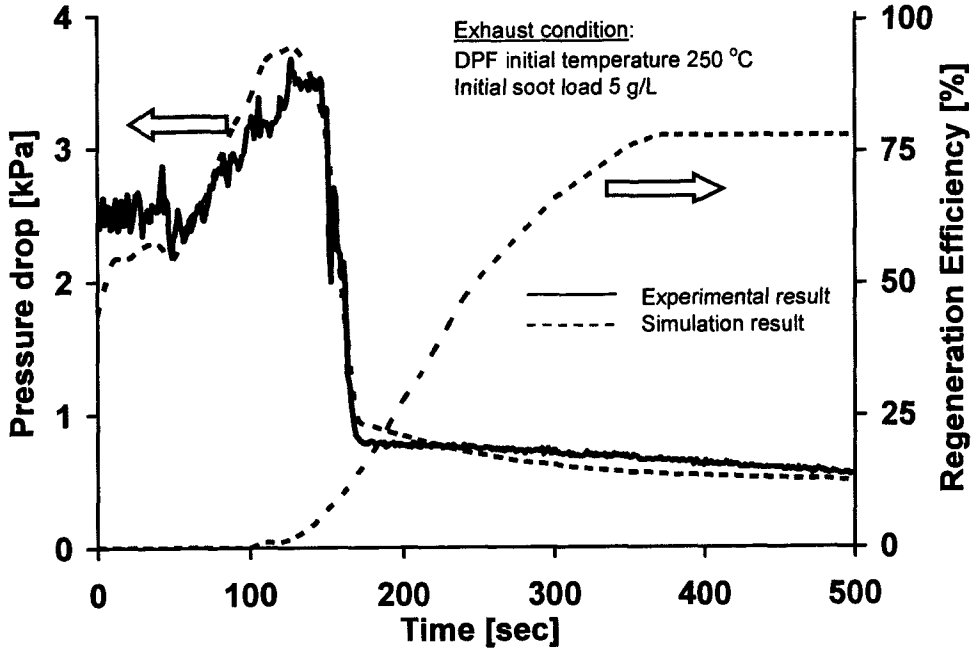

Figure 4-3: Regeneration Model Validation

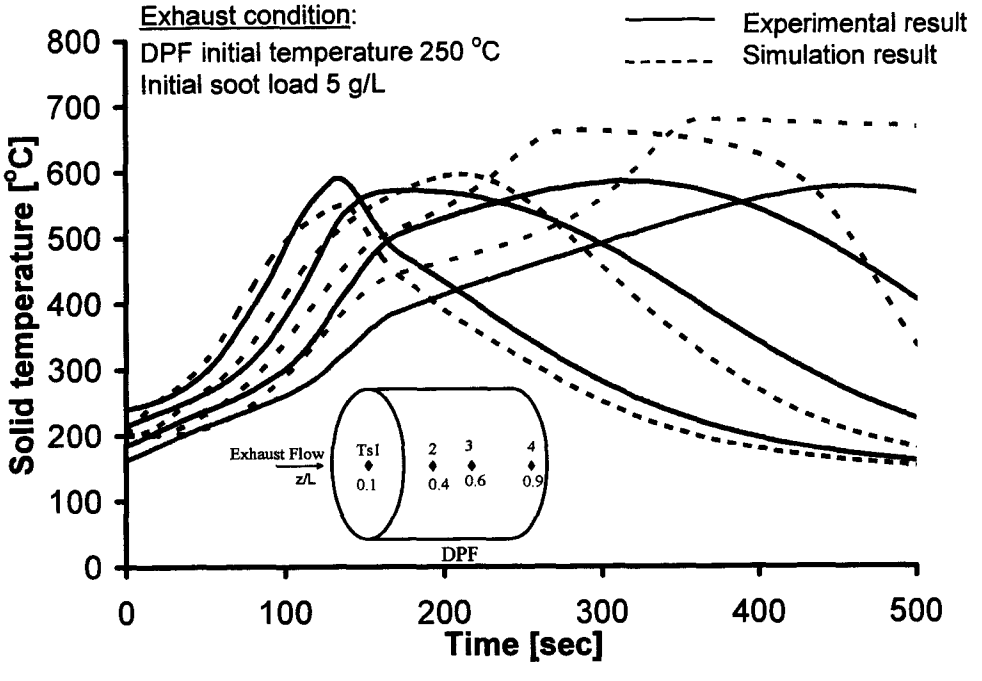

Figure 4-4: Regeneration Thermal Response Validation

From the Figure 4-3 and Figure 4-4 it is seen that the simulation and the experimental data are in reasonable agreement with one another. The simulated pressure drop is within

± 0.25 kPa and the temperatures are comparable within ± 70 °C with the experimental results. It is noticed that the timing of the regeneration is governed by the reaction kinetics. Based on the validation some important calibration parameters describing the thermo physical process during DPF regeneration are tabulated in the Table 4-1. Additional calibration parameters are tabulated in Table C-2 of APPENDIX C.

Table 4-1: Important Calibration Parameters

Parameter	Value	Unit
F	28.45	-
μ	2.97×10^{-5}	Pa·s
κ_s	1.54×10^{-15}	m^2
κ_p	5.55×10^{-15}	m^2
Nu	3.81	-
c_{ps}	1.1	kJ/kg·K
c_{pp}	1.52	kJ/kg·K
ρ_s	1400	kg/m^3
ρ_p	140	kg/m^3
λ_s	0.85	W/m·K
λ_p	2.1	W/m·K
k_{accum}	2500	-

Theoretical and experimental investigations are carried out on the energy efficiency of various active flow conditions to initiate and sustain aftertreatment operation without reaching the conditions of substrate overheating. Thermal response of the DOC-DPF is also analysed for active flow conditions with the simulation results.

4.1. EXPERIMENTAL INVESTIGATION

A single cylinder engine is used with a DOC-DPF unit to perform tests on active and passive flow control strategies. The thermocouples are placed inside the exhaust pipe to record the exhaust gas temperature at the inlet of DOC (Tg in) and the aftertreatment substrate at various locations (DOC 1, 2 and DPF 1, 2) as shown in the Figure 4-5. The DOC-DPF system is placed approximately 300 mm downstream of an external fuel injector. The exhaust gas heater is installed before the fuel injector to enhance supplemental fuel vaporization, and to complement with additional heat energy to the exhaust stream. The exhaust gas samples are taken before and after the DOC-DPF system and are analyzed with exhaust gas analysers for the readings of the CO, NO, HC and O_2 concentrations. A smoke meter is also attached in order to monitor the volumetric soot concentration of the PM in the exhaust stream.

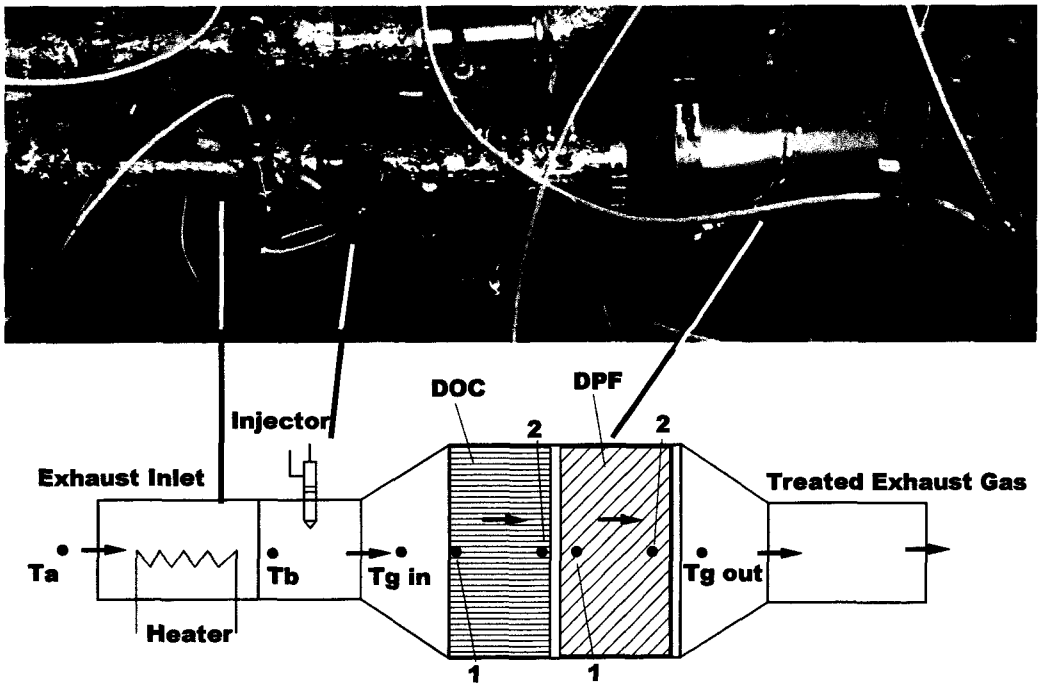

Figure 4-5: Experimental Setup for Aftertreatment System

The thermal response of the substrate is recorded through a dedicated data acquisition system consisting of thermocouples, differential pressure sensor, hotfilm anemometer based exhaust gas flow meter, and a system of computer network to record and analyse the experimental results online for diagnosis. The supplemental fuel delivery is controlled with an independent controller, solenoid injector and a pressure regulator. The fuel delivery rate is controlled by a computer program connected to the solenoid by an electronic counter card. Depending on the frequency and the duty cycle of the digital counter signal the fuel flow rate is controlled. A calibrated lookup table of fuel flow rate versus frequency and duty cycle is referred in the control algorithm. The heater is controlled with an independent variable DC power supply. The thermocouples placed at various locations of the exhaust stream records the exhaust gas temperature. From the difference in the temperatures before and after the heater and the mass flow rate reading, the net rate of external heat energy delivery rate is calculated from the equation 4.1. The rate of exothermic heat released to the exhaust gas due to DOC reaction is similarly calculated. The rate of fuel energy delivered through the external injector is calculated from the rate fuel injected into the exhaust stream.

$$P_{heater} = \dot{m}_{gas}\, c_{pg} \left(T_b - T_a\right) \tag{4.1}$$

$$P_{DOC} = \dot{m}_{gas}\, c_{pg} \left(T_{g\,out} - T_{g\,in}\right) \tag{4.2}$$

$$P_{fuel} = \dot{m}_{fuel}\, LHV_{fuel} \tag{4.3}$$

The objective of the experiment is to investigate the effect of exhaust gas temperature and the supplemental energy on the catalytic activity of DOC for the active aftertreatment conditions. The engine condition is maintained at 1420 RPM at 32 Nm corresponding to the exhaust mass flow rate of 9.5 g/s and exhaust gas temperature of 250 °C at the inlet of

DOC-DPF. The external fuel energy of 1.997 kW is delivered corresponding to the rate of fuel delivery of 47 mg/s through the external fuel injection system. Different cases are run with the different external heating conditions and exhaust gas temperatures at the inlet of DOC and summarized in the Table 4-2. An analysis is carried out to investigate the energy efficient pathways to initiate regeneration in DPF. Additionally study is carried out to investigate the effects of the supplemental heating of the exhaust stream. The external heating power is controlled by varying the electrical current across the heating coil which is embedded in a honeycomb ceramic substrate structure in the exhaust pipe upstream of the external fuel injector. The mass air flow sensor used for the purpose is a hot-film anemometer based calibrated device installed in the intake line of the engine. It is assumed that the mass flow rate in the intake and the exhaust fo the engine are equal neglecting the mass of fuel injected in-cylinder. The DOC-DPF setup in the experiment is given in Table C-3 of APPENDIX C.

Table 4-2: Experimental Test Cases

Case	External Fuel Energy [kW]	External Heating Energy [kW]	Temperature above threshold for catalytic activity	Exhaust Gas Temperature at the inlet of DOC [°C]
T1	1.997	0.000	No	250
T2	1.997	0.650	Yes	290
T3	1.997	0.800	Yes	300

From the experimental investigation of case T1, it is observed that when the exhaust gas temperature is kept below the threshold temperature for the catalytic activity in DOC, the supplemental fuel energy delivered into the DOC is wasted without any chemical conversion in the DOC channel.

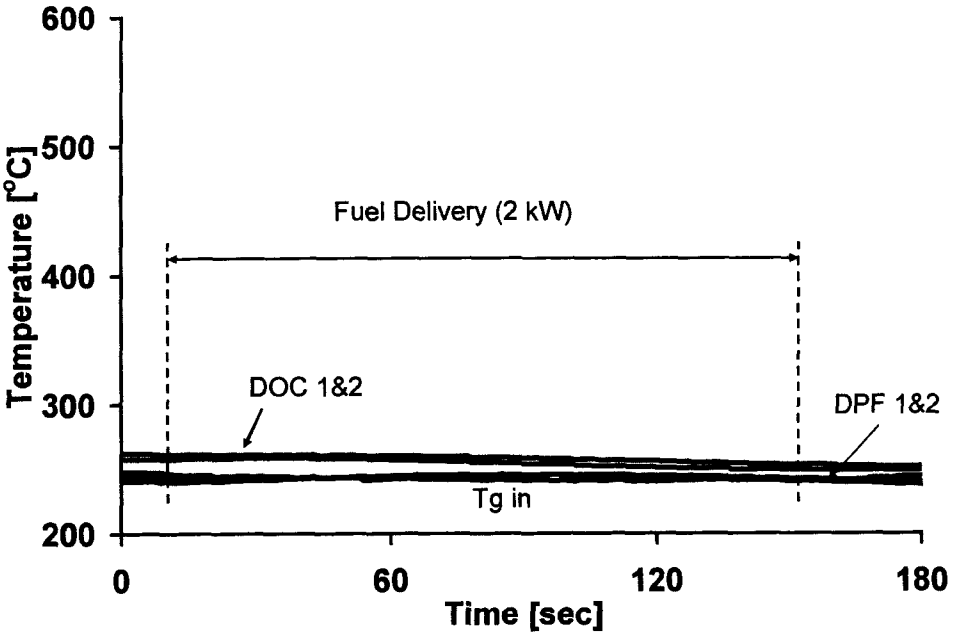

Figure 4-6: Experimental Result (Case T1)

It is also observed that there is no rise in the temperature of the DOC-DPF system indicating no catalytic activity occurring inside the DOC. The experimental results in the Figure 4-6 show that the DPF regeneration condition cannot be reached without sustainable catalytic activity in the DOC. The performance analysis of DOC for the case is shown in the following Table 4-3.

Table 4-3: DOC Performance Analysis (Case T1)

Time [sec]	O_2 Concentration [%]		CO Concentration [ppm]		Gas Temperature [°C]	
	Before DOC	After DOC	Before DOC	After DOC	Before DOC	After DOC
0	11.8	11.7	9.8	9.8	248.3	252.8
90	10.9	10.7	177.7	176.5	241.1	254.7
180	12.6	12.6	125.0	125.0	244.1	252.9

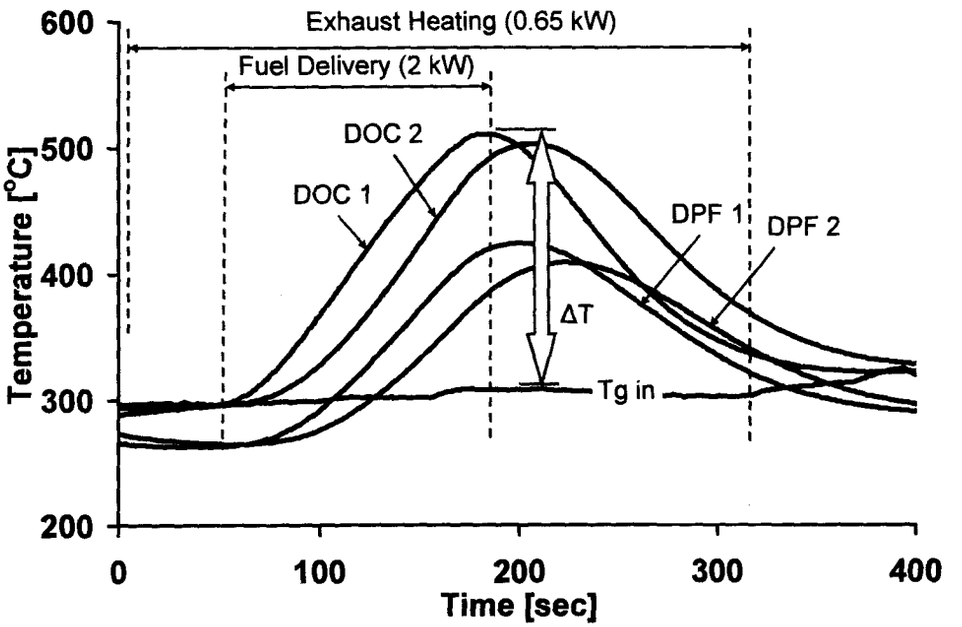

Figure 4-7: Experimental Result (Case T2)

From the experimental investigation of the case T2, it is observed that the significant catalytic activity occurs when the exhaust gas temperature is above the "light off" temperature for DOC activity. The thermal response from the Figure 4-7 indicates that the temperature of the substrate of DOC rise by $\Delta T = 120\ ^{\circ}C$ due to the exothermic reactions occurring in the catalyst site of the DOC. The energy released due to the chemical reactions are taken up by the exhaust gas which in turn helps to raise the substrate temperature of the DPF from 250 °C to 415 °C in 100 seconds by forced convection. Therefore the catalytic activity in DOC helps in initiating conditions favourable to soot regeneration in DPF. The catalytic activity in DOC also helps to chemically convert the harmful exhaust pollutant species as shown in the Table 4-4. It is to be noted due to the number of chemical reactions taking place inside the DOC, the

accurate measurements of the exhaust species concentration is highly improbable though, an estimate of the conversion efficiency can be obtained. The exhaust gas temperature at the inlet of the DOC-DPF system is raised by the exhaust gas heating with the heater.

Table 4-4: DOC Performance Analysis (Case T2)

Time [sec]	O_2 Concentration [%]		CO Concentration [ppm]		Gas Temperature [°C]	
	Before DOC	After DOC	Before DOC	After DOC	Before DOC	After DOC
0	11.9	11.9	12.7	12.6	296.4	285.5
100	10.6	10.3	129.9	51.8	299.3	294.4
200	12.6	11.2	129.9	63.5	308.2	431.8
300	13.4	12.1	129.7	20.0	302.4	380.4
400	10.8	10.6	12.6	11.7	319.4	314.5

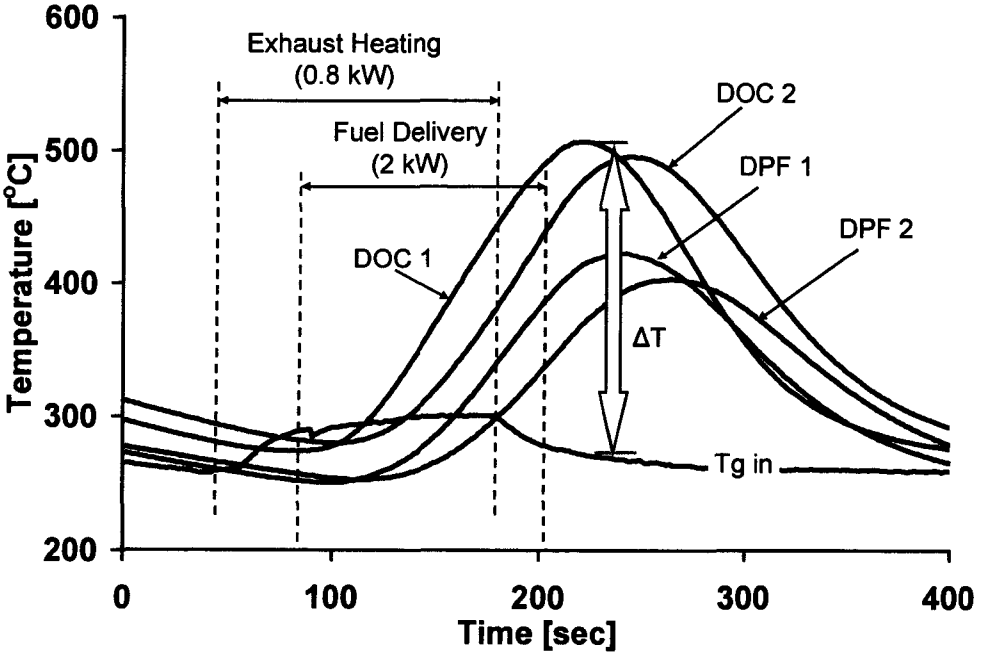

Figure 4-8: Experimental Result (Case T3)

It is noticed that the performance of DOC is attributed to the exhaust temperature consistent with the findings of other researchers as mentioned in the literature review. The experimental investigation of the case T3 shows that the additional heat from the exhaust heater enhances the DOC performance. The thermal response of the DOC-DPF substrate is presented in the Figure 4-8 and the performance analysis is summarized in the Table 4-5. The exhaust heater with 0.8 kW heat power is turned ON 30 seconds prior to the starting of the external fuel injection. The external heater in the upstream of injector helps to raise the exhaust temperature above the vaporisation temperature of diesel fuel thereby enhancing the fuel vaporisation and mixing [24, 25, 26]. The advantage of the exhaust gas heater is twofold. First of all it is to enhance fuel vaporisation and mixing and the second is to provide the additional heat energy to rise the exhaust temperature during low load operations of the diesel engine.

Table 4-5: DOC Performance Analysis (Case T3)

Time [sec]	**O_2 Concentration [%]**		**CO Concentration [ppm]**		**Gas Temperature [°C]**	
	Before DOC	After DOC	Before DOC	After DOC	Before DOC	After DOC
0	13.5	13.4	8.8	6.8	265.1	300.5
100	13.5	12.2	27.7	9.77	291.2	270.9
200	13.6	10.7	181.4	85.9	279.4	364.5
300	13.4	12.6	190.8	23.4	261.6	406.7
400	13.2	12.4	18.5	8.8	259.2	293.5

From the Figure 4-8, it is observed that the temperature of the substrate of DOC rise by $\Delta T = 220\ ^{\circ}C$ from 300 °C to 510 °C. The duration of supplemental energy delivery is

maintained for 120 seconds. The substrate temperature of DPF rises to 420 °C indicating condition favourable to initiate soot regeneration.

An energy efficiency analysis is carried out and a comparison is made between various experimental cases as shown in the Figure 4-9. The energy comparisons are for the fuel energy delivered (assuming LHV_{fuel} to be 42.7 kJ/g), heating energy delivered and the energy from the exothermic reactions in terms of the absolute energy over the duration of the experimental case interval. It is observed that the energy released to the exhaust gas from the exothermic reactions in DOC facilitates soot regeneration in DPF. The energy efficiency of the DOC exothermic reaction is defined as the ratio of energy released and the total energy delivered by heater and the supplemental fuel.

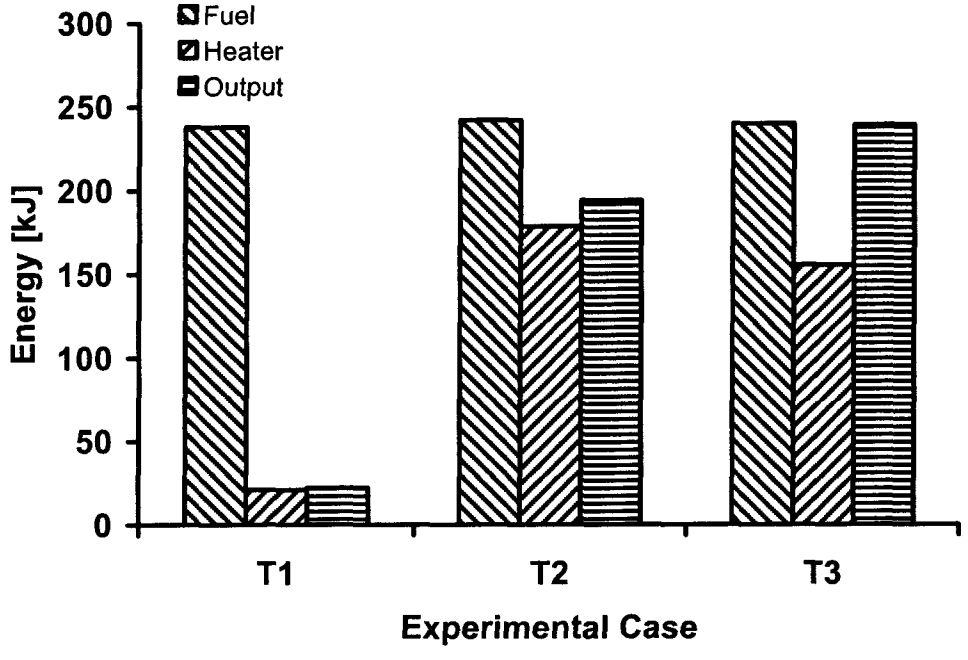

Figure 4-9: Energy Analysis of Experimental Cases

It is observed that the energy efficiency of the DOC increases with the increase of inlet exhaust temperature of DOC. This is explained by the fact that the DOC performance improves with the increase of substrate temperature. The exothermic heat released and the DOC conversion efficiency is dependent on the substrate temperature.

Table 4-6: Energy Efficiency Analysis of DOC

Energy Parameter	Experimental Case		
	T1	T2	T3
Fuel Energy [kJ] (*a*)	237.8	241.7	239.7
Supplemental Heat [kJ] (*b*)	20.9	178.3	155.3
Energy Released [kJ] (*c*)	22.1	193.8	238.9
Energy Efficiency [%] $(\frac{c}{a+b}\times 100)$	8.5	46.1	60.5

4.2. SIMULATION RESULTS

Simulations are carried out with the various active flow conditions for the DOC-DPF systems. A comparison of the FR and the NFR strategies are demonstrated through simulations on DPF regeneration. The temperatures Ts1, Ts2, Ts3 and Ts4 are recorded at the different locations along the axial directions of DPF (z/L) during the simulation as indicated in the Figure 4-10 below.

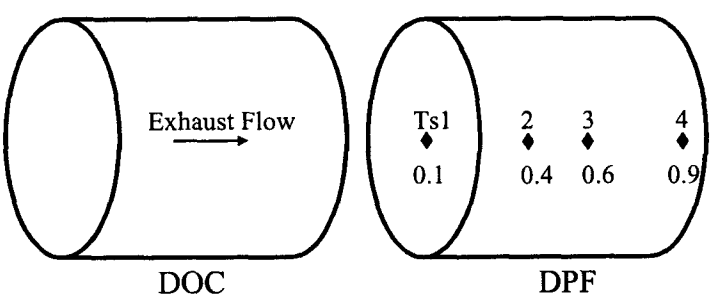

Figure 4-10: Simulation Setup

The DOC-DPF system that is chosen for the simulation is commonly used for the diesel automotive applications, as shown in the Table C-3 of APPENDIX C.

Table 4-7: DOC – DPF Setup Parameters

Parameter	Value	Unit
Substrate Material Density	1.4	kg/L
Substrate Heat Capacity	0.80	kJ/kg.K
Substrate Thermal Conductivity	22.6	W/m.K
DOC Catalyst Loading	1.5	g/L

The objectives of the theoretical investigations are to carry out the thermal response and the energy efficiency analysis with different active flow strategies in the diesel aftertreatment system. The main focus of the simulation is to study DPF regeneration and to get a better understanding of the various pathways to initiate safe and efficient regenerations in the DPF. The energy required initiating such conditions in the DOC and the DPF are quantified.

4.2.1 CASE S1: COMPARISON BETWEEN FR AND NFR SETUP FOR DPF REGENERATION

The simulations are carried out to demonstrate the heat retention capabilities of the FR setup during cooling of DOC – DPF system by the exhaust gas. During this conditions the heat is retained at the center portion of substrate while the the flow of the exhaust gas is changed periodically. The substrate temperature profile oscillates periodically due to FR operation and therefore the temperature of the substrate center is retained for a considerable amount of time. The FR frequency is the time for each of the forward and the reverse flow through the aftertreatment system.

Table 4-8: Simulation Conditions (Case S1)

Parameter	Value	Unit
Exhaust Gas Temperature	250	°C
Initial DPF Temperature	500	°C
Initial DPF Soot Load	5	g/L
Inlet THC	5000	ppm
Inlet CO	2000	ppm
Inlet O_2	10	%
Exhaust Mass Flow Rate	8	g/s
FR Time Period	10	seconds

The transient thermal response, the soot cake profile and the fraction of soot regeneration are compared between the FR and the NFR setup. In FR system, the substrate's center temperature can be retained above the catalytic "light off" temperature to sustain conditions favourable to enable aftertreatment operation such as regeneration in DPF device. The regeneration efficiency is a representation of the fraction of soot oxidised with respect to the initial soot load at a particular time instant. For example if the intial soot load of DPF is 5 g/L and after 10 min of the regeneration operation, the soot load remaining in the DPF is 2.5 g/L then the regeneration efficiency achieved till 10 min of regeneration operation is termed as 50 %.

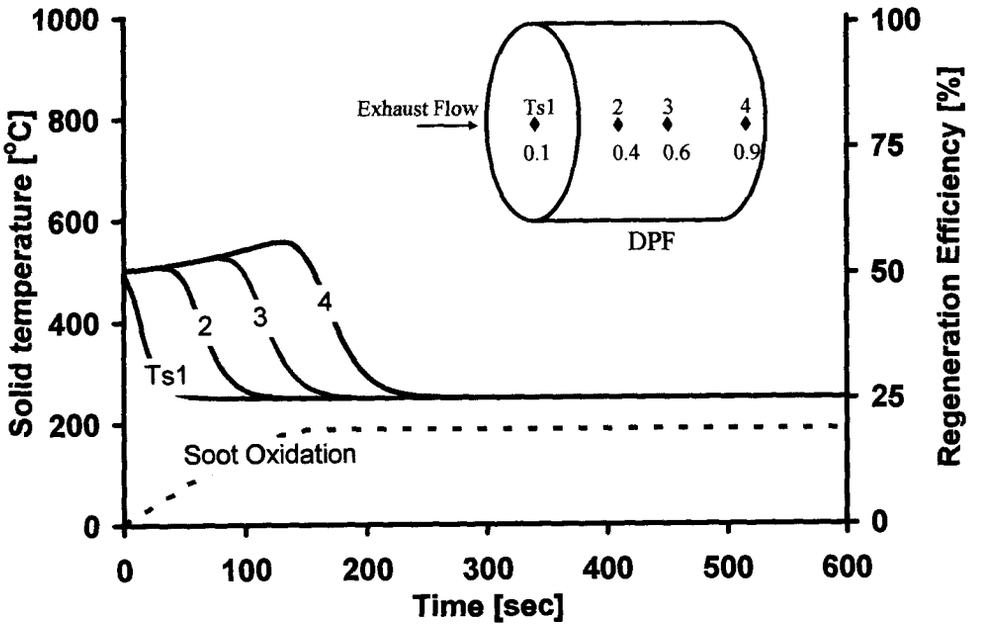

Figure 4-11: Transient Response of DPF regeneration (NFR)

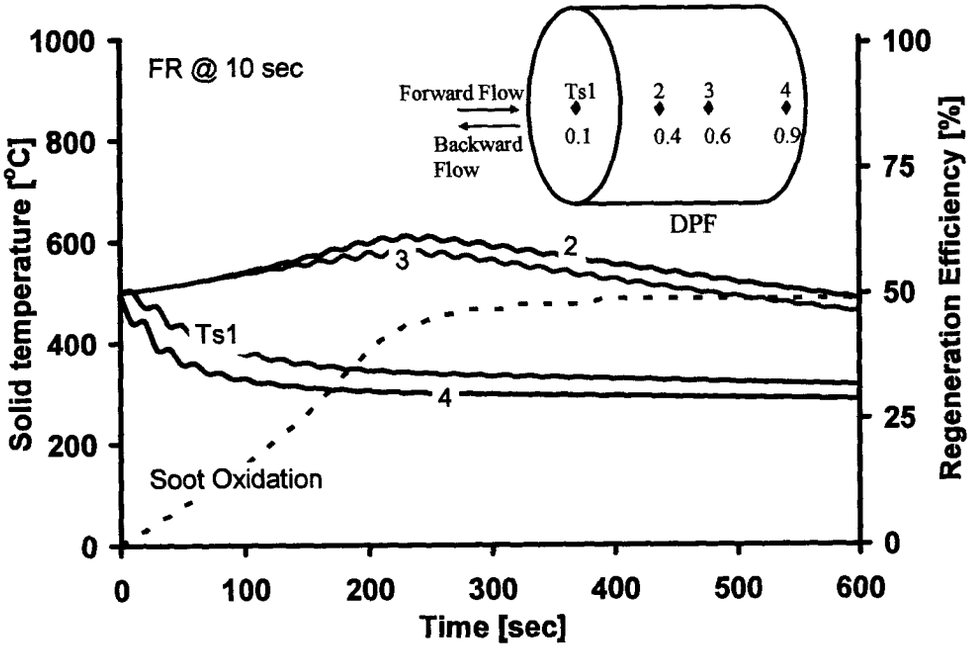

Figure 4-12: Transient Response of DPF (FR)

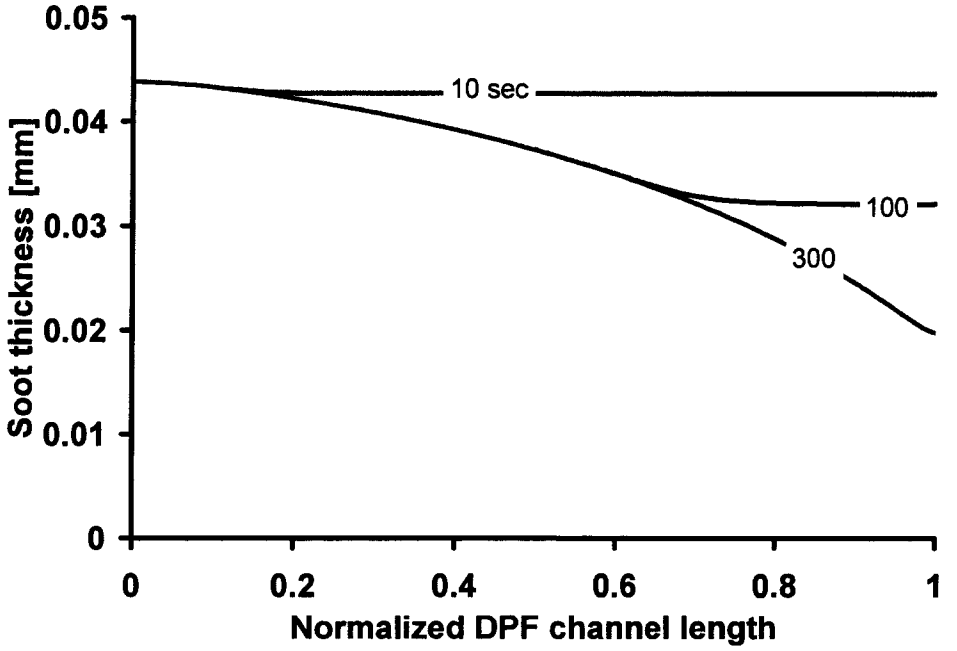

Figure 4-13: Soot Profile (NFR)

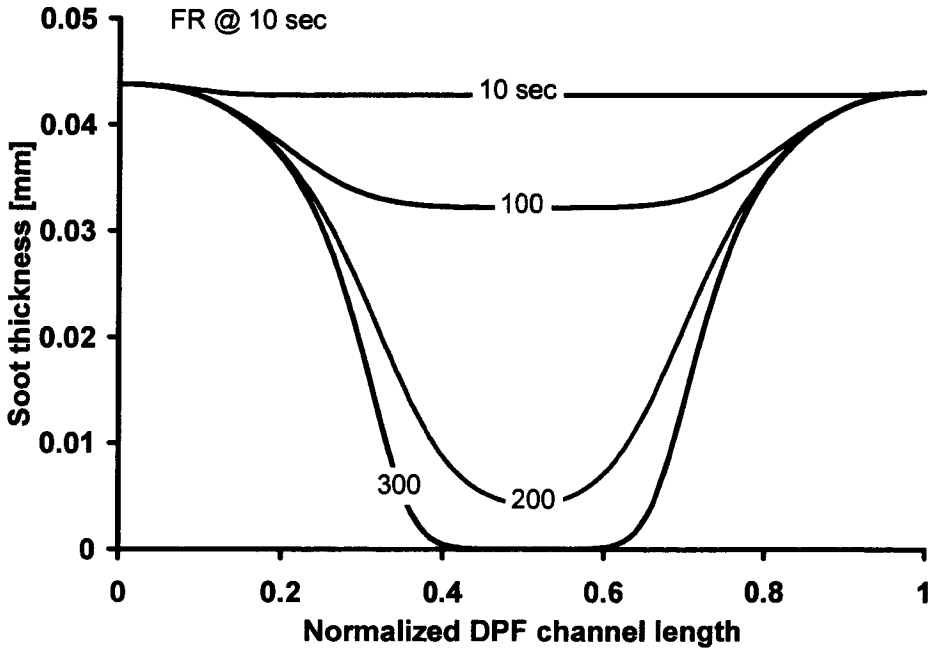

Figure 4-14: Soot Profile (FR)

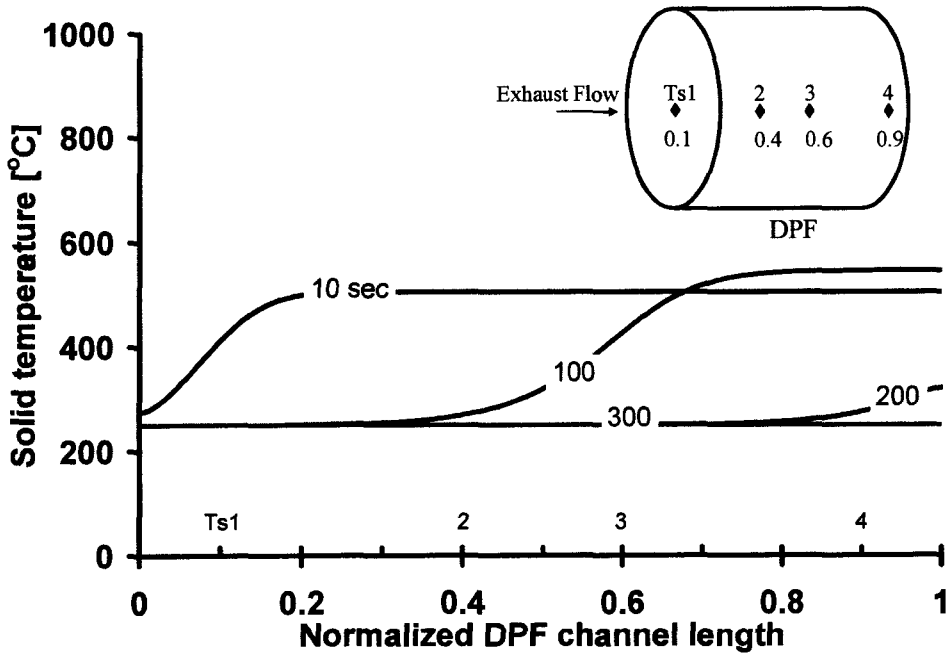

Figure 4-15: Temperature Profile (NFR)

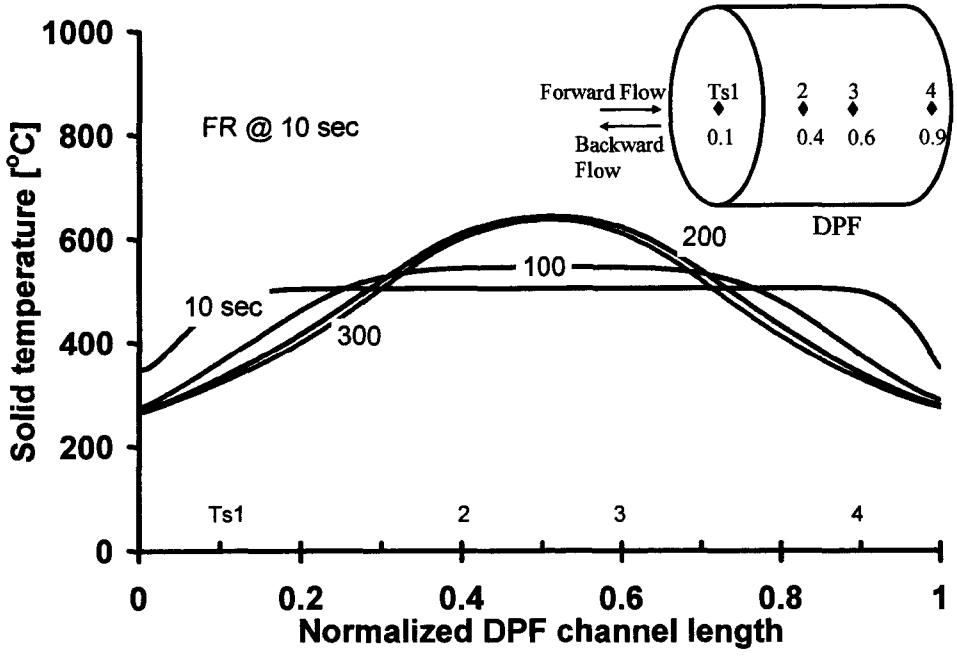

Figure 4-16: Temperature Profile (FR)

From the results of the thermal response and the soot cake thickness, it is observed that for cooling process the FR setup is more effective in retaining conditions favourable to regeneration for longer time duration. It is also evident from the soot profile that the regeneration is sustained in the center of the DPF substrate while the boundary region cools down to the temperature of the exhaust gas.

4.2.2 CASE S2: EXHAUST GAS TEMPERATURE VARIATION FOR DPF REGENERATION

The main objectives of this set of simulations are to identify objectively the energy efficient pathway to initiate soot regeneration conditions in the DOC-DPF system. The cases with different initial temperatures and the inlet gas temperatures are simulated to analyse the energy required to initiate and sustain regenerations inside DPF. The inlet temperature of the exhaust gas can be varied by installing an exhaust gas heater similar to the heater used in the experiment at the flow rates ranging from 2 to 15 g/s. The rise in the exhaust temperature depends on the exhaust gas flow rate and the energy supplemented by the exhaust heater. The supplemental heat energy can be effectively delivered in the low exhaust space velocities corresponding to the low flow rate loop of the PF system. From the experimental results it is observed if the DOC is placed before the DPF, the setup will facilitate to accomplish regeneration provided that the DOC attains calaytic "light off". Once the "light off" condition is reached, the DOC catalytic activity can be sustained by controlled addition of the supplemental fuel. The exothermic reactions of fuel oxidation inside the DOC channels counter balance the convective heat loss to the cooler exhaust gas. The exhaust gas picks up the convective heat from the DOC channel and helps to sustain the regeneration in the DPF in the downstream. The simulation conditions are summarized in the Table 4-9.

Table 4-9: Simulation Conditions (Case S2)

Parameter	Value			Unit
	Case			
	S2A	S2B	S2C	
Exhaust Gas Temperature	310	300	290	°C
Initial DOC Temperature	310	300	290	°C
Initial DPF Temperature	310	300	290	°C
Initial DPF Soot Load	5			g/L
Inlet THC	5000			ppm
Inlet CO	2000			ppm
Inlet O_2	10			%
Exhaust Mass Flow Rate	10			g/s

In the following simulations the DOC is positioned before the DPF so that the catalytic activity in the DOC helps to achieve regeneration conditions in DPF. Sufficient amount of external fuel is injected in the upstream of DOC with the initial temperature of DOC just above the temperature to sustain catalytic activity. The simulation results of the transient thermal response along with the fraction of soot regeneration (regeneration efficiency) are presented for different cases. The soot profiles at different time as the regeneration progresses are also shown. An energy efficiency comparison is made by analyzing the fraction of soot regenerated with the total quantity of the supplemental energy delivered for the purpose. It is assumed that the supplemental fuel injected in the exhaust stream is fully vaporized before entering to the DOC. The supplemental fuel delivery rate of 50 mg/s in an exhaust stream of approximately 10 g/s corresponds to 5000 ppm of THC by mass as indicated in the Table 4-9.

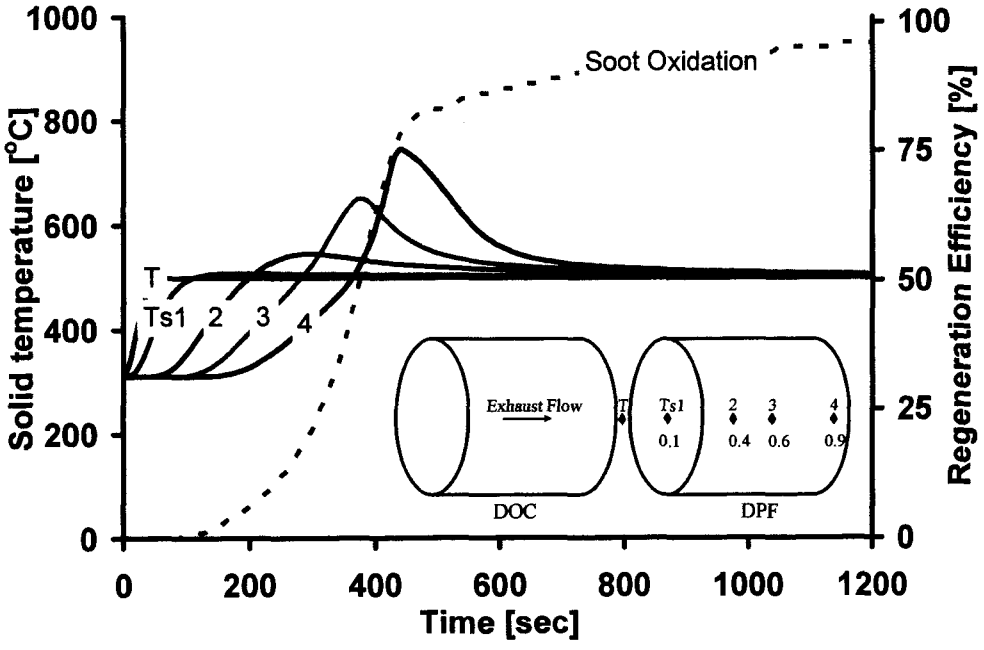

Figure 4-17: Transient Simulation Results (Case S2A)

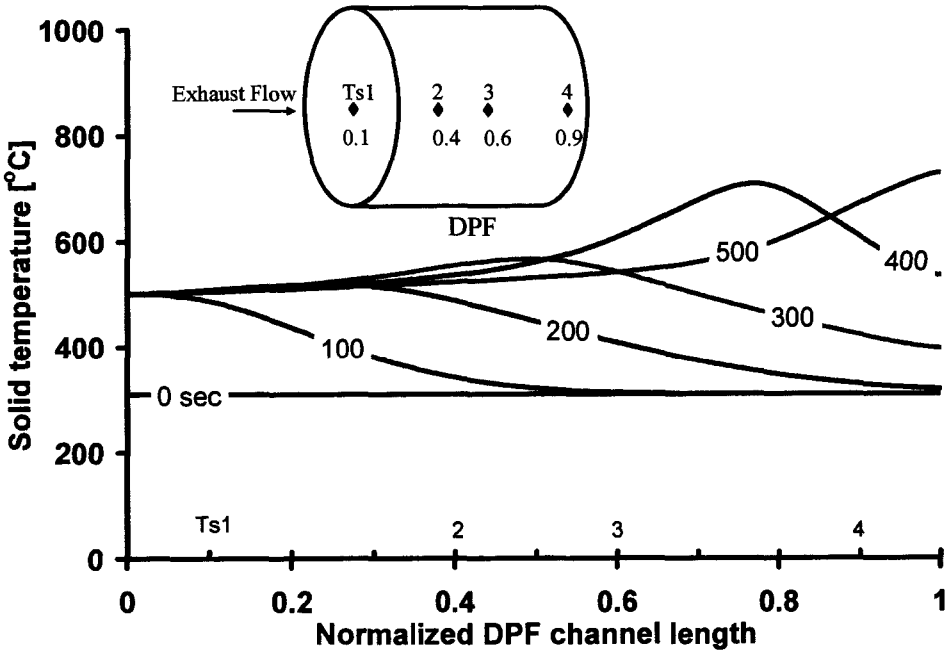

Figure 4-18: Thermal Response Simulation (Case S2A)

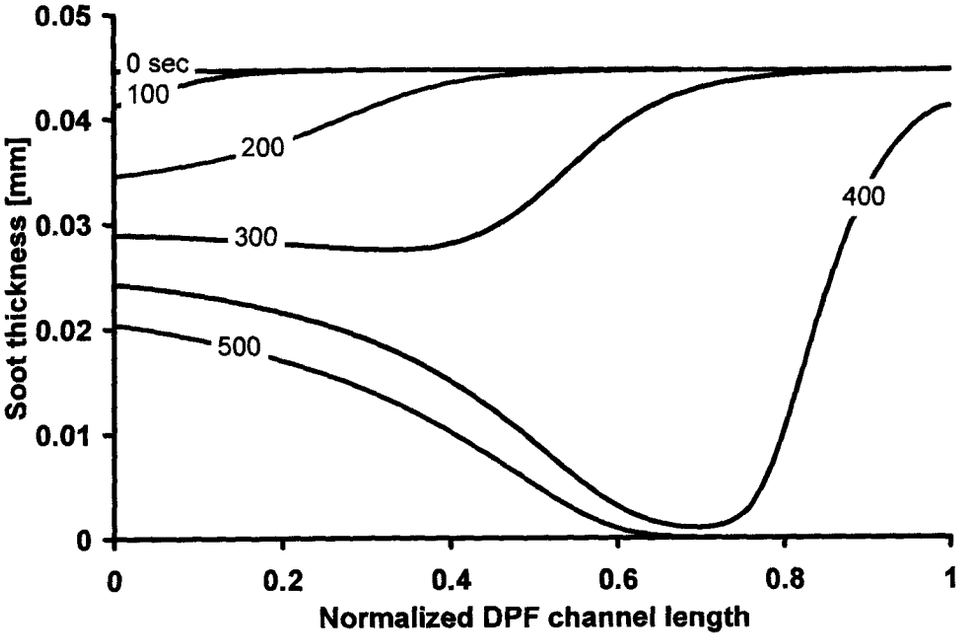

Figure 4-19: Soot Oxidation Simulation (Case S2A)

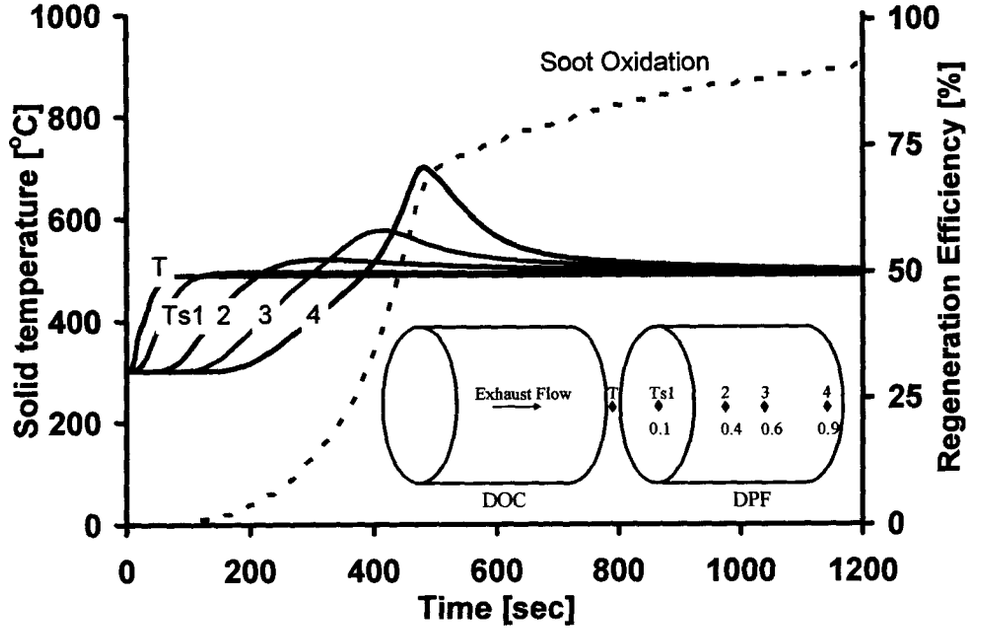

Figure 4-20: Transient Simulation Results (Case S2B)

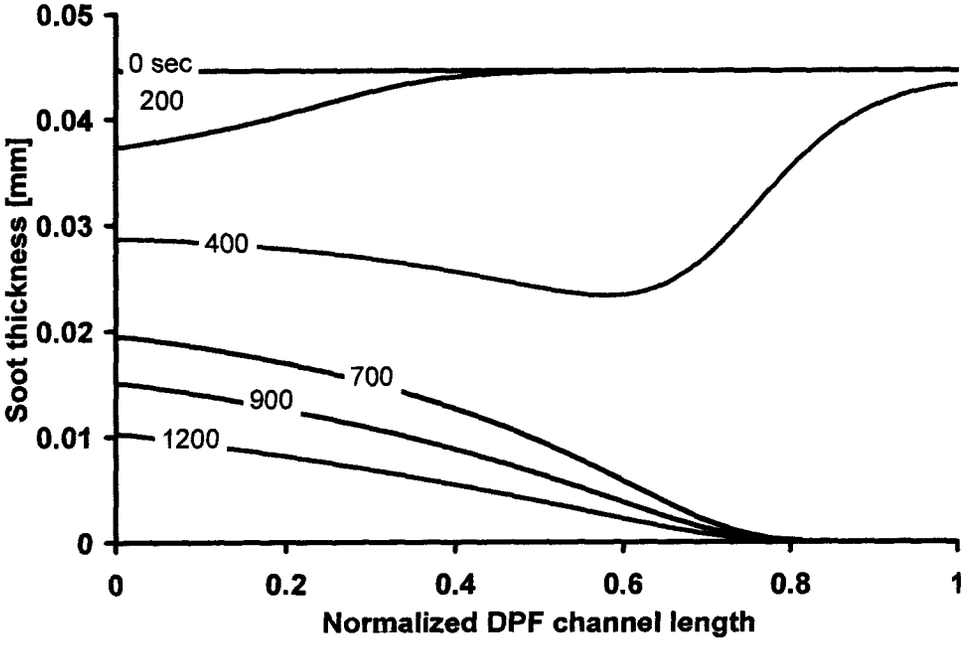

Figure 4-21: Soot Oxidation Simulation (Case S2B)

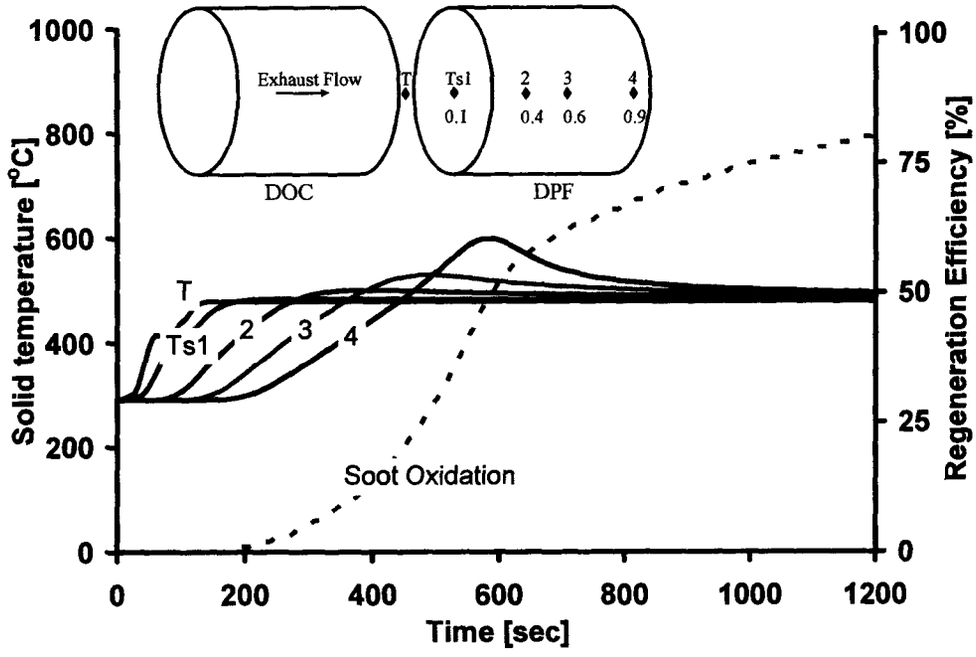

Figure 4-22: Transient Simulation Results (Case S2C)

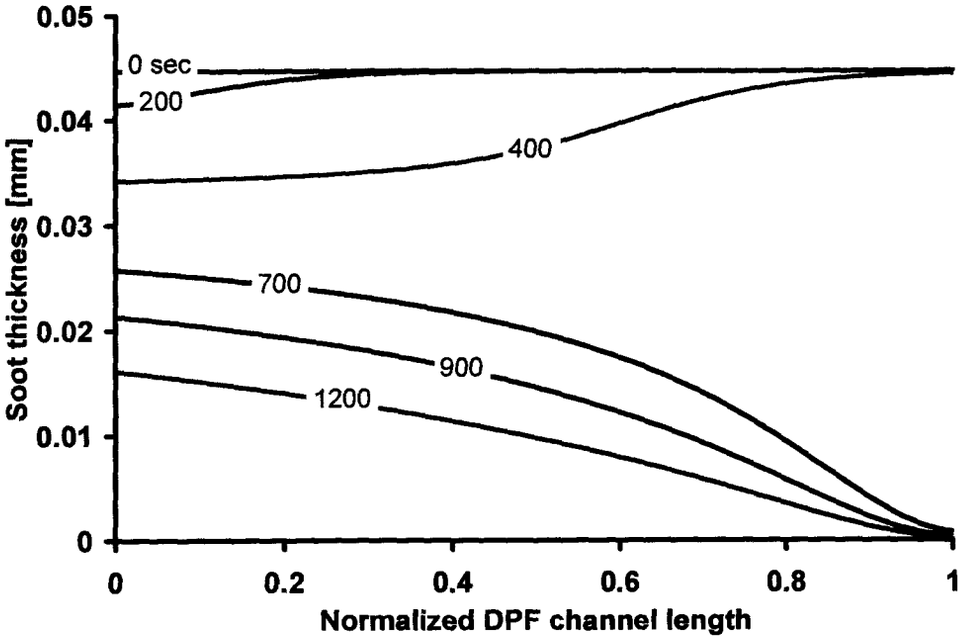

Figure 4-23: Soot Oxidation Simulation (Case S2C)

The simulations are repeated with other inlet temperatures of the exhaust gas and the initial temperatures of the substrate. The progress of regeneration in DPF with the 5 g/L initial soot loading is compared between the different cases of the initial substrate temperatures and the inlet exhaust gas temperatures and shown in the Figure 4-24. It is observed that if the temperature is kept below the DOC "light off", then the regeneration in DPF is not initiated. From the simulation results presented it is seen that the DOC-DPF system is capable of regeneration once the temperature is maintained above 290 °C.

It can be argued that in order to initiate and complete regeneration by energy efficient method an additional supplemental heater may be installed in the diesel exhaust system. The offset of additional heater cost, the PR setup and the additional heat energy can be recovered by the energy saved during the regeneration process in DPF.

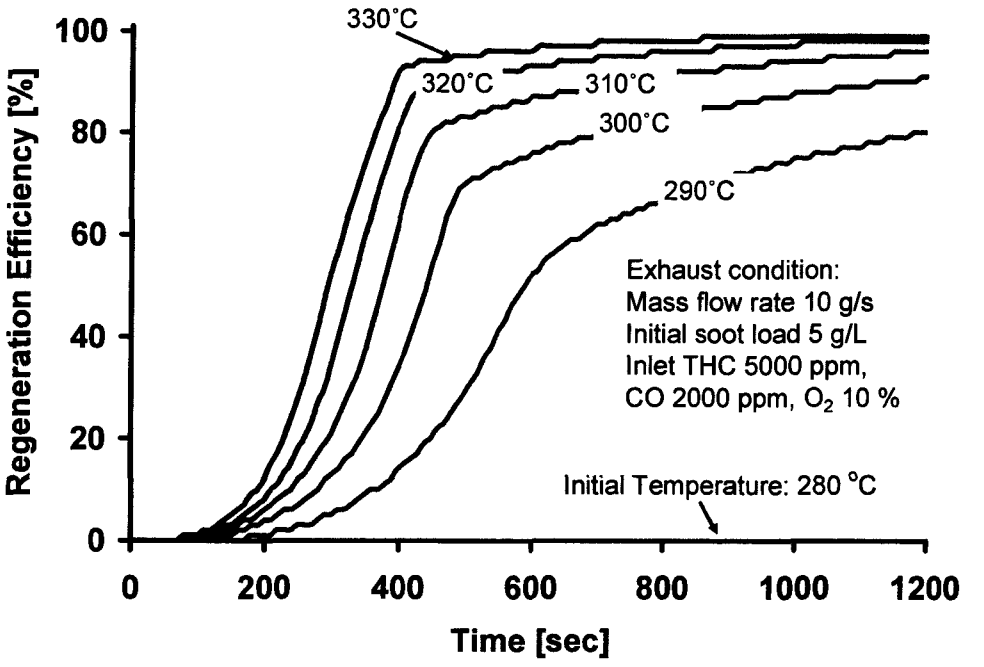

Figure 4-24: Comparison of Regeneration Efficiency for Different Exhaust Temperature

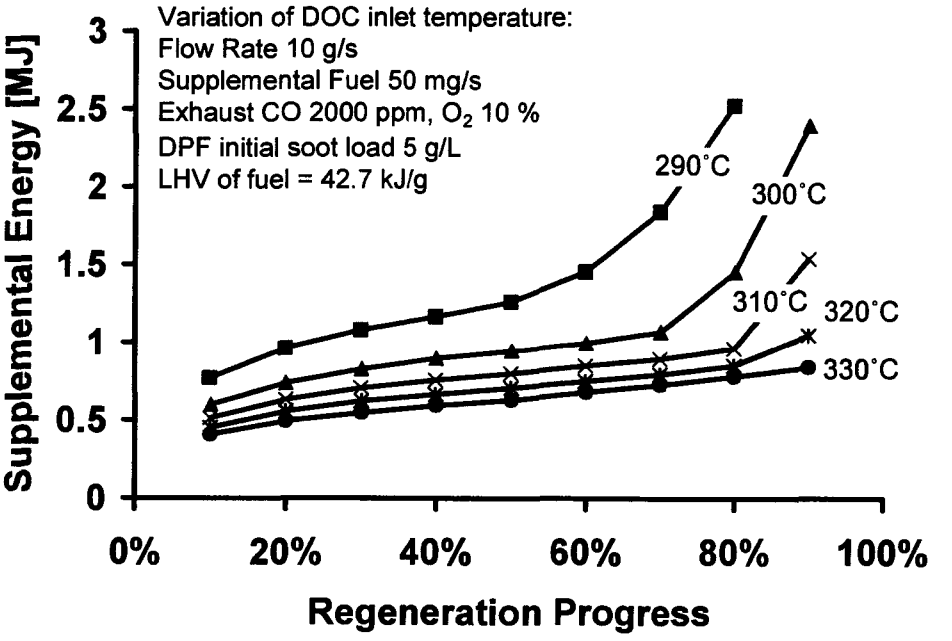

Figure 4-25: Energy Efficiency Analysis with Regeneration Progress

It is noted that the rate of regeneration reduces with its progress. However 80 % of the regeneration is accomplished within initial 400 seconds with 330 °C initial temperature. This indicates that considerable amount of energy can be saved by switching to next mode of PR operation sequence when only 70 to 80 % of regeneration is accomplished. In other words the energy efficiency of regeneration process will deteriorate once the rate of regeneration starts to decline.

4.2.3 CASE S3: EXHAUST FLOW RATE VARIATION FOR DPF REGENERATION

Simulations are carried out with the different exhaust flow rate in the PR flow. The primary objective of this set of simulations is to provide a guideline to effectively control the regeneration process in a safe and energy efficient manner. With the low exhaust mass flow rate along with the moderate rate of supplemental energy in the PR regeneration loop, the supplemental energy density amount may be high. This can potentially run the regeneration out of control often resulting in overheating. On the other hand the supplemental energy is wasted with the high exhaust gas mass flow rate and moderate rate of supplemental fuel delivery due to the low energy density. Therefore an optimum balance between the exhaust mass flow rate and the supplemental fuel delivery rate is required to carry out regeneration effectively, serving the purpose of the PR setup to accomplish regeneration and save supplemental energy. A summary of the simulation cases is shown in the Table 4-10. To demonstrate the effect of variations of the exhaust mass flow rates the exhaust gas temperature at the inlet of DOC-DPF is kept constant along with supplemental fuel delivery rate. It is noted that with the variations in the exhaust mass flow rate only, the effective energy concentration of fuel in the exhaust stream is changed keeping the rate of supplemental energy delivery constant.

Table 4-10: Simulation Conditions (Case S3)

Parameter	Value			Unit
	Cases			
	S3A	S3B	S3C	
Exhaust Mass Flow Rate	10	5	2.5	g/s
Exhaust Gas Temperature	310			°C
Initial DOC Temperature	310			°C
Initial DPF Temperature	310			°C
Initial Soot Load	5			g/L
Supplemental Fuel	50			mg/s
Inlet CO	2000			ppm
Inlet O_2	10			%

It is assumed that the fuel delivered by the external injector is vaporised completely before reaching the DOC channel. The simulation case S3A is identical to the case S2A. The supplemental fuel rate of 50 mg/s with exhaust flow rate of 10 g/s corresponds to 5000 ppm of THC by mass at the inlet of DOC.

The transient thermal response and fraction of soot oxidised were analysed and presented along with the soot profile during the regeneration at different time instant. The diffusion heat and mass transfer becomes dominant at the low exhaust gas velocities. The simulation model ignores free convection and radiation heat transfers and also the gas phase conduction and diffusion mass transfer. Therefore the simulation model has limitations in simulating thermal response at low flow rates lesser than 2 g/s. However a guidline to conduct controlled regeneration can be outlined from the following results.

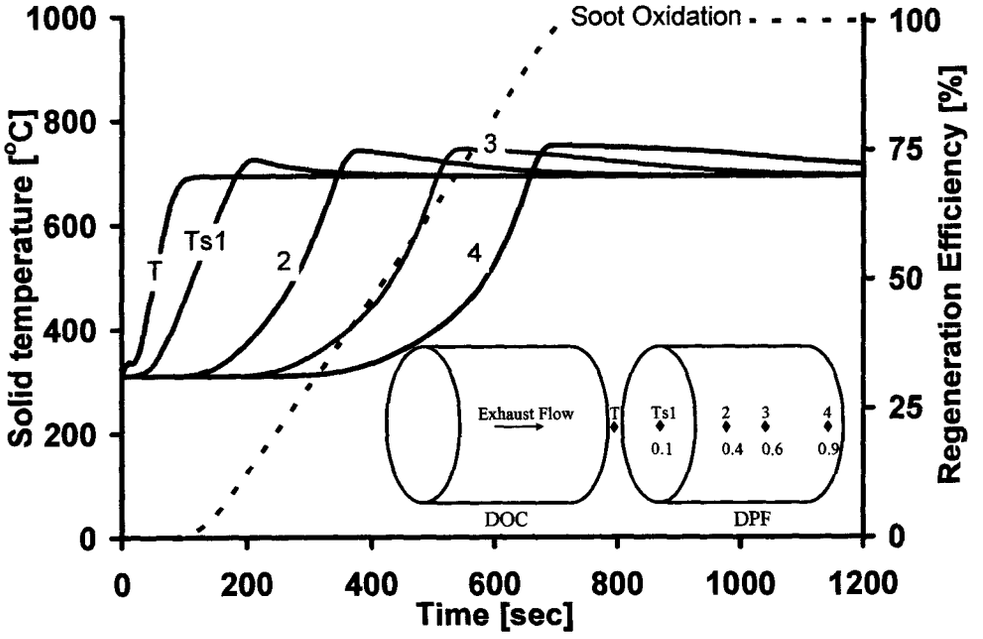

Figure 4-26: Transient Simulation Result (Case S3B)

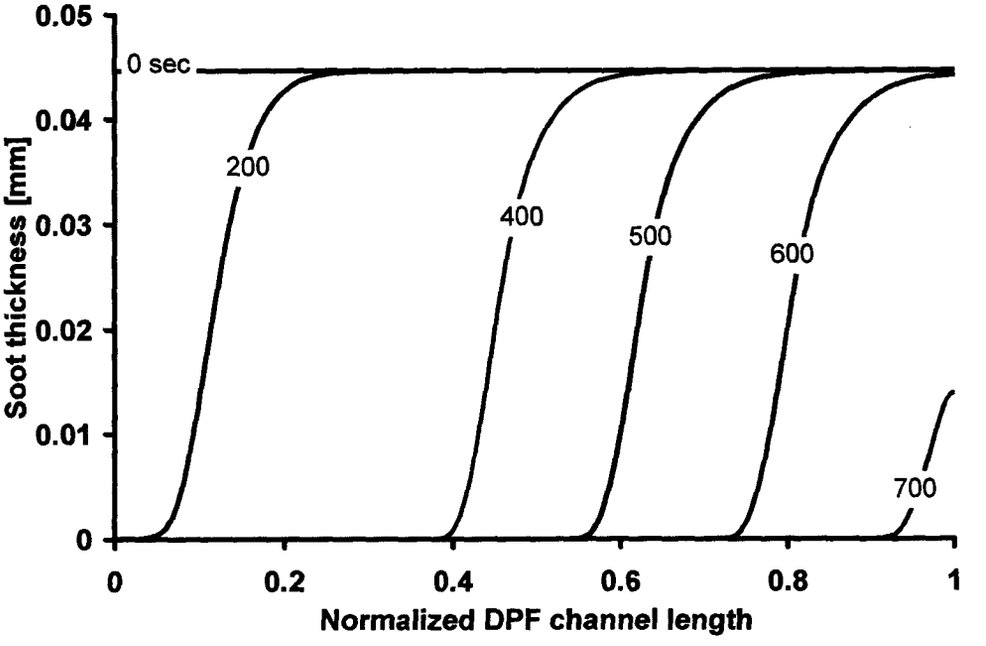

Figure 4-27: Soot Oxidation Simulation (Case S3B)

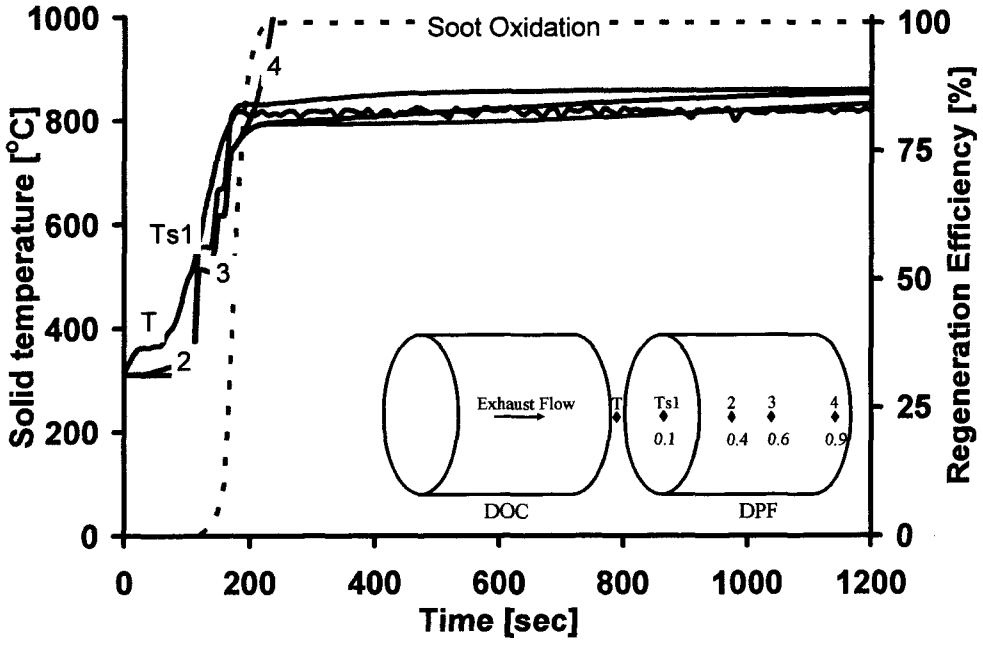

Figure 4-28: Transient Simulation Results (Case S3C)

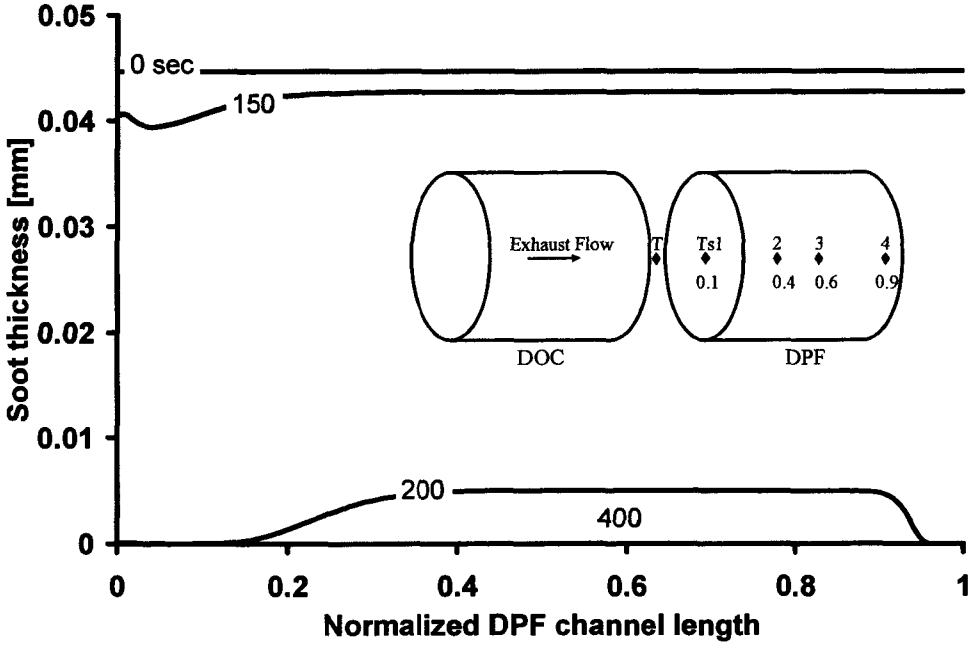

Figure 4-29: Soot Oxidation Simulation (Case S3C)

It is observed from the simulation results of the case S3C that the overheating occurs at the location corresponding to $z/L = 0.9$. This can be explained in terms of rate of heat released due to the oxidation reaction of soot is compensated with the rate of cooling by the cold exhaust gas. Due to the low exhaust flow rate, the residence time of exhaust gas increases considerably in the DPF channel and the convective heat transfer increases. Therefore the exhaust gas reaching the outlet of DPF channel is heated by the regeneration heat released at the inlet of the channel. From the simulation results of the case S3B it is noted that soot is oxidised locally and the reaction progresses from the inlet side of the DPF channel and the rate of soot oxidation remains constant throughout the regeneration process. This is therefore a very good example of energy efficient soot regeneration without overheating. An energy analysis of the simulation cases with partial and full regenerations is shown in the Figure 4-30 below.

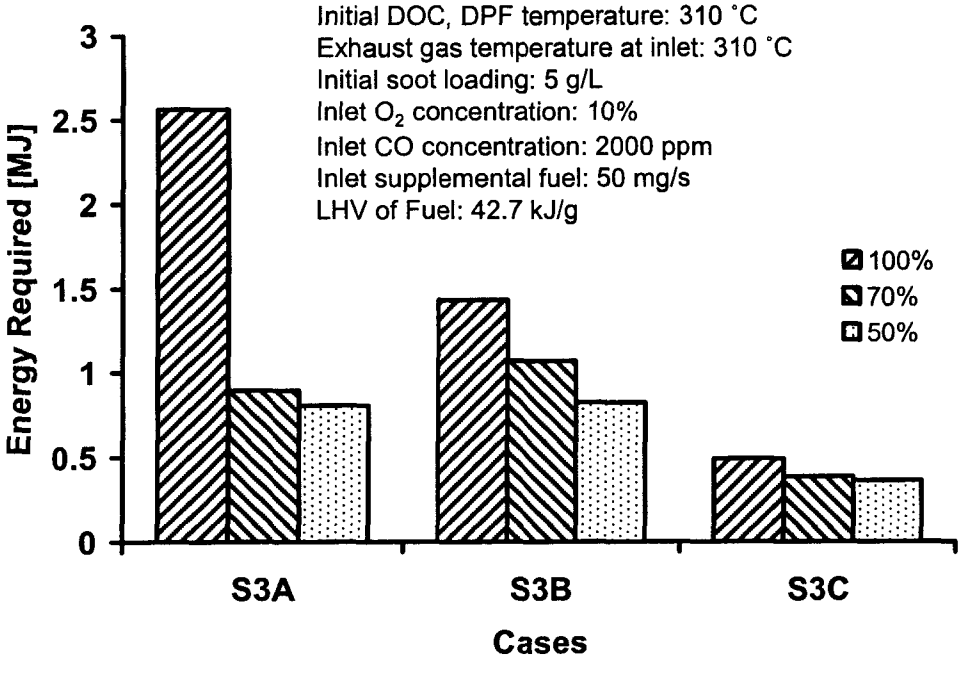

Figure 4-30: Supplemental Energy for Regeneration

CHAPTER V

5. CONCLUSIONS AND RECOMMENDATIONS

A thermal response analysis of the DOC and DPF has been carried out. A one dimensional mathematical model has been developed along with a computer program in order to simulate the DOC and DPF operation under various passive and active flow control conditions. Flow field representing pressure and velocity of the exhaust gas along with mass and energy transfers between the different phases of DOC and DPF channels were calculated. The model has been validated with the experimental results. An experimental investigation has been carried out to study the effects of the supplemental energy in the form of external fuel and exhaust heating on the DOC thermal response. An energy efficient pathway to reach DPF regeneration condition has been discussed along with the results. Complementary simulation cases are also presented to establish guidelines to control chemical reactions in a safe and energy efficient way. Theoretical investigation shows that energy efficiency can be improved by the active flow control strategies under certain conditions of exhaust gas flow rate, temperature and supplemental energy delivery.

The work presented here can be essentially used by the designers of the diesel aftertreatment devices to optimise its operation cost against the cost of manufacturing. This work can also assist engineers to control the active flow operations such as flow reversal and parallel flow techniques for the safe and energy efficient operations of the diesel aftertreatment devices such as the DOC and the DPF. The model developed in this work can be used and developed further for advanced simulations on diesel aftertreatment performances.

5.1. DIESEL OXIDATION CATALYST

The DOC performance based on the chemical conversion of pollutant exhaust gas species is dependent on the temperature of the substrate. The DOC is enabled to perform chemical conversions only above certain temperature otherwise knows as "light off". In active flow configurations, the DOC plays an important role to activate soot regeneration in the DPF. The exothermic heat released from the DOC to the exhaust gas often enables the condition favourable to initiate regeneration in DPF. The DOC "light off" temperature can be achieved by increasing exhaust temperature through either in-cylinder techniques such as post injection or increasing manifold temperature by adjusting VGT or by other active control strategies such as independently heating exhaust gas. In this work an energy efficiency analysis is carried between various active control strategies to enable and sustain catalytic activity in the DOC. Theoretical studies presented in this work indicates that once the catalytic activity is initiated, the temperature of DOC can be maintained higher than the "light off" temperature through the sustainable exothermic reactions in the catalyst site. If however the balance between the exothermic heat release rate and the rate of heat lost to exhaust gas is disturbed, the DOC can either potentially overheat or can cool down below "light off" temperature. Therefore in order to control DOC activity without overheating the substrate temperature and its time derivative along the channel length should be monitored. The length derivative of substrate temperature indicates the thermal stress of the substrate.

5.2. DIESEL PARTICULATE FILTER

The DPF eliminates the SPM from the exhaust stream by the method of deep bed filtration and soot cake deposition. Over the period of time, the accumulated PM in the DPF channel clogs the passage of exhaust gas resulting in higher pressure drop across DPF. Increased back pressure in the exhaust affects the performance of the engine. In practical automotive applications, the DPF is regenerated during vehicle operation by chemically oxidizing the soot in the DPF channel thereby restoring the back pressure to the acceptable limits. Theoretical and experimental investigations have been carried out to identify the energy efficient corridor to initiate and sustain safe regeneration with the various active flow control configurations. Effects of the various active control schemes on the thermal response characteristics of DPF substrate are analyzed and a guideline is outlined based on such analysis. It is observed that the supplemental fuel can be saved considerably by accurately predicting the rate of regeneration from the real time monitoring of temperature, pressure and mass flow rate of the exhaust gas through the DPF. It is recommended that during the PR operation, an optimum exhaust flow rate can save energy without having the risk of overheating the substrate. It is also observed that during low load operations, the temperature of the DPF can be maintained favourable to the conditions for regeneration through FR operation.

5.3. RECOMMENDATIONS FOR FUTURE WORK

The mathematical model developed assuming the PM as dry soot for accumulation and regeneration characteristics. Dry soot is generated during pyrolysis of fuel in the in-cylinder combustion process in the absence of oxygen. However the SOF which is otherwise known as the wet soot is also filtered in the DPF channel. The model

can be improved to consider the effects of regeneration also on wet soot. An experiment using synthetic organic substance to represent SOF can give insights to the physical phenomenon of such filtration and regeneration. A distillation and vaporisation characteristics can be obtained through fractional distillation process of SOF.

The mathematical model can be expanded to consider the effect of free convection and diffusion mass transfer during low exhaust flow rate. The effect of radiation and convection through the inlet and outlet faces may also be taken into account. A three dimensional model can also be developed based on the one dimensional model developed in this work.

An experimental study of DOC-DPF performance at various active flow control operation conditions may be performed to validate the theoretical findings of this work.

The FORTRAN program may be converted to SIMULINK S-functions to develop model based feed forward algorithm integrated with an engine control system. Such integrated model may be useful to the automotive manufacturers to develop engine management system that can implement various active and passive flow control techniques in their vehicles, to initiate and sustain DPF regeneration and DOC activity in a safe and efficient manner.

REFERENCES

1. Reader G. T., Banerjee S., Wang M., Zheng M., "Energy Efficiency Analysis of Active Flow Operations in Diesel Engine Aftertreatment", SAE 2006-01-3286, 2006.
2. Asad U., Banerjee S., Reader G.T., Wang M., Zheng M., "Energy Efficiency Analysis between In-cylinder and External Supplemental Fuel Strategies", SAE 2007-01-1125, 2007.
3. Zheng M., Reader G.T., Hawley G., "Diesel Engine Exhaust Gas Recirculation – A Review On Advanced Novel Concepts", Journal of Energy Conversion and Management 45 (2004) 883-900, 2004.
4. Asad U., "Thermal Response Analysis from In-cylinder Combustion to Exhaust Aftertreatement", MASc Thesis, University of Windsor, Canada, May 2006.
5. Zheng M., Asad U., Reader G. T., Ting D., S. K., "A Preliminary Thermal Response Analysis of Exhaust Pipe Plenums for Diesel Aftertreatment Improvement" SAE 2006-01-3310, 2006.
6. Zheng M., Reader G. T., "Energy efficiency analyses of active flow aftertreatment systems for lean burn internal combustion engines", Journal of Energy Conversion and Management 45 (2004) 2473-2493, 2004.
7. Zheng M., Mirosh E. A., Klopp W., Uland D. A., Pardell M. E., Newman P. E., Matros Y. S., "Development of Compact Reverse-Flow Catalytic Converter for Diesel Dual-Fuel Lev", SAE 1999-01-3558, 1999.

8. Padilla A. T., "Development of Models to Study the Emissions, Flow and Kinetic Characteristics from Diesel Oxidation Catalysts and Particulate Filters", PhD Dissertation, Michigan Technological University, 2005.
9. Padilla A. T., Johnson J. H., Yang S. L. , Baumgard K. L., "An Expermental and Numerical Study of the Performance Characteristics of the Diesel Oxidation Catalyst in a Continuosly Regeneration Particulate Filter", SAE 2003-01-3176, 2003.
10. Setiabudi A., Makkee M., Moulijn J. A., "An optimal NOx assited abatement of diesel soot in an advanced catalytic filter design", Journal of Applied Catalysis 42 (2003) 35-45, 2003.
11. Heck R. M., Farrauto R. J., "Catalytic Air Pollution Control – Commercial Technology", John Wiley & Sons, Inc., 1995.
12. Davis C. N., "Air Filtration", Academic Press Inc. 1973.
13. Zheng M., Wang D., Reader G. T., Wang M., "Empirical and Theoretical Investigations of Active-flow Control on Diesel Engine After-treatment", SAE 2006-01-0465, 2006.
14. Zheng, M., Reader, G. T., Wang D., Zuo J., Wang M., Mirosh E., Van der Lee A. H., Liu B., "A Thermal Analysis of Active-Flow Control on Diesel Engine Aftertreatment", SAE 2004-01-3020, 2004.
15. Zheng M., Wang D., Reader G. T., "Boundary-Layer-Enhanced Recuperation for Diesel Particulate Filter Regeneration Under a Periodic Flow Reversal Operation", SAE 2005-01-0951, 2005.

16. Zheng M., Reader G. T., Wang D., Zuo J., Kumar R., Mulenga M. C., Asad U., Ting D. S. K., Wang M., "Thermal Response Analysis on the Transient Performance of Active Diesel Aftertreatment", SAE 2005-01-3885, 2005.

17. Bisset Edward J., "Mathematical Model of the Thermal Regeneration of a Wall-Flow Monolith Diesel Particulate Filter", Chemical Engineering Science Vol. 39, Nos. 7/8 pp 1233-1244, 1984.

18. Konstandopolous A.G., Johnson J.H., "Wall-Flow Diesel Particulate Filters – Their Pressure Drop and Collective Efficiency", SAE 890405, 1989

19. Konstandopolous A.G., Kostoglou M. Skaperdas E., Papaioannou E., Zarvalis D., Kladopoulou E., "Fundamental Studies of Diesel Particulate Filters: Transient Loading, Regeneration and Aging", SAE 2000-01-1016, 2000.

20. Huynh C.T., Johnson J.H., Yang S.L., Bagley S.T., Warner J.R., "A One-Dimensional Computation Model for Studying the Filtration abd Regeneration Characteristics of a Catalyzed Wall-Flow Diesel Particulate Filter", SAE 2003-01-0841, 2003.

21. Koltsakis G.C., Stamelos A.M., "Modeling Catalytic Regeneration of Wall-Flow Particulate Filters", Ind. Eng. Chem. Res. 35, pp 2-13, 1996.

22. Corning Inc. Website www.corning.com/docs/environmentaltechnologies/co.pdf accessed on 13th November 2006.

23. Internal Communications with Corning Inc. of USA, December 2005.

24. Zheng M., Mulenga M. C., Reader G. T., Wang M., Ting D. S. K., "Influence of Biodiesel Fuel on Diesel Engine Performance and Emissions in Low Temperature Combustion", SAE 2006-01-3281, 2006.

25. http://zenstoves.net/CHRIS/ODS.pdf accessed on 6th April 2006.

26. Zheng M., Mulenga M. C., Reader G. T., Tan Y., Wang M., Tjong J. S., "Neat Biodiesel Fuel Engine Tests and Preliminary Modelling", SAE 2007-01-0616, 2007.

27. Ko R. S-J., "Investigation of EGR Reforming", MASc Thesis, University of Windsor, Canada, November 2005.

APPENDICES

APPENDIX A

A. FORTRAN CODE AND THE INPUT FILES

A.1 Calculation Time Loop of Main Program

```
dzdoc=Ldoc/(n-1)
dzdpf=Ldpf/(n-1)
t=0
frcycle=0
revflow=0
time(0)=0
regres(0)=0
regini=sum(wp)
if(regini.eq.0) then
        regini=1.0d-10
end if
if(wp0.le.0) then
        wp0=1.0d-10
end if
do i=1,n
if(wp(i).le.0) then
wp(i)=1.0d-10
end if
continue
end do
do i=1,n
if(wpp(i).le.0) then
wpp(i)=1.0d-10
end if
continue
end do

T1res(0)=Tsdpf(loc1*n)-273.0d0
T2res(0)=Tsdpf(loc2*n)-273.0d0
T3res(0)=Tsdpf(loc3*n)-273.0d0
T4res(0)=Tsdpf(loc4*n)-273.0d0
Tmidres(0)=Tsdpf(0.5*n)-273.0d0
Tgdocoutres(0)=Tgintrans(0)-273.0d0
dPres(0)=0.0d0

do i=1,n
Tgres(0,i)=Tgintrans(0)-273.0d0
Tsdpfres(0,i)=Tsdpf(i)-273.0d0
Tsres(0,i)=Tsp(i)-273.0d0
Tg1res(0,i)=Tgintrans(i)-273.0d0
Tg2res(0,i)=Tgintrans(i)-273.0d0
wpres(0,i)=wp(i)*1.0d3
v1res(0,i)=u1(i)
v2res(0,i)=u2(i)
vwres(0,i)=0
p1res(0,i)=patomtrans(1)
p2res(0,i)=patomtrans(1)
continue
end do

write(*,*)
'Time(s),SVDOC(1/h),SVDPF(1/h),DPFin(C),T1(C),T2(C),T
3(C),T4(C)'
call line

if(flowrev) then
simintr=dt_fr
frcycle=1
else
simintr=tminpt
end if

1000 continue
if((flowrev).and.frcycle.ne.1) then
write(*,*)
write(*,*) 'Flow reversal Operation'
do i=1,n
wp(i)=wpprev(n+1-i)
Tsdpf(i)=Tsdpfprev(n+1-i)
Ts(i)=Tsprev(n+1-i)
YsCO(i)=YsCOprev(n+1-i)
YsHC(i)=YsHCprev(n+1-i)
YsNO(i)=YsNOprev(n+1-i)
YsO2(i)=YsO2prev(n+1-i)
ws(i)=wsprev(n+1-i)
continue
end do
end if

do tloop=1,int(simintr/dt)
t=t+1
time(t)=t*dt
guess=.true.
if(DOCDPF) then
if(t.gt.1) then
Tgp=Tg
Tsp=Ts
YgCOp=YgCO
YsCOp=YsCO
YgHCp=YgHC
YsHCp=YsHC
YgNOp=YgNO
YsNOp=YsNO
YgO2p=YgO2
YsO2p=YsO2
end if
uz(1:1000)=(gfrintrans(t)/(deng(Tgintrans(t))))/(Ncdoc*ddoc
**2)
Tgindoc=Tgintrans(t)
YgCOindoc=Ycointrans(t)
YgHCindoc=Yhcintrans(t)
YgNOindoc=Ynointrans(t)
YgO2indoc=Yo2intrans(t)
! DOC Simulation for one single loop
rguz=uz(1)*deng(Tgindoc)
Tg(1)=Tgindoc
YgCO(1)=Ygcoindoc
YgHC(1)=Yghcindoc
YgNO(1)=Ygnoindoc
YgO2(1)=Ygo2indoc
do i=1,n
if(i.ne.n) then
```

```
Tg(i+1)=Tg(i)+(4*dzdoc*(Tsp(i)-
Tgp(i))*(hcoe(Tgp(i),ddoc)))/(cpg*ddoc*rguz)
! Exhaust gas energy balance
if((Tgp(i+1)-Tsp(i+1))*(Tg(i+1)-Tsp(i+1)).lt.0) then
Tg(i+1)=Tg(i) ! Thermal oscillation protection for explicit
scheme
end if
end if
continue
end do
do i=1,n
To simulate one channel of DOC
if((i.gt.1).and.(i.lt.n)) then
ae0=lamdasdoc*(1-svfdoc)/ncdoc/dzdoc
aw0=lamdasdoc*(1-svfdoc)/ncdoc/dzdoc
ae(i)=flex*ae0
aw(i)=flex*aw0
aps=densdoc*cpsdoc*(1-svfdoc)/ncdoc*dzdoc/dt
sp=-hcoe(Tg(i),ddoc)*ssfdoc/ncdoc
sc=hcoe(Tg(i),ddoc)*ssfdoc/ncdoc*Tg(i)+(ssfdoc/ncdoc)*qD
OC(i)
ap(i)=aps+ae(i)+aw(i)-flex*sp*dzdoc
b(i)=(aps-(1-flex)*(ae0+aw0)+(1-flex)*sp*dzdoc)*Tsp(i)+(1-
flex)*ae0*Tsp(i+1)+(1-flex)*aw0*Tsp(i-1)+sc*dzdoc
else if(i.eq.1) then      ! Left Boundary
ae0=lamdasdoc*(1-svfdoc)/ncdoc/dzdoc
aw0=0.0d0
ae(1)=flex*ae0
aw(1)=flex*aw0
sp=-hcoe(Tg(1),ddoc)*ssfdoc/ncdoc
sc=hcoe(Tg(1),ddoc)*ssfdoc/ncdoc*Tg(1)+(ssfdoc/ncdoc)*q
DOC(1)
ap(1)=0.5d0*aps+ae(1)+aw(1)-flex*sp*0.5d0*dzdoc
b(1)=(0.5d0*aps-(1-flex)*(ae0+aw0)+(1-
flex)*sp*0.5d0*dzdoc)*Tsp(1)+(1-
flex)*ae0*Tsp(2)+sc*0.5d0*dzdoc
else if(i.eq.n) then      ! Right Boundary
ae0=0.0d0
aw0=lamdasdoc*(1-svfdoc)/ncdoc/dzdoc
ae(n)=flex*ae0
aw(n)=flex*aw0
sp=-hcoe(Tg(n),ddoc)*ssfdoc/ncdoc
sc=hcoe(Tg(n),ddoc)*ssfdoc/ncdoc*Tg(n)+(ssfdoc/ncdoc)*q
DOC(n)
ap(n)=0.5d0*aps+ae(n)+aw(n)-flex*sp*0.5d0*dzdoc
b(n)=(0.5d0*aps-(1-flex)*(ae0+aw0)+(1-
flex)*sp*0.5d0*dzdoc)*Tsp(n)+(1-flex)*aw0*Tsp(n-
1)+sc*0.5d0*dzdoc
end if
continue
end do
call tdma(ap,ae,aw,b,n,Ts)
do i=1,n
if((Ts(i)-Tsp(i)).gt.10.0d0) then
Ts(i)=Tsp(i)+10.0d0
end if
continue
end do
do i=1,n
uz(i)=rguz/deng(Tg(i))
continue
end do

! To solve mass balance of spiecies in the DOC channel
! Oxidation Reactions Considered in the odel are
! CO + 0.5 O2-> CO2 (kCO,hrrCO)
! HC + 4.5 O2 -> 3 CO2 + 3 H2O (kHC,hrrHC)
! NO + 0.5 O2 -> NO2 (kNO,hrrNO)
const=(rguz*Adoccell/Mexh) ! Number of moles influx,
moles/sec
do i=1,n
GCO(i)=1.0d0/(1.0d0+K1CO*exp(-(Ts(i)-273.0d0-
K2CO)/K3CO))*min(1.0d0,(YgO2p(i)+1.0d-
6)/(YgCOp(i)+1.0d-6)*2.0d0)
GHC(i)=1.0d0/(1.0d0+K1HC*exp(-(Ts(i)-273.0d0-
K2HC)/K3HC))*min(1.0d0,(YgO2p(i)+1.0d-
6)/(YgHCp(i)+1.0d-6)*2.0d0/9.0d0)
GNO(i)=1.0d0/(1.0d0+K1NO*exp(-(Ts(i)-273.0d0-
K2NO)/K3NO))*min(1.0d0,(YgO2p(i)+1.0d-
6)/(YgNOp(i)+1.0d-6)*2.0d0)
kCO(i)=ACO*exp(-EaCO/(R*Ts(i)))
kHC(i)=AHC*exp(-EaHC/(R*Ts(i)))
kNO(i)=ANO*exp(-EaNO/(R*Ts(i)))
rCO(i)=min(kCO(i)*DOCLOAD*SSFDOC*dzdoc*GCO(i),
kaCO*DOCLOAD*SSFDOC*dzdoc*abs(YgCOp(i)-
YsCOp(i)))
rHC(i)=min(kHC(i)*DOCLOAD*SSFDOC*dzdoc*GHC(i),
kaHC*DOCLOAD*SSFDOC*dzdoc*abs(YgHCp(i)-
YsHCp(i)))
rNO(i)=min(kNO(i)*DOCLOAD*SSFDOC*dzdoc*GNO(i),
kaNO*DOCLOAD*SSFDOC*dzdoc*abs(YgNOp(i)-
YsNOp(i)))
rO2(i)=0.5*rCO(i)+4.5*rHC(i)+0.5*0.5*rNO(i)
if((i.ne.1).and.(i.ne.n)) then
YgCO(i+1)=YgCO(i-1)-rCO(i)/const
YgHC(i+1)=YgHC(i-1)-rHC(i)/const
YgHC(i+1)=YgHC(i-1)-rHC(i)/const
YgO2(i+1)=YgO2(i-1)-rO2(i)/const
if(YgCO(i+1).le.0.0d0) YgCO(i+1)=0.0d0
if(YgHC(i+1).le.0.0d0) YgHC(i+1)=0.0d0
if(YgNO(i+1).le.0.0d0) YgNO(i+1)=0.0d0
if(YgO2(i+1).le.0.0d0) YgO2(i+1)=0.0d0
YsCO(i)=YgCO(i-1)-YgCO(i+1)
YsHC(i)=YgHC(i-1)-YgHC(i+1)
YsNO(i)=YgNO(i-1)-YgNO(i+1)
YsO2(i)=YgO2(i-1)-YgO2(i+1)
elseif(i.eq.1) then
YgCO(2)=YgCO(1)-rCO(1)/const
YgHC(2)=YgHC(1)-rHC(1)/const
YgNO(2)=YgNO(1)-rNO(1)/const
YgO2(2)=YgO2(1)-rO2(1)/const
if(YgCO(2).le.0.0d0) YgCO(2)=0.0d0
if(YgHC(2).le.0.0d0) YgHC(2)=0.0d0
if(YgNO(2).le.0.0d0) YgNO(2)=0.0d0
if(YgO2(2).le.0.0d0) YgO2(2)=0.0d0
YsCO(1)=YgCO(1)-YgCO(2)
YsHC(1)=YgHC(1)-YgHC(2)
YsNO(1)=YgNO(1)-YgNO(2)
YsO2(1)=YgO2(1)-YgO2(2)
else
YsCO(n)=YgCO(n-1)-YgCO(n)
YsHC(n)=YgHC(n-1)-YgHC(n)
YsNO(n)=YgNO(n-1)-YgNO(n)
YsO2(n)=YgO2(n-1)-YgO2(n)
end if
continue
end do
YgCOp=YgCO
YgHCp=YgHC
YgNOp=YgNO
YgO2p=YgO2
YsCOp=YsCO
YsHCp=YsHC
YsNOp=YsNO
YsO2p=YsO2
do i=2,n-1
YgCO(i)=(YgCOp(i-1)+YgCOp(i+1))*0.5d0
```

```
YgHC(i)=(YgHCp(i-1)+YgHCp(i+1))*0.5d0
YgNO(i)=(YgNOp(i-1)+YgNOp(i+1))*0.5d0
YgO2(i)=(YgO2p(i-1)+YgO2p(i+1))*0.5d0
YsCO(i)=(YsCOp(i-1)+YsCOp(i+1))*0.5d0
YsHC(i)=(YsHCp(i-1)+YsHCp(i+1))*0.5d0
YsNO(i)=(YsNOp(i-1)+YsNOp(i+1))*0.5d0
YsO2(i)=(YsO2p(i-1)+YsO2p(i+1))*0.5d0
continue
end do
do i=1,n
qDOC(i)=(YsCO(i)*hrrCO+YsHC(i)*hrrHC+YsNO(i)*hrrN
O)*const/(ssfdoc/ncdoc)
continue
end do
Tgoutdoc=Tg(n) ! The Gas temperature is adjusted to the
DOC out temperature
YgO2outdoc=YgO2(n)
Tgindpf=Tgoutdoc
YgO2indpf=YgO2outdoc
else
Tgoutdoc=Tgintrans(t)
Tgindpf=Tgintrans(t)
YgO2indpf=Yo2intrans(t)
end if
! Boundary Conditions
uindpf=(gfrintrans(t)/(deng(Tgintrans(t))))/(Ncdpf*ddpf**2)
u1(1)=uindpf
u2(1)=uindpf/5.0d0
Tg1(1)=Tgindpf
Tg2(1)=Tgindpf
YPMdpf(1)=ystintrans(t)/(deng(Tgintrans(t))*1.0d6)
do while((u1(n).ge.u1(1)/20.0).or.(u1(n).le.0.0).or.(p2(n)-
patomtrans(t).ge.20.0).or.guess)
guess=.false.
! To guess the boudary conditions (p1(1) and p2(1))
if(p2(n).ge.patomtrans(t)) then
p1(1)=p1(1)-5.0D0
p2(1)=p2(1)-5.0D0
end if
if(u1(n).lt.0) p2(1)=p2(1)+1.0d0
if(u1(n).ge.u1(1)/20) p2(1)=p2(1)-5.0d0
2000 continue
do i=1,n-1
! Calculate uw(i)
uw(i)=(p1(i)-
p2(i))/(viscg(Tsdpf(i))*(wp(i)/permeabsoot+wsdpf/permeabd
pf))
u1(i+1)=u1(i)-
dzdpf*4/ddpf*deng(Tsdpf(i))*uw(i)/deng(Tg1(i))
if(u1(i+1).lt.0) then     ! P2(1) Guess Wrong
p2(1)=p2(1)+1.0d0
goto 2000
end if
u2(i+1)=u2(i)+dzdpf*4/ddpf*deng(Tsdpf(i))*uw(i)/deng(Tg2
(i))
! Soot Accumulation Model
YPMdpf(i+1)=YPMdpf(I)-
k_accum*YPMdpf(I)*uw(i)*dzdpf/u1(i)
if(YPMdpf(i+1).le.0) YPMdpf(i+1)=1.0d-10
! To Calculate Temperature of next control volume
Tg1(i+1)=Tg1(i)+dzdpf*4/ddpf*(hcoe(Tg1(i),ddpf)-
Cpg*deng(Tsdpf(i))*uw(i))*(Tsdpf(i)-
Tg1(i))/(Cpg*deng(Tg1(i))*u1(i))
if((Tg1(i).gt.Tsdpf(i)).and.(Tg1(i+1).lt.Tsdpf(i)))
Tg1(i+1)=Tsdpf(i)
! To prevent Solution Divergence
if(((Tg1(i+1)-Tg1(i)).gt.10.0d0).and.(t.gt.50.0d0))
Tg1(i+1)=Tg1(i)+10.0d0
if(Tg1(i+1).lt.0.0d0) goto 9995
Tg2(i+1)=Tg2(i)+dzdpf*4/ddpf*(hcoe(Tg2(i),ddpf)+Cpg*de
ng(Tsdpf(i))*uw(i))*(Tsdpf(i)-
Tg2(i))/(Cpg*deng(Tg2(i))*u2(i))
if((Tg2(i).gt.Tsdpf(i)).and.(Tg2(i+1).lt.Tsdpf(i)))
Tg2(i+1)=Tsdpf(i)
if(((Tg2(i+1)-Tg2(i)).gt.10.0d0).and.(t.gt.50.0d0))
Tg2(i+1)=Tg2(i)+10.0d0
if(Tg2(i+1).lt.0) goto 9995
! To Calculate Pressure of next control volume
p1(i+1)=p1(i)-(deng(Tg1(i+1))*(u1(i+1)**2)-
deng(Tg1(i))*(u1(i)**2))-
dzdpf*cfric*viscg(Tg1(i))*u1(i)/(ddpf**2)
p2(i+1)=p2(i)-(deng(Tg2(i+1))*(u2(i+1)**2)-
deng(Tg2(i))*(u2(i)**2))-
dzdpf*cfric*viscg(Tg2(i))*u2(i)/(ddpf**2)
continue
end do
uw(n)=(p1(n)-
p2(n))/viscg(Tsdpf(n))/(wp(n)/permeabsoot+wsdpf/permeabd
pf)
continue
end do
! To Calculate the soot amount for next time step
Tsdpfp=Tsdpf
Tg1p=Tg1
Tg2p=Tg2
do i=1,n
call
chemr1(odr,Tsdpf(i),deng(Tsdpf(i)),uw(i),YgO2indpf,wp(i),c
at)
! To prevent sudden increase of temperature causing solution
divergence
if((Tsdpf(i)-Tsdpfp(i)).gt.10.0d0) then
Tsdpf(i)=Tsdpfp(i)+10.0d0
end if
call
chemr2(cdr,hreact,rno2(i),Tsdpf(i),wp(i),YgO2indpf,ws(i)*
Mexh/MNO2)
if((Tsdpf(i)-Tsdpfp(i)).gt.10.0d0) then
Tsdpf(i)=Tsdpfp(i)+10.0d0
end if
wpp(i)=wp(i)
m_accum=(YPMdpf(i)-YPMdpf(i+1))*gfrintrans(t)*dt
w_accum=m_accum/(0.5*Ncdpf)/denssoot/(4*ddpf*dzdpf)
wp(i)=wp(i)-cdr*wp(i)*dt*MCB*1000.0/denssoot-
MCB/MO2*odr*dt/denssoot+w_accum
if(wp(i).le.0) wp(i)=1.0d-10      ! No soot
heatdpf(i)=hreact+dh/MO2*odr
continue
end do
! To find out the temperature for the next time step using the
differential equation of form ap.Tp=ae.Te+aw.Tw+B to solve
heat conduction equation
do i=2,n-1
ae0=(lamdassoot*wpp(i)+lamdasdpf*wsdpf)/dzdpf
aw0=(lamdassoot*wpp(i)+lamdasdpf*wsdpf)/dzdpf
ae(i)=flex*ae0
aw(i)=flex*aw0
apold=denssoot*cpssoot*wpp(i)*dzdpf/dt
aps=densdpf*cpsdpf*wsdpf*dzdpf/dt
sp=-(hcoe(Tg1(i),ddpf)+hcoe(Tg2(i),ddpf))
sc=hcoe(Tg1(i),ddpf)*Tg1(i)+hcoe(Tg2(i),ddpf)*Tg2(i)+heat
dpf(i)
ap(i)=apold+aps+ae(i)+aw(i)-flex*sp*dzdpf
b(i)=(apold+aps-(1-flex)*(ae0+aw0)+(1-
flex)*sp*dzdpf)*Tsdpf(i)+(1-flex)*ae0*Tsdpf(i+1)+(1-
flex)*aw0*Tsdpf(i-1)+sc*dzdpf
continue
end do
```

```
! Left Boundary
ae0=lamdassoot*wpp(1)/dzdpf+lamdasdpf*wsdpf/dzdpf
aw0=0.0d0
ae(1)=flex*ae0
aw(1)=flex*aw0
apold=denssoot*cpssoot*wpp(1)*dzdpf/dt
sp=-(hcoe(Tg1(1),ddpf)+hcoe(Tg2(1),ddpf))
sc=hcoe(Tg1(1),ddpf)*Tg1(1)+hcoe(Tg2(1),ddpf)*Tg2(1)+h
eatdpf(1)
ap(1)=0.5d0*apold+0.5d0*aps+ae(1)-flex*sp*0.5d0*dzdpf
b(1)=(0.5d0*(apold+aps)-(1-flex)*ae0+(1-
flex)*sp*0.5d0*dzdpf)*Tsdpf(1)+(1-
flex)*ae0*Tsdpf(2)+sc*0.5d0*dzdpf
! Right Boundary
ae0=0.0d0
aw0=lamdassoot*wpp(n)/dzdpf+lamdasdpf*wsdpf/dzdpf
ae(n)=flex*ae0
aw(n)=flex*aw0
apold=denssoot*cpssoot*wpp(n)*dzdpf/dt
sp=-(hcoe(Tg1(n),ddpf)+hcoe(Tg2(n),ddpf))
sc=hcoe(Tg1(n),ddpf)*Tg1(n)+hcoe(Tg2(n),ddpf)*Tg2(n)+h
eatdpf(n)
ap(n)=0.5d0*apold+0.5d0*aps+aw(n)-flex*sp*0.5d0*dzdpf
b(n)=(0.5d0*(apold+aps)-(1-flex)*aw0+(1-
flex)*sp*0.5d0*dzdpf)*Tsdpf(n)+(1-flex)*aw0*Tsdpf(n-
1)+sc*0.5d0*dzdpf
call tdma(ap,ae,aw,b,n,Tsdpf)
do i=1,n
if((Tsdpf(i)-Tsdpfp(i)).gt.10.0d0) then
Tsdpf(i)=Tsdpfp(i)+10.0d0
end if
continue
end do
! To find out the soot particulate thickness in the DPF wall
do i=2,n-1
aw(i)=dno2*ddpf/dzdpf+0.5*u1(i)*ddpf
ae(i)=dno2*ddpf/dzdpf-0.5*u1(i)*ddpf
ap(i)=2.0*dno2*ddpf/dzdpf+4.0*uw(i)*dzdpf
b(i)=-
4.0*km*rno2(i)*wp(i)/wp0*(1/dt)*mno2*wp(i)*dzdpf/deng(
Tsdpf(i))/(km+uw(i))
continue
end do
! Left Boundary
aw(1)=0
ae(1)=dno2*ddpf/dzdpf-2.0/3.0*u1(1)*ddpf
ap(1)=3.0*dno2*ddpf/dzdpf+4.0*uw(1)*dzdpf
b(1)=2.0*dno2*ddpf*YNO2intrans(t)*1.0d-
6*MNO2/Mexh/dzdpf+2.0/3.0*u1(1)*ddpf*YNO2intrans(t)*
1.0d-6*MNO2/Mexh-
4.0*km*rno2(1)*wp(1)/wp0*(1/dt)*MNO2*wp(1)*dzdpf/de
ng(Tsdpf(1))/(km+uw(i))
! Right Boundary
aw(n)=dno2*ddpf/dzdpf+2.0/3.0*u1(n)*ddpf
ae(n)=0
ap(n)=aw(n)+4.0*uw(n)*dzdpf
b(n)=-
4.0*km*rno2(n)*wp(n)/wp0*(1/dt)*MNO2*wp(n)*dzdpf/de
ng(Tsdpf(n))/(km+uw(n))
wgpdpf=wgdpf
call tdma(ap,ae,aw,b,n,wgdpf)
do i=1,n
if(wgdpf(i).lt.0.0) wgdpf(i)=1.0d-10
ws(i)=(ws(i)+wgdpf(i)-
rno2(i)*wp(i)/wp0*(1/dt)*MNO2*wp(i)/deng(Tsdpf(i))/(km
+uw(i)))/2.0
if(ws(i).lt.0.0) ws(i)=1.0d-10
continue
end do

! To record result for output file
do i=1,n
if(revflow.eq.0) then
Tsres(ceiling(time(t)/dt_out),i)=Ts(i)-273.0d0
Tgres(ceiling(time(t)/dt_out),i)=Tg(i)-273.0d0
Tsdpfres(ceiling(time(t)/dt_out),i)=Tsdpf(i)-273.0d0
wpres(ceiling(time(t)/dt_out),i)=wp(i)*1.0d3
p1res(ceiling(time(t)/dt_out),i)=p1(i)
p2res(ceiling(time(t)/dt_out),i)=p2(i)
v1res(ceiling(time(t)/dt_out),i)=u1(i)
v2res(ceiling(time(t)/dt_out),i)=u2(i)
vwres(ceiling(time(t)/dt_out),i)=uw(i)*1.0d3
Tg1res(ceiling(time(t)/dt_out),i)=Tg1(i)-273.0d0
Tg2res(ceiling(time(t)/dt_out),i)=Tg2(i)-273.0d0
else if(revflow.eq.1) then
Tsres(ceiling(time(t)/dt_out),i)=Ts(n+1-i)-273.0d0
Tgres(ceiling(time(t)/dt_out),i)=Tg(n+1-i)-273.0d0
Tsdpfres(ceiling(time(t)/dt_out),i)=Tsdpf(n+1-i)-273.0d0
wpres(ceiling(time(t)/dt_out),i)=wp(n+1-i)*1.0d3
p1res(ceiling(time(t)/dt_out),i)=p1(n+1-i)
p2res(ceiling(time(t)/dt_out),i)=p2(n+1-i)
v1res(ceiling(time(t)/dt_out),i)=u1(n+1-i)
v2res(ceiling(time(t)/dt_out),i)=u2(n+1-i)
vwres(ceiling(time(t)/dt_out),i)=uw(n+1-i)*1.0d3
Tg1res(ceiling(time(t)/dt_out),i)=Tg1(n+1-i)-273.0d0
Tg2res(ceiling(time(t)/dt_out),i)=Tg2(n+1-i)-273.0d0
end if
continue
end do
T1res(ceiling(time(t)/dt_out))=Tsdpf(loc1*n)-273.0d0
T2res(ceiling(time(t)/dt_out))=Tsdpf(loc2*n)-273.0d0
T3res(ceiling(time(t)/dt_out))=Tsdpf(loc3*n)-273.0d0
T4res(ceiling(time(t)/dt_out))=Tsdpf(loc4*n)-273.0d0
Tmidres(ceiling(time(t)/dt_out))=Tsdpf(0.5*n)-273.0d0
Tgdocoutres(ceiling(time(t)/dt_out))=Tgoutdoc-273.0D0
dPres(ceiling(time(t)/dt_out))=p1(1)-p2(n)
regres(ceiling(time(t)/dt_out))=1.0d0-sum(wp)/regini
do i=1,n
if(wp(i).le.0) then
wp(i)=1.0d-10
end if
continue
end do
do i=1,n
if(wpp(i).le.0) then
wpp(i)=1.0d-10
end if
continue
end do
if((flowrev).and.(revflow.eq.1)) then
write(*,50)
time(t),int((uz(1)/Ldoc)*3600),int((u1(1)/Ldpf)*3600),int(Tg
indpf-273),int(Tsdpf((1-loc1)*n)-273),int(Tsdpf((1-loc2)*n)-
273),int(Tsdpf((1-loc3)*n)-273),int(Tsdpf((1-loc4)*n)-273)
else
write(*,50)
time(t),int((uz(1)/Ldoc)*3600),int((u1(1)/Ldpf)*3600),int(Tg
indpf-273),int(Tsdpf(loc1*n)-273),int(Tsdpf(loc2*n)-
273),int(Tsdpf(loc3*n)-273),int(Tsdpf(loc4*n)-273)
end if
50 format(1x,f6.1,1x,i7,1x,i7,1x,i4,1x,i4,1x,i4,1x,i4,1x,i4)
continue
end do

if((flowrev).and.(frcycle.lt.(int(tminpt/dt_fr)))) then
frcycle=frcycle+1
wpprev=wp
Tsdpfprev=Tsdpf
Tsprev=Ts
```

```
YsCOprev=YsCO
YsHCprev=YsHC
YsNOprev=YsNO
YsO2prev=YsO2
wpprev=wpp
wsprev=ws
if(revflow.eq.0) then
revflow=1 ! Odd Cycle
else if(revflow.eq.1) then
revflow=0 ! Even Cycle
end if
goto 1000
end if

! SUBROUTINE TO CALCULATE HEAT TRANSFER
COEFFICIENT
FUNCTION HCOE(TG,DIA)
DOUBLE PRECISION HCOE,TG,NU,DIA,LAMDAG,CPG
COMMON /BLOCK1/          CPG,NU
LAMDAG=0.0186D0+4.41D-5*TG+3.64D-9*TG*TG
HCOE=NU*LAMDAG/DIA
RETURN
END

! SUBROUTINE TO CALCULATE THE GAS DENSITY
FUNCTION DENG(TG)
DOUBLE PRECISION DENG,TG
DENG=1.823D0-0.3115D0*((TG-
273.0D0)/100)+0.01694D0*((TG-273.0D0)/100.0D0)**2
RETURN
END

! SUBROUTINE TO CALCULATE THE GAS VISCOSITY
FUNCTION VISCG(TG)
DOUBLE PRECISION VISCG,TG,CVISC,SVISC
COMMON /BLOCK2/ CVISC,SVISC
VISCG=CVISC*(TG**1.5)/(TG+SVISC) ! SUTHERLAND
EQUATION
RETURN
END

! SUBROUTINE TO CALCULATE OXYGEN
DEPLETION RATE
SUBROUTINE CHEMR1(ODR,T,DENG,V,YO2,W,CAT)
IMPLICIT DOUBLE PRECISION (A-H,O-Z)
DOUBLE PRECISION K,K1,K_THM,K_CAT
LOGICAL CAT
COMMON /BLOCK3/
A_THM,K_THM,E_THM,A_CAT,K_CAT,E_CAT
COMMON /BLOCKCONST/ R
SP1=5.5D7 ! Specific Area of Deposit Layer (1/m)
IF(CAT) THEN ! For Catalytic Regeneration
A=A_CAT ! Soot Oxidation Compleateness Index
K=K_CAT ! Collision Frequency Factor (m/(s*K))
E=E_CAT  ! Apparant Activation Energy (J/mol)
ELSE ! For Thermal Regeneration
A=A_THM ! Soot Oxidation Compleateness Index
K=K_THM ! Collision Frequency Factor (m/(s*K))
E=E_THM ! Apparant Activation Energy (J/mol)
END IF
K1=K*T*EXP(-E/(R*T)) ! Using Arrehenius Equation to
Calculate Oxidation Rate of Soot
ODR=DENG*V*YO2/A*(1.0D0-EXP(-SP1*K1*W*A/V))
RETURN
END

! SUBROUTINE TO CALCULATE CARBON
DEPLETION RATE
SUBROUTINE
CHEMR2(CDR,HREACT,R3,T,WP,YO2,YNO2)
IMPLICIT DOUBLE PRECISION (A-H,O-Z)
DOUBLE PRECISION K1,K3,K1_NO2,K3_NO2
COMMON /BLOCK4/
P1_NO2,P2_NO2,P3_NO2,K1_NO2,E1_NO2,K3_NO2,E3_
NO2
COMMON /BLOCK5/ DHCO,DHCO2,DHNO2
COMMON /BLOCKCONST/ R
K1=K1_NO2
E1=E1_NO2
P1=P1_NO2
P2=P2_NO2
P3=P3_NO2
K3=K3_NO2
E3=E3_NO2
FCO=1.0/(1.0+P1*YO2**P2*EXP(P3/R/T))
R1=FCO*K1*EXP(-E1/R/T)*YO2
R2=(1.0-FCO)*K1*EXP(-E1/R/T)*YO2
R3=K3*EXP(-E3/R/T)*YNO2
CDR=R1*2.0+R2+R3
HREACT=(R1*DHCO+R2*DHCO2+R3*DHNO2)*WP*10
00.0
RETURN
END

! SUBROUTINE TO SOLVE TRI-DIAGONAL MARIX
ARRAY
SUBROUTINE TDMA(A,B,C,D,N,X)
DOUBLE PRECISION A(N),B(N),C(N),D(N),X(N)
B(1)=B(1)/A(1)
D(1)=D(1)/A(1)
! FORWARD ELIMINATION
DO I=2,N
B(I)=B(I)/(A(I)-C(I)*B(I-1))
D(I)=(D(I)+C(I)*D(I-1))/(A(I)-C(I)*B(I-1))
CONTINUE
END DO
! BACKWARD SUBSTITUTION
X(N)=D(N)
DO I=N-1,1,-1
X(I)=B(I)*X(I+1)+D(I)
CONTINUE
END DO
RETURN
END
```

A.2 Input File

```
Diesel Engine Aftertreatment Simulation - Input File

----------File Selection----------
property.dat        ! Property data file
calibration.dat     ! Calibration file
transient.dat       ! Transient input file
profile.dat         ! Profile selection (Initial condition)
output              ! Output file name _*.dat

----------Simulation Selection----------
N ! Use transient data, Yes (Y) or No (N)
N ! Use profile selection, Yes (Y) or No (N)

----------Sub-model Selections----------
T ! THERMAL (T) or CATALYTIC (C) regeneration
N ! Use DOC model (DOC + DPF), Yes (Y) or No (N)
```

```
S ! Straight flow (S), Flow reversal (R)

----------Specifications of the DOC & DPF----------
1          ! DOC  Material, (1) -> Cordierite (2) -> SiC (3) -
> Stainless Steel
06.0       ! DOC  Length, (in)
5.66       ! DOC  Diameter, (in)
400.0      ! DOC  Cell Density, (cpsi)
8.0        ! DOC  Wall Thickness, (milli-inch)

1          ! DPF Material, (1) -> Cordierite (2) -> SiC (3) ->
Stainless Steel
06.0       ! DPF Length, (in)
5.66       ! DPF Diameter, (in)
200.0      ! DPF Cell Density, (cpsi)
19.0       ! DPF Wall Thickness, (milli-inch)
1.54e-13   ! DPF Wall permeability, (m^2)

----------Initial Conditions----------
05.0     ! Initial Soot Loading, (g/L)
1        ! Initial Soot Layer Distributions
************************************************
* 1 - Uniform Distribution ( y = h )                *
* 2 - Linear Increase ( y = 2*h/L * x )             *
* 3 - Linear Decrease ( y = -2*h/L * x + 2*h )      *
* 4 - Quadratic Incrase ( y = 3*h/L^2 * x^2 )       *
* 5 - Quadratic Decrese ( y = 3*h/L^2 * x^2 - 6*h/L * x +
3*h ) *
* 6 - Triangular increase and decrease (ymax=2*h)
*
* 7 - Rectangular hump in 25% of the DPF length at the
middle  *
* 8 - Triangular hump in 50% of the DPF length at the
middle  *
************************************************
100.0    ! DOC Substrate Initial Temperature, (Celsius)
100.0    ! DPF Substrate Initial Temperature, (Celsius)
```

A.3 Calibration File

```
Diesel Engine Aftertreatment Simulation - Calibration file

----------Chemical Reaction Kinetics (DPF)----------
************************************************
*  Simple Mechanism                  *
*  Reaction: C + a*O2 -> 2(a-0.5)CO2 + 2(1-a) CO   *
*  Reaction Rate: r1 = k*T*exp(-E/RT)        *
************************************************
Thermal Regeneration
0.5        ! a, Soot Oxidation Completeness Index
3.0        ! k, Collisions Frequency Factor, (m/(s*K))
1.5e5      ! E, Apparent Activation Energy, (J/mol)

Catalytic Regeneration
0.8        ! a, Soot Oxidation Completeness Index
2.8        ! k, Collisions Frequency Factor, (m/(s*K))
1.1e5      ! E, Apparent Activation Energy, (J/mol)

************************************************
*  Carbon - Reaction Mechanism                *
*  Reactions:                                 *
*  (1) 2C + O2 -> 2CO                         *
*  (2)  C + O2 -> CO2                         *
*  (3)  C + NO2 -> CO + NO                    *
*  Reaction Rates:                            *
*  (1) r1 = f_CO*k1*exp(-E1/RT)*y_O2          *
*  (2) r2 = (1-f_CO)*k1*exp(-E1/RT)*y_O2      *
*  (3) r3 = k3*exp(-E3/RT)*y_NO2              *

----------Exhaust Gas Conditions (Static case)----------
-
100.0      ! Exhaust Gas Temperature, (Celsius)
75.60      ! Exhaust Gas Flowrate, (g/s)
10.0       ! Exhaust O2 Concentration, (%)
01.0       ! Exhaust SOOT Concentration, (mg/m^3)
001.0      ! Exhaust NO Concentration, (ppm)
001.0      ! Exhaust NO2 Concentration, (ppm)
0001.0     ! Exhaust HC Concentration, (ppm)
0001.0     ! Exhaust CO Concentration, (ppm)
1.00       ! Atmospheric Pressure (bar)

----------Running Parameters----------
120        ! Simulation time, (s)
1          ! Output data point time interval (s)
10         ! Flow reversal frequency (s)
250        ! Total number of elements in z direction for
result output
N          ! To monitor simulation run

----------Temperature Sensor Location----------
-
0.083      ! Normalized Location of Ts1
0.361      ! Normalized Location of Ts2
0.638      ! Normalized Location of Ts3
0.917      ! Normalized Location of Ts4

----------Transient file data----------
Time (sec) Exhaust temperature (deg C)      Exhaust GFR
(g/s)      O2 (%)    Soot (mg/m^3)      NO (ppm) NO2
(ppm)      HC (ppm) CO (ppm) Pressure Atomospheric
(bar)

----------Profile file data----------
DOC surface temperature (deg C)          DPF surface
temperature (deg C)          DPF soot load (mm)

*  f_CO = 1/(1+P1*y_O2^P2*exp(P3/RT)          *
************************************************
0.02       ! P1, Constant
0.21       ! P2, Constant
3000.0     ! P3, Constant
5.0e8      ! k1, Reaction Rate Constant
1.5e5      ! E1, Activation Energy, (J/mol)
1.0e4      ! k3, Reaction Rate Constant
500        ! E3, Activation Energy, (J/mol)
2.21e5     ! DHCO, Heat of Formation of CO (J/mol)
3.93e5     ! DHCO2, Heat Release from CO2 Oxidation
(J/mol)
0.53e5     ! DHNO2, Heat Release from NO2 Oxidation
(J/mol)
0.8        ! Alpha, Soot Oxidation Completeness Index,
Constant
3.61e5     ! DH1, Heat of Formation of CO2 (J/mol)
0.9e5      ! DH2, Heat of Formation of CO (J/mol)
1.36e-6    ! DNO2, NO2 Diffusion Coefficient (1/sqm)
3.66       ! Sh, Sherwood Number

----------Physical properties (DPF)----------
28.45      ! Friction coefficient of DPF channel wall
2500       ! Soot accumulation coefficient

----------General properties----------
3.61       ! Nusselt Number
```

----------DOC Calibration----------
20.0 ! K1CO, DOC Conversion Factor
100.0 ! K2CO, DOC Conversion Factor
20.0 ! K3CO, DOC Conversion Factor
10.0 ! k1HC, DOC Conversion Factor
300.0 ! k2HC, DOC Conversion Factor
10.0 ! k3HC, DOC Conversion Factor
10.0 ! k1NO, DOC Conversion Factor
200.0 ! k2NO, DOC Conversion Factor
10.0 ! k3NO, DOC Conversion Factor
5.32e5 ! ACO, Preexponential factor for DOC reaction kinetics (CO Oxidation)
1.72e5 ! AHC, Preexponential factor for DOC reaction kinetics (HC Oxidation)
8.05e5 ! ANO, Preexponential factor for DOC reaction kinetics (NO Oxidation)
1.5e5 ! EaCO, Activation energy of CO Oxidation (J/mol)
1.5e5 ! EaHC, Activation energy of HC Oxidation (J/mol)
1.5e5 ! EaNO, Activation energy of NO Oxidation (J/mol)
1.0e-5 ! kaCO, Diffusion coefficient of CO (m2/s)
1.0e-5 ! kaHC, Diffusion coefficient of HC (m2/s)
1.0e-5 ! kaNO, Diffusion coefficient of NO (m2/s)
1.0e-5 ! kaO2, Diffusion coefficient of O2 (m2/s)
2.21e8 ! hrrCO, Heat Release from CO Oxidation (J/mol)
2.40e11 ! hrrHC, Heat Release from HC Oxidation (J/mol)
5.30e7 ! hrrNO, Heat Release from NO Oxidation (J/mol)

A.4 Property File

Diesel Engine Aftertreatment Simulation - Property file

----------General Material Properties----------
Cordierite
1100 ! Specific Heat, (J/(kg*K))
1400 ! Density, (kg/m^3)
0.850 ! Thermal Conductivity (W/(m*K))

SiC
800 ! Specific Heat, (J/(kg*K))
3150 ! Density, (kg/m^3)
1150 ! Thermal Conductivity (W/(m*K))

Stainless Steel
580 ! Specific Heat, (J/(kg*K))
7900 ! Density, (kg/m^3)
22.60 ! Thermal Conductivity (W/(m*K))

----------Soot Layer Properties----------
1510.0 ! Specific Heat, (J/(kg*K))
140.0 ! Density, (kg/m^3)
2.1 ! Thermal Conductivity (W/(m*K))
5.55e-15 ! Permeability, (m^2)

----------DOC Property----------
1.5 ! DOC Catalyst Loading (g/L)

----------Exhaust Gas Property----------
1090.0 ! Specific Heat, (J/(kg*K))

APPENDIX B

B. DERIVATIONS OF PDE

The control volume method is employed to derive the mass, the momentum and the energy equations from Reynolds's transport theory. The control volume shown in the Figure B-1 is at a location set $z = z$ from the inlet of DOC and at the time $t = t$. The entire DOC channel length is divided into equal and identical geometrical sections of size $\Delta x \Delta y \Delta z$. To setup one dimensional model of DOC, $\Delta x = \Delta y = d$ is considered. A representative scalar term ψ_g is defined to represent any scalar property of exhaust gas to be considered for conservation law to derive mathematical equations. An Upwind differencing scheme is applied to derive the discretised equations.

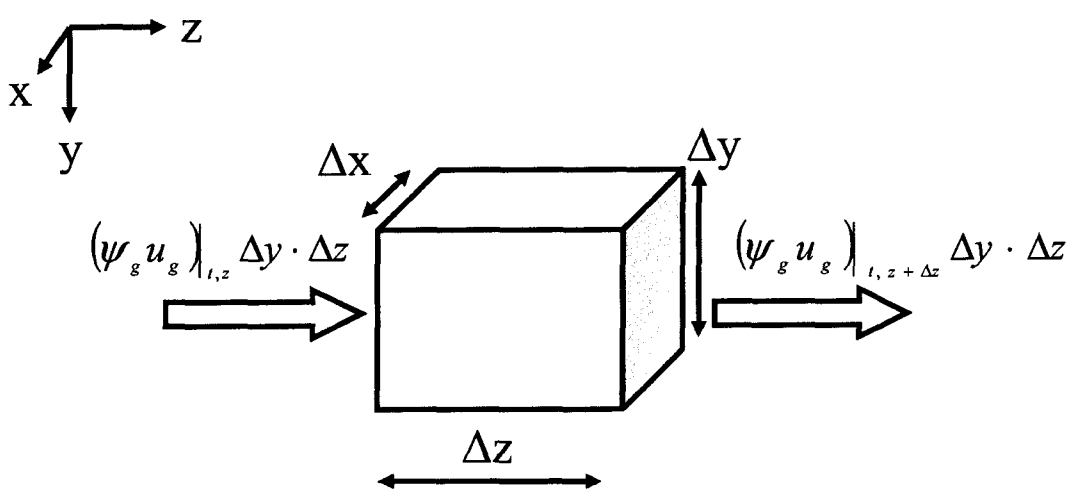

Figure B-1: Control volume of exhaust gas

The generalized Reynolds's transport equation for the conservation of scalar property ψ_g inside the control volume is written in the equation B.1. The total time derivative of a rate of change of a scalar property is sum total of local time derivative and the net flux into the control volume.

$$\frac{\partial}{\partial t}\iiint_{CV}\psi_g \rho_g dV + \iint_{CS}\psi_g \rho_g \vec{u}\cdot d\vec{S} = \frac{D\psi_g}{Dt} \tag{B.1}$$

From the generalized transport equation applying $\psi_g = 1$, the equation of mass conservation is derived. In compressible flow, the net rate of mass accumulation in the control volume is equal to the net rate of mass inflow into the control volume. From second law of thermodynamics, the energy conservation equation for the control volume in Reynolds's transport form can be written as:

$$\frac{\partial}{\partial t}\iiint_{CV}\left(e_i + \frac{1}{2}u_z^2 + gy\right)\rho_g dV + \iint_{CS}\left(e_h + \frac{1}{2}u_z^2 + gy\right)\rho_g \vec{u}\cdot d\vec{S} = \dot{Q} - \dot{W} \tag{B.2}$$

The equation above is written assuming the scalar property as energy. Similarly exhaust species concentration can be obtained using the scalar property equal to the mass concentration of the species in the exhaust gas. Using the mass conservation the PDE for exhaust species concentration can be calculated.

APPENDIX C

C. ADDITIONAL FIGURES AND TABLES

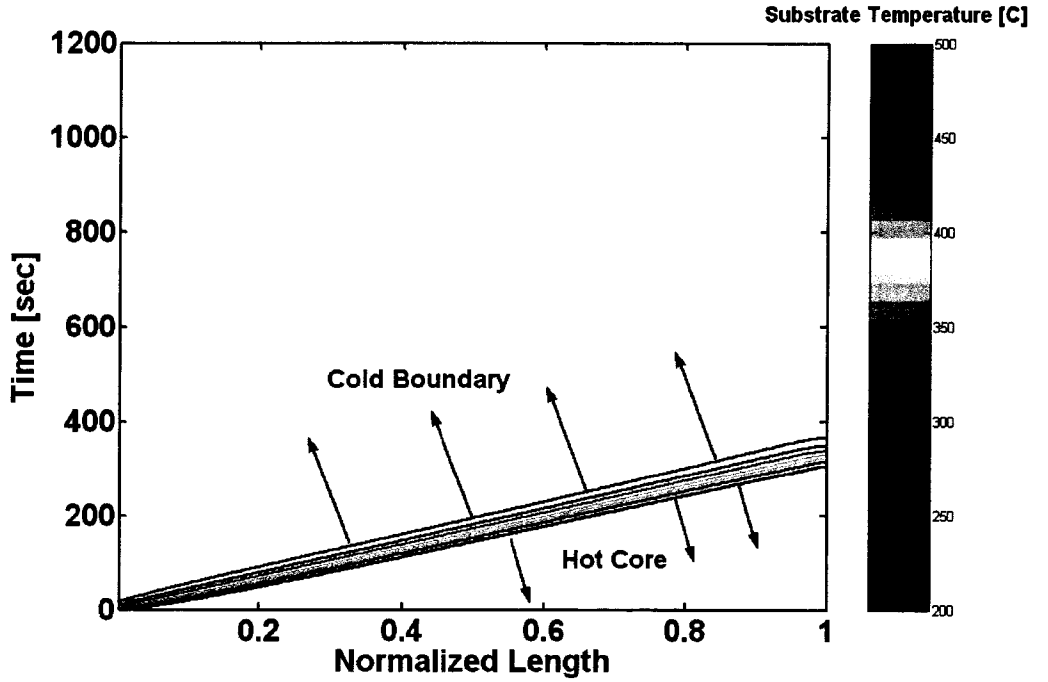

Figure C-1: Propagation of Cold Boundary in NFR (Cooling Process)

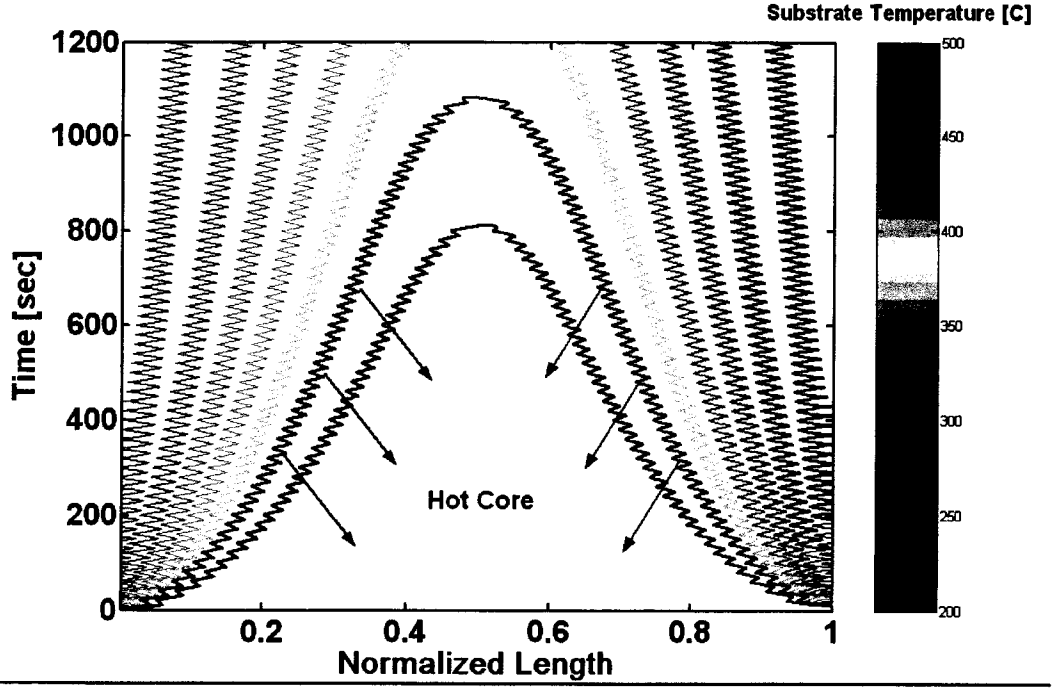

Figure C-2: Propagation of Cold Boundary in FR (Cooling Process)

Table C-1: Source of Uncertainty in Exhaust Mass Flow Measurement

Source of Uncertainty	Relative uncertainty [%]
Calibrator	3.0
Linearization	0.5
A/D resolution	0.4
Probe positioning	0.0
Cold junction temperature variations	0.2
Ambient Temperature variation	1.1
Ambient pressure variation	0.6
Ambient Humidity variation	0.6
Total	6.4

Table C-2: Additional Calibration Parameter

Parameter	Value	Unit
κ_p	5.55×10^{-15}	m^2
κ_s	1.54×10^{-13}	m^2
A_{CO}	5.32×10^{5}	-
A_{HC}	1.72×10^{5}	-
A_{NO}	8.05×10^{5}	-

Table C-3: Experimental DOC-DPF Setup

	Value	Unit
DOC Diameter	5.66	inch
DOC Length	6	inch
DOC Wall Thickness	8	mil
DOC Cell Density	400	cpsi
DPF Diameter	5.66	inch
DPF Length	6	inch
DPF Wall Thickness	19	mil
DPF Cell Density	200	cpsi
Substrate Material	Cordierite	-
Catalyst Alloy	Pd-Rh	-

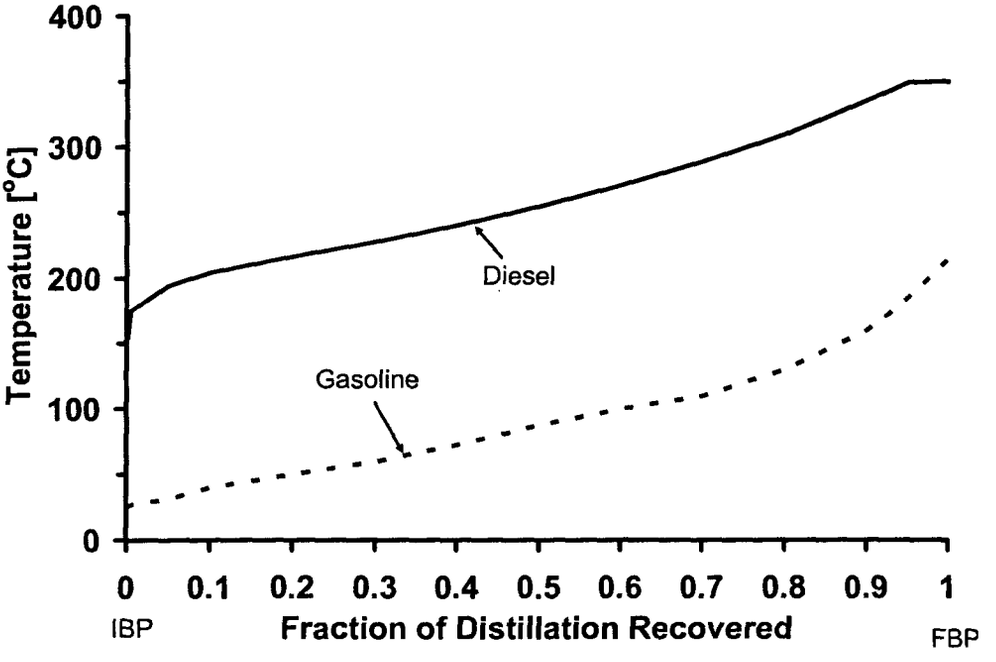

Figure C-3: Distillation Curve of Diesel and Gasoline

APPENDIX D

D. CALIBRATION OF EXTERNAL INJECTOR

The external fuel injector is calibrated using diesel fuel at different injection pressures and nozzle opening time. The injector nozzle opening is controlled by a solenoid that is connected to a counter signal and a power supply. The counter signal is generated by a control algorithm using NI-LABVIW ® program energies and de energies the solenoid resulting in opening and closing of injector nozzle. Due to the nature of electrical delay of signal and mechanical inertia with the solenoid mass, the commanded there is a difference between commanded and actual opening time of the injector nozzle. Therefore it is necessary to calibrate the nozzle discharge efficiency with the commanded opening time. Using the calibration results [27], a lookup table is generated and is used by the injection control program to compensate for the electrical and mechanical delay. The fuel injection is therefore accurately controlled by diagnosing the injection pressure.

If the frequency of commended counter signal is f_{inj} and the duty cycle is dc_{inj} then the commanded injection duration per opening of nozzle is given by t_{inj} as given by the equation D.1.

$$t_{inj} = \frac{dc_{inj}}{f_{inj}} \tag{D.1}$$

The fuel flow rate $\dot{m}_{fuel}$ is given by the injection pressure p_{inj}, exhaust gas pressure at the location of external injection p_{loc}, the density of the fuel in the injector nozzle ρ_{fuel}, the nozzle opening area A_{nozzle} and the discharge efficiency η_{inj}.

$$\dot{m}_{fuel} = \eta_{inj} A_{nozzle} \sqrt{2\rho_{fuel} \cdot (p_{inj} - p_{loc})} \tag{D.2}$$

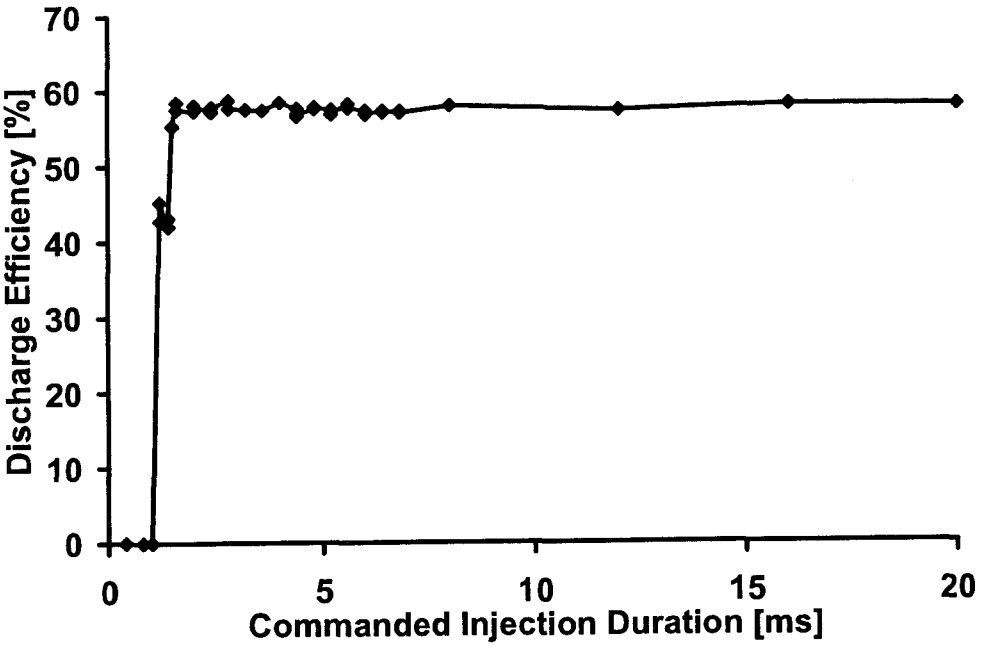

Figure D-1: Injector Calibration Lookup Table

VITA AUCTORIS

NAME:	Siddhartha Banerjee
PLACE OF BIRTH:	Kolkata, India
YEAR OF BIRTH:	1981
EDUCATION:	Jodhpur Park Boys School, Kolkata 1997-1999
	Bengal Engineering and Science University, Shibpur 1999-2003, B.E., Mechanical Engineering